Integrins and SPARC

Potential implications for cardiac remodeling

Dissertation zur Erlangung des

Naturwissenschaftlichen Doktorgrades

der Bayerischen Julius-Maximilians-Universität Würzburg

Vorgelegt von

Rongxue Wu

aus Kunming, China

Würzburg, 2006

Eingereicht am:

Betreuer der Promotion:

Medizinische Universitätsklinik: Prof. Dr.Georg Ertl

Fakultät für Biologie. PD. Dr.Christof Hauck

Tag des Promotionskolloquiums:

Doktorurkunde ausgehändigt am:

Dedicate to my great parents and my whole family

献给我伟大的父亲和母亲

Content

Chapter 1. General introduction

Charpter 2. Characterization of Cardiac specific excision of β1 integrin gene in mice-Influence on the transcriptional response after transversal aortic constriction

Chapter 3. Transient expression of SPARC in response to myocardial infarction in mice

Chapter 4. Fibroblast migration is modulated by SPARC

Chapter 5. Materials

Chapter 6.Methods

Appendices

Acknowledgements

I would like to express my sincere gratitude to the following people and institutions for their help and support during the preparation of this thesis.

My deep gratitude belongs to my study leader and supervisor, Prof. Dr. Georg Ertl, for giving me the opportunity to conduct my doctorate work at his institute. For all his encouragement, trust, help and kindness. It is an honour to be one of his PhD students.

So many thanks to Dr. Martin Laser, his kind help from the first day, when I reached Germany till even after he left the lab. For giving me the interesting project, guiding and teaching me how to think and work independently. Also for dealing with frustrating times and solving problems as well as his support during these years and especially to his family for the hospitality during my first months in Germany; I have improved step by step due to his strict demands.

I appreciate so much the help of PD Dr Christof Hauck, for giving me the opportunity to work in his lab and guiding my research there. For his extremely motivating scientific discussions and encouragement during all my studies in Germany; for reviewing the manuscripts and for his suggestions and advice on my work.

My deep gratitude to Dr Oliver Ritter, for a very scientifically stimulating work atmosphere and his encouragement, prompt help in all the preparation of the thesis and my papers; for all his help and support on my study and research work.

I am indebted to Dr Kai Schuh, for all his valuable help, for discussion, advice and observations of my work, for critically reviewing the manuscript of the article, for his always being helpful and smiling.

I am deeply thankful to Hong Hang and Kai Hu, for teaching me with patience several experimental procedures, for helping me to overcome many difficulties in a foreign country. I also would like to thank them for their hospitality of Chinese dinner in their family.

I am grateful to Prof. Dr. Wolfram Voelker, for giving me his support to attend scientific meetings and his always positive smile. My gratitude also to Dr. Theo Pelzer and all my colleagues in molecular cardiology lab, Natalie Burkard, Virginia Jazbutyte, Matthias Hallhuber, Cornelia Heindl, Jenny Muck and Paula Arias, for creating such a nice relaxing atmosphere in the lab and all their help, advice and smiles. Especially I would like to thank Paula for her encouragement and such a great and lovely friendship.

Furthermore, I would like to express my gratitude to all the people in the institute for ''Infektionsbiologie der Universität Würzburg'' for their advise and for providing a friendly working atmosphere.

Finally, I owe a debt of gratitude to my family, Papa Chanyuan, Mami Baolian, Taoyun, Ronghan and Bonnie…Thanks for just being always there sharing with me happiness and tears. Thanks for all your love and confidence.

Summary

The massive remodeling of the heart tissue, as observed in response to pressure overload or myocardial infarction, is considered to play a causative role in the development of heart failure. Alterations in the heart architecture clearly affect the mechanical properties of the heart muscle, but they are rooted in changes at the cellular level including modulation of gene expression. Together with integrins, the transmembrane receptors linking the extracellular environment to the cytoskeleton, extracellular matrix (ECM) proteins and matricellular proteins are key components of the remodeling process in the heart. Therefore, this thesis was aimed at analysing the role of integrins in the regulation of gene expression and heart muscle performance during cardiac wound repair induced by pressure overload or myocardial infarction (MI).

To investigate the contribution of integrin $\beta 1$, we characterised the response of mice with a conditional, cardiac-specific deletion of the integrin $\beta 1$ gene in an experimental model of pressure overload by aortic banding (AB). In particular, we measured physiological alterations and gene expression events in the stressed heart in the presence or absence of integrin $\beta 1$. Interestingly, mice containing a knock-out allele and the ventricular myocyte-specific conditional allele of the integrin $\beta 1$ gene were born and grew up to adulthood. Though these animals still exhibited minor amounts of integrin $\beta 1$ in the heart (expressed by non-myocytes), these mice displayed abnormal cardiac function and were highly sensitive to AB. Whereas a compensatory hypertrophic response to pressure overload was observed in wildtype mice, the integrin $\beta 1$-deficient mice were not able to undergo heart tissue remodeling. Furthermore, ECM gene expression was altered and, in particular, the increased expression of the matricellular protein SPARC after AB was abolished in integrin $\beta 1$– deficient mice.

Interestingly, we also found a transient upregulation of SPARC mRNA during heart remodeling after MI using cDNA macroarrays. Indeed, increased SPARC protein levels were observed starting at day 2 (2.55 ± 0.21fold, $p<0.01$), day 7 (3.72 ± 0.28 fold, $p<0.01$) and 1 month (1.9 ± 0.16 fold, $p<0.01$) after MI, which could be abolished by using an integrin α_v inhibitor in vivo. Immunofluorescence analysis of

heart tissue demonstrated that the increased SPARC expression was confined to the infarcted area and occurred together with the influx of fibroblasts into the heart.

In vitro, either TGF-β1 or PDGF-BB stimulated SPARC expression by fibroblasts. Inhibition of integrin α_v did not interfere with TGF-β1 or PDGF induced SPARC secretion as determined by ELISA assays or Western blot. However, secretion of TGF-β1 and PDGF-BB by cardiomyocytes was induced by vitronectin, a ligand of integrin α_v, and this response was blocked by the integrin α_v inhibitor. Functionally, SPARC modulated the migratory response of fibroblasts towards ECM proteins suggesting that the local deposition of SPARC following MI contributes to scar formation.

Taken together, our combined in vivo and in vitro data demonstrate that several integrin subunits play critical roles during tissue remodeling in the injured heart. Integrin-dependent gene expression events such as the upregulation of SPARC following MI are critical to orchestrate the healing response. These processes appear to involve complex cross-talk between different cell types such as cardiomyocytes and fibroblasts to allow for locally confined scar formation. The elucidation of the sophisticated interplay between integrins, matricellular proteins such as SPARC, and growth factors will undoubtedly provide us with a better and clinically useful understanding of the molecular mechanisms governing heart remodeling.

Zusammenfassung

Der enorme Umbau des Herzgewebes, wie man ihn nach Drucküberlastung des Ventrikels oder MyokardInfarkt beobachten kann, gilt als eine der kausalen Ursachen des Herzversagens. Die Veränderungen in der Architektur des Herzens beeinflussen die mechanischen Eigenschaften des Herzmuskels, begründet sind sie jedoch in Anpassungsprozessen auf der zellulären Ebene vor allem in einer Modulation der Expression bestimmter Gene. Gemeinsam mit Integrinen, den Transmembran-Rezeptoren, welche die extrazelluläre Umgebung mit dem intrazellulären Zytoskelett verbinden, gehören Proteine der extrazellulären Matrix (ECM) und matrizelluläre Proteine zu den Schlüsselkomponenten, die den Umbauprozess im Herzen steuern. Aus diesen Gründen hatte diese Doktorarbeit zum Ziel, die Rolle der Integrine für die Regulation der Genexpression und die Leistungsfähigkeit des Herzmuskels während der durch Drucküberlastung oder myokardialen Infarkt (MI) hervorgerufenen Wundheilungsprozesse zu analysieren.

Um die Beteiligung von Integrin β1 zu untersuchen, wurde ein experimentelles Modell der Drucküberlastung im Mausherzen (*aortic banding*; Konstriktion der Aorta; AB) eingesetzt, wobei Mäuse mit einer konditionalen, Herz-spezifischen Deletion des Integrin β1 Gens untersucht wurden. Ein besonderes Augenmerk wurde dabei auf die physiologischen Unterschiede und eine veränderte Genexpression im gestressten Herzen in An- oder Abwesenheit von Integrin β1 gelegt. Interessanterweise wurden die Mäuse, welche eine Kombination aus Integrin knock-out Allel und dem Kardiomyozyten-spezifischen konditionalen knock-out Allel von Integrin β1 aufwiesen im normalen Mendelschen Verhältnis geboren und wuchsen normal auf. Obwohl diese Tiere immer noch geringe Mengen von Integrin β1 in ihrem Herzen aufwiesen (exprimiert von nicht-Myozyten), besaßen diese Mäuse eine veränderte Herzfunktion und waren sehr sensitiv gegenüber AB. Im Gegensatz zu der kompensatorischen hypertrophischen Reaktion, die in Wildtyp Mäusen zu beobachten war, zeigte sich in den Integrin β1–defizienten Mausherzen kein Gewebeumbau. Auch die erhöhte Expression von verschiedenen ECM Proteinen, insbesondere die verstärkte Expression des matrizellulären Proteins SPARC, unterblieb nach AB in den Integrin β1–defizienten Tieren.

Interessanterweise konnte auch eine transiente Erhöhung der SPARC mRNA während der Umbauprozesse im Herzen in Folge von myokardialem Infarkt (MI) mittels cDNA Makroarrays festgestellt werden. In der Tat fanden sich größere

Mengen von SPARC bereits 2 Tage (~2,5-fach erhöht), 7 Tage (~4-fach erhöht) und 1 Monat (~2-fach erhöht) nach MI, während ein spezifischer Inhibitor der Integrin α_v Untereinheit diese Hochregulation von SPARC in vivo verhinderte. Immunfluoreszenz Untersuchungen von Herzgewebe verdeutlichten, dass sich die erhöhte Expression von SPARC auf das Infarktareal beschränkte, dass die Expression von SPARC nach einer anfänglichen Erhöhung im Verlauf von 1 Monaten wieder auf das Anfangsniveau zurückging und dass die verstärkte Expression von der Einwanderung von Fibroblasten in das ischämische Herzgewebe begleitet war.

In vitro stimulierten die Wachstumsfaktoren TGF-β1 und PDGF-BB die Expression von SPARC durch Fibroblasten. Wie sich an Hand von ELISA und Western Blot Untersuchungen feststellen ließ, war die Inhibition von Integrin α_v nicht in der Lage, die durch TGF-β1 oder PDGF induzierte Sekretion von SPARC zu beeinflussen. Jedoch zeigte sich, dass Vitronektin, ein Ligand von Integrin α_v, sowohl die Sekretion von TGF-β1 als auch von PDGF-BB durch Kardiomyozyten induzierte und diese Reaktion wurde durch den Integrin α_v Inhibitor komplett unterdrückt. In funktioneller Hinsicht wirkte SPARC auf die durch ECM Proteine induzierte Migration von Fibroblasten ein, so dass man davon ausgehen kann, dass die lokale Freisetzung von SPARC nach myokardialem Infarkt zur Wundheilung im Herzen beiträgt.

Zusammenfassend läßt die Kombination der in vivo und in vitro erhobenen experimentellen Daten den Schluss zu, dass mehrere Integrin Untereinheiten eine entscheidende Rolle während der Gewebeumbildung im Herzen spielen. Integrin-abhängige Genexpressionsereignisse wie beispielsweise die erhöhte Expression von SPARC nach MI sind entscheidend an der Koordination der Wundheilung beteiligt. Diese Prozesse scheinen auf einer komplexen Wechselwirkung und Kommunikation zwischen verschiedenen Zelltypen wie Kardiomyozyten und Fibroblasten zu beruhen, um lokal begrenzt eine Heilung und Vernarbung des verletzten Gewebes zu regulieren. Die Aufklärung des fein abgestimmten Wechselspiels zwischen Integrinen matrizellulären Proteinen wie SPARC und Wachstumsfaktoren wird sicherlich zu einem besseren und klinisch nutzbarem Verständnis der molekularen Mechanismen des Gewebeumbaus im Herzen beitragen.

Chapter 1

General introduction

1. GENERAL INTRODUCTION

When the heart has to work too hard to maintain adequate blood output, it can begin to change shape, with the left ventricle often growing larger, less flexible and weaker. Prolonged compensation for these impairments can change both the heart structure and its function. This combination is known as remodeling of the heart

1.1. Myocardial infarction and cardiac hypertrophy

Cardiovascular diseases, in particular hypertrophic and ischemic heart disease, are leading cause of death in industrialized countries. Remodeling of the myocardium is the major mechanism underlying disability and death in recent cardiovascular diseases (Ertl, Gaudron et al. 1993)

1.1.1.   Acute events upon acute myocardial infarction

When a coronary artery becomes totally blocked, the inadequate arterial oxygen supply to the myocardium produces an acute myocardial infarction (MI). As a result of acute ischemia after MI, excitation–contraction uncoupling occurs determining cardiac systolic and diastolic dysfunction. Myocardial ischemia has been viewed for many decades as an all-or-none process that causes myocardial necrosis when prolonged and severe, but the effects are transient when it is brief, mild or prompt reperfusion occurs (Braunwald and Kloner 1982; Cohn 1993). Persistence of ischemia leads to irreversible cell death. Ischemic necrosis is diagnostic pathognonomic of acute myocardial infarction. Apoptosis may represent an important pathophysiological mechanism causing progressive cardiomyocyte loss and left ventricular dilation after acute myocadial infarction. (Abbate, Biondi-Zoccai et al. 2002) Adaptative processes after myocardial ischemia play an important role in the progression of left ventricular remodeling. Either occlusion of a coronary artery or chronic severe coronary artery stenosis leads to myocardial cell loss with consecutive necrosis and scar formation. Following myocardial ischemia reactive neovascularization (angiogenesis) occurs in the myocardial regions bordering and remote from the scar. Ischemic necrosis is diagnostic pathognonomic of acute myocardial infarction

Apoptosis may represent an important pathophysiological mechanism causing progressive cardiomyocyte loss and left ventricular dilation after acute myocardial infarction (AMI).(Abbate, Biondi-Zoccai et al. 2002). Apoptosis represents the major form of death, being several times more common than necrosis. Myocardial apoptosis peaks at 4-12 h in AMI and is persistently demonstrable up to 10 days (Cohn 1993; Cheng, Kajstura et al. 1996) (Olivetti, Abbi et al. 1997). Necrosis of cardiomyocyte is usually completed within 24-48 h following coronary occlusion, phagocytosis and removal of cellular debris by inflammatory cells starts at 24 h (Lodge-Patch 1951; Fishbein, Maclean et al. 1978). A reduction in myocardial apoptosis have already been shown to contribute to improve the prognosis and symptoms in patients with post-infarction heart failure.(Holtz 1998). Characteristically, features of acute inflammation are observed within the first 24-72 h and are associated with further reduced cardiac performance, while macrophages infiltrate the infarcted myocardium days later. Myocardial infarction involves scar-formation mechanisms in which inflammation, proliferation, cell differentiation, apoptosis and angiogenesis all play a role. After an inflammatory phase in which polymorphon nuclear neutrophils colonized the scar, granulation tissue set in with a proliferation of myofibroblasts and growth of new blood vessels. These cells disappeare from the scar gradually, leaving behind a matrix rich in collagen and devoid of any contractile properties.

1.1.2. Left ventricular remodeling and hypertrophy in myocardial infarction

Two myocardial processes are initiated by acute myocardial infarction: hypertrophy of the residual myocardium and a change in left ventricular chamber dimension. In response to a transmural myocardial infarction (MI), the left ventricle (LV) undergoes significant remodeling (Pfeffer and Braunwald 1990). The sequence of these events appears to be critically dependent on the size of the infarct and its distensibility, on the load placed on the myocardium, on the metabolic state of adjacent and remote myocardium, and on the degree of activation of tissue hormone systems. Hypertrophy may occur transversely (concentric) or longitudinally (eccentric). Myocardial injury following MI induce LV remodeling events that continue for months and even years. The chamber may enlarge because of cell lengthening or slippage or because of infarct expansion. In vivo, left ventricular remodeling after myocardial

infarction involves hypertrophy generally attributed to increased cardiac workload. Transient hypoxia may contribute to cardiac hypertrophy in ischemic heart disease independent of cardiac workload. Furthermore, increase for the surviving myocardium may activate signalling cascades that induce cardiac hypertrophy, functional deterioration and failure. Hypertrophy is an adaptive response to compensate for impaired cardiac function. (El Jamali, Freund et al. 2004). Remodeling is a repair process. It can follow myocardial infarction, mechanical overload (for example, in hypertension or valvular heart disease), and also occurs in inflammation and dilated cardiomyopathy. Remodeling can be an (early) adaptive process followed by a maladaptive (late) phase and involves all cells that are present in the myocardium - the myocyte, the interstitial cells, the vascular endothelium, and the immune cells. Despite the varying etiology that these different aspects of heart disease share, a similar sequence of molecular, biochemical and mechanical events that can lead to heart failure, myocyte hypertrophy, extensive extracellular matrix production and fibrosis. The rearrangement of the components of the ventricular wall and subsequent development of chronic heart failure after ischemic myocardial injury plays an important role in the development of cardiac failure after myocardial infarction. Although left ventricular remodeling appears to represent an adaptive process serving to preserve stroke volume (and cardiac output) following myocardial injury, the enlargement process may have undesirable long-term effects on global left ventricular function and on clinical prognosis. Recent observations suggested that this long process has a deleterious effect on LV function and prognosis. (Abbate, Biondi-Zoccai et al. 2002). Fortunately, recent experimental and clinical evidence demonstrates that ventricular remodeling and its deleterious consequences may be preventable.

1.1.3. Alterations in cardiac gene expression after myocardial infarction and hypertrophy

Recent technological advances in the production of cDNA microarrays have made it possible to profile gene expression of tens of thousands of genes simultaneously (Brown and Botstein 1999). More than 200 genes were identified that showed differential expression in response to myocardial infarction. (Stanton, Garrard et al. 2000). It is clear that substantial alterations in gene expression are needed to afford such profound changes within cells of the remodeling myocardium. Alterations in

expression of several genes have been described in the experimental model of MI in rat. Changes in actin and myosin gene expression are associated with alterations in cytoskeleton and contractile apparatus in surviving cardiomyocytes (Meggs, Tillotson et al. 1990). Fibrosis of LV myocardium is, in part, the result of elevated collagen and fibronectin expression. (Murakami, Kusachi et al. 1998). Atrial natriuretic peptide mRNA and protein levels in the cardiomyocyte are increased in response to MI as a compensatory response to improve hemodynamics (Mendez, Pfeffer et al. 1987). In addition, certain cytokine genes, transforming growth factor beta 1 (TGF-beta(1)) interleukins 1ß and 6, and tumor necrosis factor-α are transcriptionally regulated in the remodeling MI rat heart. (Dai, Dheen et al. 2002).

Cardiac hypertrophy is accompanied by distinct qualitative and quantitative changes in gene expression. Specific changes have been observed in cardiomyocytes during the development of cardiac hypertrophy (Cooper 1987; Ruwhof and van der Laarse 2000) e.g. quantitative and qualitative changes in gene expression, rapid induction of proto-oncogenes (such as c-fos. C-jun, and c-myc) and heat shock protein genes (such as hsp 70). which are the first response hemodynamic overload (Izumo, Nadal-Ginard et al. 1988). As a later event, the expression of several genes that encode sarcomeric proteins is switched to expression of fetal isoforms, for example transition from cardiac α-actin to skeletal α actin. Hypertrophy is characterized by an increase in cell size in the absence of cell division, actin, and from the α-form of myosin heavy chain (MHC) to the β-MHC form in rodents (Schwartz, de la Bastie et al. 1986). In addition, several changes in isogene expression of proteins involved in energy metabolism have been described (Revis, Thomson et al. 1977; Meerson and Javich 1982). Furthermore, the expression of atrial natriuretic peptide (ANP) that is restricted to the atria shortly after birth, is reappearing in the ventricles upon hemodynamic overload (Mercadier, Samuel et al. 1989). Besides the qualitative changes in gene expression described above, there are also quantitative changes in constitutive expression of genes, i.e. stimulation of gene expression which contributes to hypertrophy, and down-regulation of genes. Several genes that encode membrane proteins are down-regulated in hypertrophied hearts, for example, the sarcoplasmic reticulum Ca^{2+}-ATPase (SERCA) gene(Anger, Lompre et al. 1998). The rate of protein synthesis is probably increased by a different mechanism although its involvement in the development of cardiac hypertrophy has to be proven.

1.2. Mechanisms and signal transduction pathways of cardiac hypertrophy

Pressure overload of the heart leads to an increase in wall stress. This frequently results in cardiac hypertrophy, which is induced by the mechanical stress on the cardiomyocytes and the activation of neuroendocrine mechanisms, particularly the renin-angiotensin-aldosterone system and the sympathetic nervous system. Myocardial hypertrophy represents an independent risk factor for cardiovascular events such as ischemic heart disease, arrhythmias, and sudden death and is a powerful predictor for the development of heart failure. (Levy, Garrison et al. 1990). Development of cardiac hypertrophy is initially beneficial since it augments the number of contractile units and reduces ventricular wall stress to normal levels according to the law of Laplace. However, the adaptation has its limits and heart failure may ensue. Furthermore, arrhythmias and ischemic heart disease may develop, which increase the risk of sudden death.

1.2.1. Stimuli inducing cardiac hypertrophy

1.2.1.1. Mechanical stress

Mechanical stress is considered to be the trigger inducing a growth response in the overloaded myocardium. Cardiac hypertrophy can be induced by hemodynamic overload even after adrenoreceptor blockade (humoral) or sympathectomy (neural)(Cooper, Kent et al. 1985). This suggested that mechanical stress itself is the primary factor for cardiac hypertrophy in response to hemodynamic overload. The view was supported by several ex vivo and vitro studies. Kiral et al demonstrated that in isolated hearts, an increased cardiac load stimulated protein synthesis (Kira, Kochel et al. 1984). Further more, alterations in gene expression in stretching cultured cardiomyocytes were observed without involvement of neural or humoral factors (Komuro, Kaida et al. 1990; Sadoshima, Jahn et al. 1992; Kira, Nakaoka et al. 1994; Vandenburgh, Solerssi et al. 1995). Moreover, the alternations in vitro experiments using stretched cardiomyocytes have been demonstrated to be similar to those in vivo hearts in response to hemodynamic overload, i.e. re-expression of fetal genes and increased protein synthesis do also occur in isolated cells in vitro. These findings demonstrated that mechanical stress is possibly the main contributor to the hypertrophy.

1.2.1.2. Growth factors and hormones

Besides mechanical loading, a range of substances, such as growth factors, cytokines, catecholamines, vasoactive peptides and hormones are involved in mediating cardiac myocyte hypertrophy(Hefti, Harder et al. 1997).(Sacca, Napoli et al. 2003) The expression and /or release of these factors have been reported in hearts that hypertrophied due to hemodynamic overload, and in cardiomyocytes that are hypertrophied due to stretch. The classic peptide growth factors can be divided into five families: epidermal growth factor (EGFs,) Fibroblast growth factor (FGFs), Insulin-like growth fachor (IGF), platelet derived growth factor (PDGFs) and transforming growth factor (TGFs). TGFβ and PDGF have been shown to cause cardiomyocyte hypertrophy in vitro systems. In the heart, PDGF is produced by non-myocytes. FGF and TGFβ can be produced by cardiac myocytes and non-myocytes(Brand and Schneider 1995; Seger and Krebs 1995), therefore, these two factors may act in a paracrine or autocrine manner in the heart. Smad proteins have been identified as the first family of putative TGF-β signal transducers (Kretzschmar, Liu et al. 1997) Upon phosphorylation by actived receptors, Smad associate with DNA binding proteins and activate gene transcription. Thus, cardiac myocytes and other cell types, such as cardiac fibroblasts, endothelial cells and vascular smooth muscle cells, may secrete growth promoting factors after a mechanical stress stimulus, which induce hypertrophy of cardiomyocytes in an autocrine/paracrine way.

1.2.2. SIGNAL TRANSDUCTION OF THE STRETCH STIMULUS

The signal transduction pathways that may be involved in mechanical stress-induced hypertrophy belong to two groups: (1) the mitogen-activated protein kinases (MAPK) pathway; and (2) the janus kinase/signal transducers and activators of transcription (JAK/STAT) pathway. The MAPK pathway can be subdivided into the extracellular-regulated kinase (ERK), the c-Jun N-terminal kinase (JNK), and the 38-kDa MAPK (p38 MAPK) pathway. Nowadays,it is known that there are several interactions between these pathways. In fact, mechanical stress appears to activate both pathways.
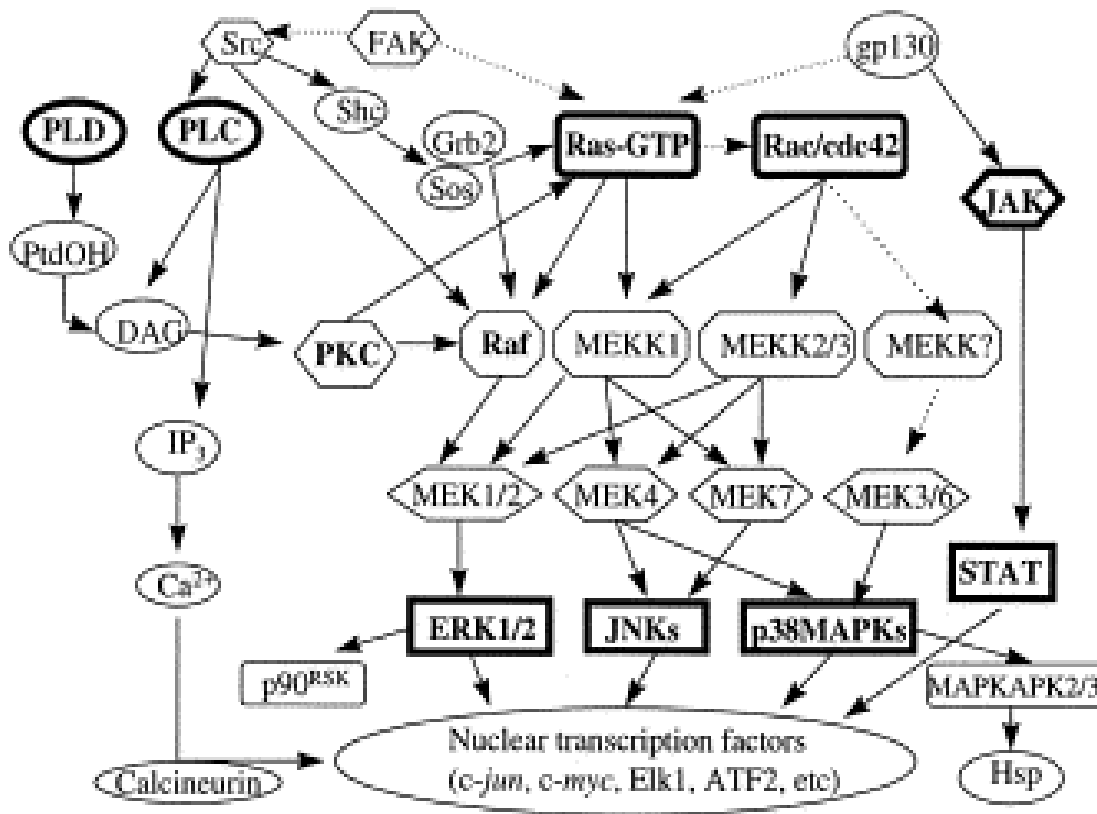
Figure 1.1 Schematic diagram of the signal transduction cascades that are involved in stress-induced cardiac hypertrophy. More informations are described in the text.

1.2.2.1 The mitogen-activated protein kinase (MAPK) pathway

1) The extracellular-regulated kinase (ERK) pathway.

The best characterized are: the 44-kDa MAPK (ERK1), the 42-kDa MAPK (ERK2), and the 63-kDa MAPK (ERK3). In the heart, ERK1 is the most highly expressed ERK. The expression of ERK3 is hardly detectable in adult heart. Substrates for ERKs are transcription factors, such as c-*jun*, and p62^{TCF} (Elk-1), and the 90-kDa S6 kinase (p90^{RSK})(Boulton, Nye et al. 1991). Mechanical stress has been reported to stimulate this pathway by activation of Ras, ERK1 and ERK2, and p90^{RSK} (Sadoshima and Izumo 1993).The precise mechanism of the stimulation of this pathway is still unknown. Moreover, stretch of cardiomyocytes caused activation of ERKs and resulted in increased expression of c-*fos* and skeletal α-actin, indicating that ERKs and mechanical stress-induced hypertrophy may be linked (Sadoshima

and Izumo 1993) Taken together, these results indicate that the ERKs may partly participate in the mechanisms of mechanical stress-induced hypertrophy.

2) The c Jun N-terminal protein kinase (JNK) pathway

The JNK pathway may be involved in mechanical stress-induced hypertrophy via phosphorylation of the transcription factors c-Jun, and ATF2 (Clerk and Sugden 1997). This activation of JNKs was independent of secreted Ang II, extracellular Ca^{2+}, and PKC. Others have found that cardiomyocytes submitted to cyclic stretch had a maximal activation of JNKs at about 5 min. Using MEKK1-transfected cardiomyocytes, Thorburn et al. (Thorburn, Xu et al. 1997). showed that overexpression of MEKK1 induced ANP expression (a marker of hypertrophy). Furthermore, these authors found that the small G protein Rho was also required for MEKK1-induced ANP expression (Thorburn, Xu et al. 1997). Controversially, Nemoto et al. found that activation of JNKs inhibited MEKK 1-induced ANP expression via a feedback loop of *c-jun*. They reported that ANP expression is activated by p38 MAPKs. Taken together, it seems that the induction of ANP expression is biphasic, first a short-living response upon JNK activation followed by a prolonged response upon p38 MAPK activation.

3) The p38 MAPK pathway

The function of the p38 pathway in myocardial hypertrophy has recently been studied. It has been observed that p38 and p38β activity were increased in a mouse model of pressure overloading and that the p38 and p38 β activity were well correlated with phenotypic ventricular hypertrophy (Wang, Harkins et al. 1997) In these experiments, introducing constitutively active MKK6 or MKK3 into cardiac myocytes elicited characteristic hypertrophic responses, including an increase in cell size, enhanced sarcomeric organization, and elevated atrial natriuretic factor expression. The two isoforms of p38 group kinase, p38 and p38β, appear to have different effects on cardiomyocyte hypertrophy: p38β seems to be more potent in inducing hypertrophy, whereas p38 appears to be more important in other function such as apoptosis. Interestingly, the hypertrophic response induced by p38 MAPKβ

included several markers of hypertrophy, i.e. an increase in cell surface area, enhanced organization of sarcomeric proteins, and induction of ANP expression (Wang, Huang et al. 1998).

1.2.2.2. The janus kinase/signal transducers and activators of transcription

The Janus kinase-signal transducer and activator of transcription (JAK-STAT) pathway

Janus –associated kinases are named after their dual functions in signal trsduction in the cytoplasm and activation of transcription in the nucleus. Binding of ligands to their cytokine rceptors, such as dardiotriphin-1 (CT-1), leads to phosphorylation and activation of the receptor-JAK complex with subsequent recruitment of STATs and activation of STATs by phosphorylation. The JAK/ STAT pathway was found to be activated in rat hearts with pressure overload-induced hypertrophy (Pan, Fukuda et al. 1997). The JAK/ STAT pathway was found to be activated in rat hearts with pressure overload-induced hypertrophy of Mechanical stretch induced rapid phosphorylation of JAK1, JAK2, Tyk2, STAT1, STAT3, and glycoprotein 130 was observed as early as 2 minutes and peaked at 5 to 15 minutes. (Tian, Cui et al. 2004). Moreover, studies clamed that the mechanical stress-induced activation may occur via gp130.

1.3.   Extracellular matrix and cardiac remodelling.

Significant remodeling of the extracellular matrix (ECM) occurs in cardiac hypertrophy and in the acute (healing) and chronic (remodelling) stage after myocardial infarction Today we know that the extracellular matrix (ECM) is important because it not only support cardiac structure but also because the ECM is essential in cardiac function and responses to pathophysiological signals. Its modifications are associated with cardiac hypertrophy and heart failure, and the molecular basis bringing a better insight into the dynamics of the ECM. The ECM is a key component in the remodeling process, and increases in collagen occur in the infarct area to replace necrotic myocytes and to form a scar. There was marked up-regulation of mRNAs for extracellular matrix (ECM) proteins and their cross-linking enzyme, such as collagens type I, III and VI, and lysyl oxidase in the injured heart. Over the last several years, it has become increasingly evident that disruption of extracellular matrix (ECM) homeostasis is a deciding factor for the progression of myocardial failure.

1.3.1 Extracellular matrix in myocardium

Although the myocytes subserve the heart's pump function, the predominant cell type by numbers in the heart is the fibroblast (not the myocyte). About two thirds of myocardial cells are fibroblasts. Cardiac fibroblasts (CF) grow in a complex tissue environment and are responsible for the production and deposition of the majority of ECM proteins in the cardiac interstitium. Several matrix proteins are expressed in the normal myocardium, including Collagens, laminin, fibronectin, and chondroitin sulphate. Collagen is the most abundant protein in the body, and collagen 1 represents about 90% of total collagen. Collagen I, collagen III, and collagen IV are the predominant collagens in the myocardium. As a whole, the ECM provides an environment for cells to migrate, grow, and differentiate, establishing a connection between cell and tissue function. The ECM is coupled to the cell through cell surface receptors, the most important ones are the integrins.

Myocardial environment
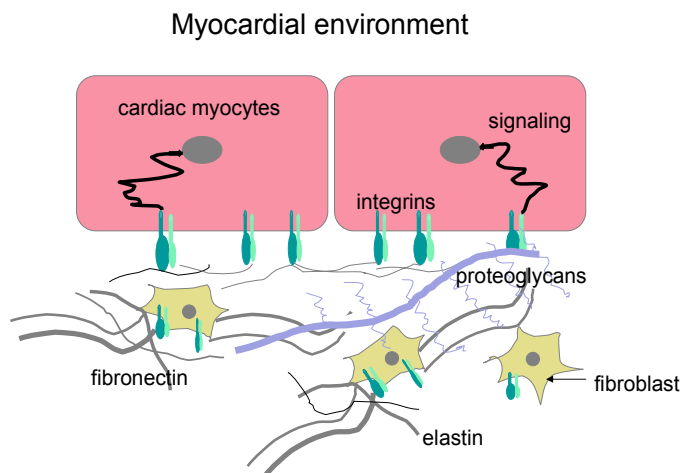
Figure 1.2 myocardial environment. Cardiac fibroblast grow in a complex tissue environment and responsible for the production and deposition of the ECM proteins, i.e. fibronectin. ECM provides an environment for cells, establishing a connection between cell and tissue function.ECM is coupled to the cell through cell surfane receptors primary of which are the integrins.

1.3.2. Collagen in the heart

Collagens, the chief components of extracellular matrix, are a tightly regulated family of proteins that determine the structural and functional integrity of heart. Collagen type I and type III comprise approximately 85% and 11% respectively of the cardiac interstitium (Weber 1989) The fibrillar collagens of the heart surround and interconnect myocytes and muscle fibers to provide for muscle fiber and myocyte alignment which imparts mechanical support to the myocardium and governs tissue stiffness. Excessive collagen deposition or pathological fibrosis is an important contributor to left ventricular (LV) dysfunction and poor outcome in hypertension, MI and heart failure. It is also an important problem in the aging heart. Antifibrotic agents that target steps in the collagen synthesis and degradation pathways therefore represent promising strategies for these diseases. Because reparative fibrosis is an essential component of healing of the infarct zone (IZ) after MI, loss of collagen fibrils and struts lead to myocyte slippage, ventricular dilation, and progressive contractile dysfunction. (D'Armiento 2002). Failed human hearts examined either at autopsy or explantation invariably exhibit alterations of the ECM primarily due to changes in collagen. Synthesis of collagens is regulated at the cellular level while deposition of proteins depend on a balance between matrix metalloproteinases (MMPs) and tissue inhibitors of matrix metalloproteinase (TIMPs).The ability of the heart to respond to mechanical and chemical stimuli by modulating the delicate balance between

synthesis and degradation of structural components of ECM has a significant impact on cardiac function.

1.3.3. Matrix Metalloproteinases (MMP) and myocardial matrix remodelling

Matrix metalloproteinases (MMPs) are a family of zinc-dependent enzymes comprised of more than 25 individual members divided into specific classes based on in vitro substrate specificity for various ECM components. MMP family is involved in a wide variety biologic processes including normal embryonic development and wound heading, as well as pathologic processes such as tumor invasion, arthritis, emphysema (Matrisian 1990). Lemaitre et al demonstrated that MMP does not always translate into tissue destruction and emphasizes the fact that MMPs are critical in the remodelling of tissues in response to injury. matrix metalloproteinases (MMPs) play an important role in atherosclerosis by degrading the extracellular matrix, which results in cardiovascular remodeling. Collagen degradation is an important step in remodelling of the collagen matrix. Collagens are degraded extracellularly by members of the of MMP family

MMPs are present in the heart and determine the interstitial architecture. Importantly, the activation of MMPs and their endogenous inhibitors (TIMPs) are associated with ventricular remodelling. Pro-fibrotic factors such as norepinephrine, angiotensin II and endothelin-1 stimulate fibrosis by modulating collagen synthesis and MMP/TIMP activity. Congestive heart failure and changes in MMP levels have been described in variety of animal models of heart failure.(Pauschinger, Chandrasekharan et al. 2004). During myocardial infarction, loss of collagen begins within minutes of the onset of ischemia, and within the first hour a marked deterioration in the structure and an actual decrease in the quantity of collagen has already occurred. This rapid initial loss of collagen is associated with enhanced activity of MMPs (Matrisian 1990). The initial degradation of collagen is followed by a rapid and progressive increase in gene expression. The generation of a transgenic mouse with constitutive expression of MMP-1 in the heart has suggested that this is an animal model of hypertrophy at 6 months of age,(Kim, Dalal et al. 2000). This transgenic model provides direct evidence that disruption of the equilibrium of ECM synthesis and degradation can play a critical role in the process of cardiac remodelling and the pathophysiology of heart failure

1.4 The extracellular connections: the role of integrins in myocardial remodeling.

Integrins are a large family of heterodimeric cell surface receptors that link the extracelluar matrix and intracellular cytoskeleton and are multifunctional, playing roles in cell organization and differentiation, migration, alteration of gene expression, and cell survival. The function as mechanotransducers has been considered the most interestingly from the cardiovascular viewpoint.

1.4.1. Integrin structure and basic signal machinery

Integrins were so named because they are both integral membrane proteins and also involved in cellular and ECM integrity. Integrins are the transmembrane receptor composed of noncovalently associated α and β subunits, with alpha subunits ranging in size from 120 to 180 kDa whereas β subunits are 90 to 110 kDa.(Ross 2002). The ingegrin family comprises more than 18α and 24 β subunits in mammals. More than 24 paired of integrins have been identified. The subunits of α and β integrin are signal transmembrane spanning proteins with the bulk of the molecule in the extracellular domain and generally short cytoplasmic domains. After ligand binding the integrin conformation is altered and subsequently the heterodimer can participate in events critical for organization of the cytoskeleton and other intercellular signalling events that might be important for cell survival or initiation of cardiac myocyte hypertrophic events. A major role of integrins in the heart is their ability to serve as a mechano-transduction device during normal development and in response to physiological and pathophysiologic signals. Integrins can signal through the membrane in either direction: The extracellular activity of integrins is regulated from the inside of the cell (inside-out signalling), while integrin banding to the ECM elicits signals that are transmitted into the cell (out side-in signalling). Integrins bind to specific ECM proteins via their large extracellular domains and the short cytoplasmic domains of integrins serve as docking sites for signalling molecules, including nonreceptor tyrosine kinases (such as FAK), adapter proteins (such as Grb-2 and p130Cas) and structural proteins (such as paxillin or talin). In addition, integrin associated molecules can connect integrins with cytoplasmic signalling enzymes as well as transmembrane growth factor receptors. Upon binding to the ECM, integrin cluster in the plane of the cell membrane and initiate an intracellular protein complex that

promotes the assembly of actin filaments. The reorganization of actin filaments into larger stress fibers, in turn, introduces more integrin clustering, hence enhancing the matrix binding and organization by integrins in a positive feedback system. Well developed aggregates have been detected by immunofluorescence microscopy and are known as focal adhesions and ECM contacts. (Giancotti and Ruoslahti 1999)

1.4.2. Integrin expression in basal and pathologic myocardium

The relative number of specific α and β integrin subunit expressed in the myocardium is small. In particular, α1, α2, α5, α7, α10 and α11 are detected in cardiomyocytes .(Ross 2002). These alpha integrin subunits appear to be only associated with splice-variants of β1 integrin, including the splice variant β1D, which is dominantly expressed in striated muscle and is the prime β1 integrin isoform expressed in postnatal heart. . Adult rat cardiac failure (CF) express a wide range of integrins including α1β1(most predominant) α2β1, α5β1, αvβ3, αvβ1 and α4β1, αvβ5, αvβ6(MacKenna, Dolfi et al. 1998) In the adult heart, integrins are the principal receptors for ECM, thus their appropriate expression and function is necessary for the normal cardiovascular function. (Keller, Shai et al. 2001). Disruption of integrin function in the murine myocardium leads to perinatal lethality, fibrosis, and abnormal cardiac performance.(Keller, Shai et al. 2001). In vitro studies have shown that disruption of α1β1 function by antibodies or adenovirus mediated inhibition resulted in altered phenotype of cultured myocytes and altered patterning of their myofibrils (Simpson, Terracio et al. 1994).

Integrins belong to the important factors, which are responsible for the process or cardiac hypertrophy. Studies in vitro have directly linked β1 integrin (both isoforms A and D) to the hypertrophic response of neonatal ventricular myocytes. The hypertrophy response caused by α1 adrenergic agents was induced by the overexpression of these integrins.(Pham, Harpf et al. 2000). Over expression of β1 integrin in the cardiomyocyte was found to increase protein synthesis and ANP expression without affection DNA synthesis. In contrast, inhibition of β1 function and signalling reduced the adrenergically mediated hypertrophy.(Ross, Pham et al. 1998; Pham, Harpf et al. 2000). Studies of integrins function in vivo have begun to be assessed in the myocardium of both rats and mice provoked to undergo morphologic hypertrophy or myocardial infarction have demonstrated the important of integrins. In

these rodent models, increased expression of β1A and β1D, α3, α7B were detected. α1and α5 integrin subunits behave like many embryonic genes in the ventricle. They are expressed in the embryonic heart, become down-regulated postnatally, and can be re-induced after mechanical loading of the heart through aortic constriction. Pressure overload of the right ventricle in a cat model has demonstrated the mobilization of β3 integrin to the cytoskeletal fraction of lysed myocardial tissue 4 hours after banding. Integrin β3 is present in both the cytosleletal and membrane bound fractions by 48 hours after pressure overload. However, the levels returned to baseline by one week. (Kuppuswamy, Kerr et al. 1997).

1.4.3. integrin signalling in the myocardium
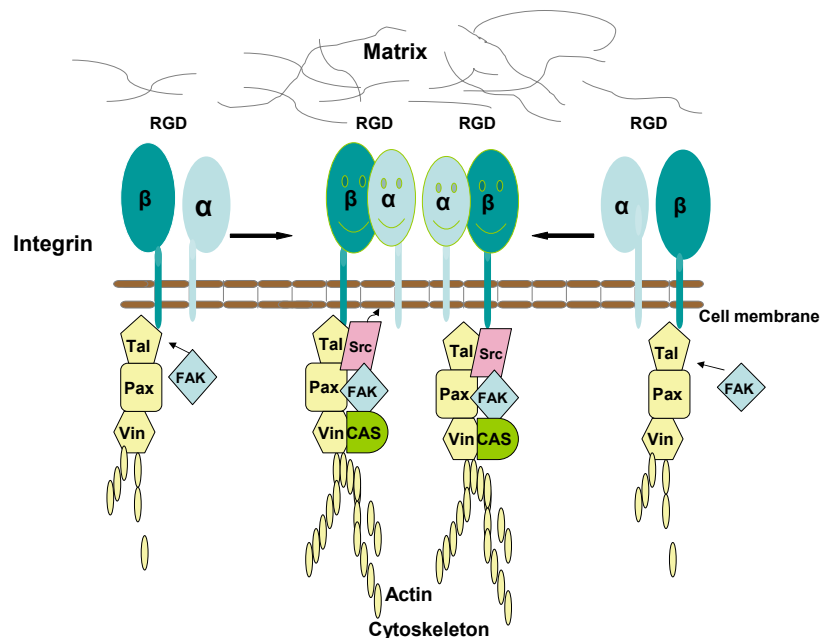
Figure.1.3 Integrin signal in myocardium. Integrin are a large family of heterodimeric cell surface transmembrane receptors composed of noncovalently associated α and β subunits. Integrins link to ECM most through RGD motif binding site. The site's conformation appears to determine which integrin a RGD tripeptide will bind. They clustered in the plane of the cell membrane and connected with a cytoskeleton and signalling complex that promotes the assembly of actin filaments. The reorganization of actin filaments into larger stress fibers, in turn introduce more integrin clustering, hence enhancing the matrix binding and organization by integrins in a positive feedback system.

The role of integrin signalling in myocardium is still incompletely understood. Integrins may be implicated in cardiac hypertrophy as mechanosensors that sense increased

work load of the heart muscle. In an integrin (β1)-dependent and matrix-specific way, integrins have been shown as mechanotransducers in cardiac cells. The integrin-dependent pathways involving FAK and Src-family kinases have been studied in some detail. There are two views on the mechanism of integrin mediated signalling, which may be complementary.

Some studies support the first view that integrins transmit signals by organizing the cytoskeleton (action filaments) through intermediary molecules including α-actinin, talin, vinculin, paxillin, and tensin, thereby stabilizing cell adhesion and regulation cell shape, morphology, and motility. (Ingber 1991; Zhang, Weinheimer et al. 2003). A large body of evidence suggests that mechanical stress is first received by integrins, and that next interlinked actin microfilaments transduce mechanical stress in concert with microtubules and intermediate filaments. Moreover, Bloom (Bloom, Lockard et al. 1996) suggested that this mechanism even could modulate gene expression. They showed that intermediate filaments transmit mechanical stress to the chromatin and hypothesized that alterations in the chromatin induce modulation of gene expression(Bloom, Lockard et al. 1996)

The second view is that integrins are regarded as true receptors capable of inducing biochemical signals within the cell that regulate gene expression and cellular growth, which based on the discovered co-localization of signaling molecules in focal adhesion complexes (FACs). Upon clustering of integrins at focal adhesion sites they recruit the non-receptor kinases FAK and Src seems to e an early event. This recruitment is followed by the association and activation of additional cytoskeletal proteins as well as signal-transducing molecules (such as Grb2, Sos, Ras, Raf, PLCγ, ERKs, and SAPKs) in the forming FACs (Miyamoto, Teramoto et al. 1995) In these FACs signaling proteins and their substrates are brought into close proximity, thereby facilitating signal transduction. In fact, integrins may induce activation of FAK with the help of Src (Parsons and Parsons 1997), which may lead to activation of the ERK pathway through Grb2-Sos-Ras or through activation of PLC γ . Integrins can also collaborate with growth factor receptors and their substrates to phosphorylate their receptor kinases and to activate ERKs and JNKs upon ligand binding (Parsons and Parsons 1997)Thus, integrins may integrate a variety of different signaling pathways that are activated by both the ECM and growth factors to establish a well-coordinated response.

1.5 Characterization of SPARC, one of the extracellular proteins

Matricellular proteins form a group of extracellular matrix (ECM) proteins that do not subserve a primary structural role, but rather function as modulators of cell-matrix interactions. Members of the group, including thrombospondin (TSP)-1,TSP-2, SPARC, tenascin (TN)-C, and osteopontin (OPN), have been shown to participate in a number of processes related to tissue repair.(Kyriakides and Bornstein 2003) SPARC (Secreted Protein Acidic and Rich in Cysteine, also known as osteonectin or BM-40), is a 32-kDa multifunctional glycoprotein that belongs to the matricellular group of proteins. It modulates cellular interaction with the extracellular matrix (ECM) by its binding to structural matrix proteins, such as collagen and vitronectin, and by its abrogation of focal adhesions, contributing to a counteradhesive effect on cells. It is expressed spatially and temporally during embryogenesis, tissue remodeling and repair. SPARC functions to regulate cell–matrix interactions and thereby influences many important physiological and pathological processes.

1.5.1. Structure and properties of SPARC

SPARC is a 32 –kD protein, but the secreted form migrates at 43 kD on SDS-PAGE, in part due to the addition of carbohydrate.(Sage, Johnson et al. 1984)The vertebrate SPARC gene encodes proteins of 298–304 amino acids (aa), including three distinct modules, as shown in Fig 1.4. Module I [aa 3–51, previously termed domain I (Lane and Sage 1994) is encoded by exons 3 and 4, is highly acidic, and binds 5–8 Ca^{2+} ions with a K_d of 10^{-3}–10^{-5} M. The structure of this module has not yet been solved. This NH_2-terminal domain contains immunodominant epitope(s) and binds to hydroxyapatite. It is the major immunological epitope of SPARC and is also the region that is the most distinct from other members of the SPARC gene family. Therefore, antibodies against SPARC have not been found to cross react with or recognize SPARC-like protein.(Yan, Sage et al. 1998)

  Module II (aa 52–132) is encoded by exons 5 and 6 and contains 10 Cys and an N-linked complex carbohydrate. The sequence encodes a structure that is homologous to a repeated domain in follistatin, a protein that binds to activin and inhibin, members of the TGF-β superfamily, and agrin, which induces aggregation of nicotinic acetylcholine receptors. Module II also contains bioactive peptides that exert

different effects on endothelial cells. Peptide 2.1 (aa 55–74), part of the EGF-like β hairpin, inhibited the proliferation of endothelial cells (Funk and Sage 1993)and peptide 2.3 (aa 113–130), containing the Cu^{2+} binding sequence GHK and part of the Kazal protease inhibitor-like region, stimulated endothelial cell proliferation and angiogenesis (Funk and Sage 1993)

Module III (aa 133–285, exons 7–9), formerly designated as the EC module also contains a sequence designated peptide 4.2 (aa 254–273), which has been shown to bind to endothelial cells and to inhibit their proliferation(Kupprion, Motamed et al. 1998). The fibril-forming collagen types I, III, and V, and the basement membrane collagen type IV, bind to the EC module of SPARC in a Ca^{2+}-dependent fashion constitutes the extracellular Ca^{2+}-binding (EC) module.
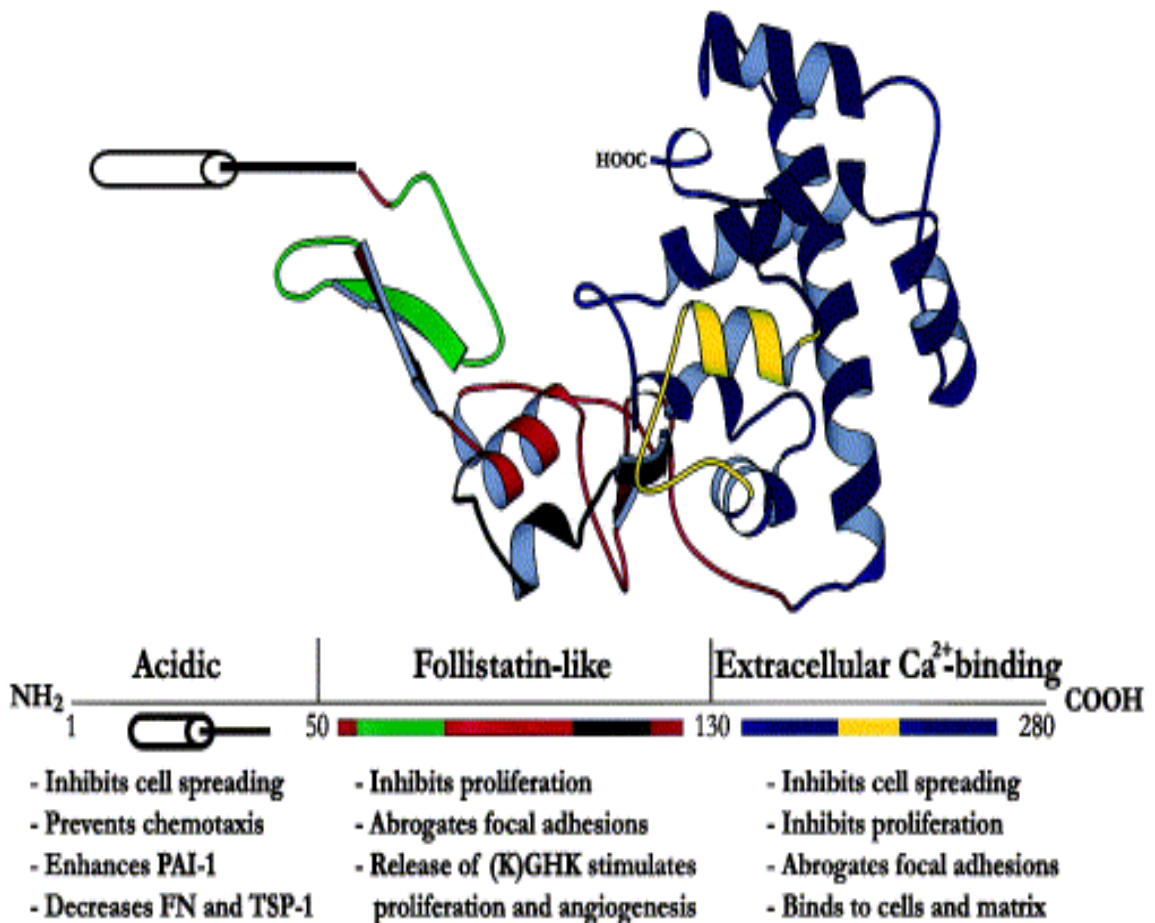
Fig 1.4. Structure of SPARC (from Rolf A. 2000). The ribbon diagram derived from crystallographic data indicates three structural modules. The follistatin-like domain, aa 53–137, is shown in red except for peptide 2.1, aa 55–74, and the (K)GHK angiogenic peptide, aa 114–130, which are shown in green and black, respectively. The EC-module (aa 138–286) is shown in blue except for peptide 4.2, aa 255–274, which is shown in yellow.

1.5.2. Expression of SPARC

SPARC is expressed at high levels in bone tissue and is distributed widely in many other tissues and cell types, and is associated generally with remodeling tissues, e.g., tissues undergoing morphogenesis, mineralization, angiogenesis, and pathological responses to injury and tumor genesis. (Maillard, Malaval et al. 1992): Although SPARC-null mice are born without obvious abnormalities, targeted disruption of the SPARC locus in mice has shown that SPARC is important for lens transparency, as SPARC-null mice develop cataracts shortly after birth. A impaired wound healing in mice deficient in SPARC has been reported.(Basu, Kligman et al. 2001): Additionally, over expression of SPARC in nematodes also resulted in developmental abnormalities that included an uncoordinated (*Unc*) phenotype in the F1 generation. Furthermore, worms overexpressing SPARC did not produce any viable offspring (Schwarzbauer, Musset-Bilal et al. 1994): These results, and the data from SPARC-null mice, indicate that the appropriate and regulated expression of SPARC is necessary for normal development.

The expression of SPARC in the heart during fetal development is high, but after birth it is reduced and almost absent during adulthood.(Sage, Vernon et al. 1989): In recent studies, the up-regulation of SPARC expression has been observed in the injured heart: Up-regulation of SPARC in the myocardium of adult rats has been seen during the remodelling of cardiac extracellular matrix during beta-adrenergic stimulation.(Masson, Arosio et al. 1998): The increase of SPARC expression in the heart was reported in response to myocardial infarction as well (Stanton, Garrard et al. 2000): SPARC mRNA expression paralleled the up-regulation of type 1 collagen mRNA after myocardial infarction implicating a role of SPARC in the process of scar formation. But so for, the protein levels of SPARC in heart have not been studied. The role of SPARC in the remodelling process in the heat is not clear. Interestingly, cardiac myocytes plated on fibronectin (FN) showed elevated expression of SPARC in vitro. Whether absence of SPARC may lead to an altered formation of collagen in the normal heart is unknown.

1.5.3. Interaction of SPARC with other proteins

Binding to cytokines is one of the major characteristics of SPARC. SPARC regulates the activity of at least three growth factors that are important for vascular

homeostasis .SPARC was shown to bind the PDGF (platelet –derived growth factor) dimers AB and BB, but not AA. PDGFs are a family of growth-regulatory molecules capable of inducing directed cell migration, proliferation and altered cellular metabolism. The specific interaction of SPARC with the B-chain prevented binding of PDGF to its receptors on smooth muscle cells. The affinity of SPARC for this important growth factor could regulate the availability of PDGF dimers and thus affect the biological response to PDGF and may consequently control proliferative repair processes. (Raines, Lane et al. 1992) That SPARC interacts with PDGF and inhibits cell proliferation induced by PDGF indicates the importance of SPARC in angiogenesis. Because both SPARC and PDGF are found in platelet α-granules, and expression of both proteins is elevated in atherosclerotic plaque and in models of kidney disease, it has been proposed that SPARC might regulate the activity or distribution of PDGF in vivo.(Floege, Alpers et al. 1992)

In addition to PDGF, VEGF, and bFGF, SPARC can also modulate the activity of TGF-β. TGF-β is an important and widely-distributed growth factor, which is associated with the rapid remodeling of connective tissues and has been shown to regulate the expression of extracellular matrix proteins ((Kingsley 1994) SPARC can magnify TGF-ß1 expression (mRNA and protein) in cultured mouse mesangial cells (Francki, Bradshaw et al. 1999)SPARC-null mesangial cells also showed significantly decreased synthesis of TGF-ß1 mRNA, and addition of SPARC to SPARC-null cells in culture restored the expression of TGF-ß1 to levels typical of wild-type cells (Francki, Bradshaw et al. 1999). Given the coincidence of TGF-ß and SPARC in embryonic development and wound healing (Sage, Decker et al. 1989)the modulation of SPARC by TGF-ß and that of TGF-ß by SPARC are likely to be significant. On contrast, TGF-ß had been shown to regulate the expression of SPARC in fibroblasts (Lane and Sage 1994) Whether TGF-β1 and SPARC interact directly or not is unknown, but it is clear that both factors participate in a feedback loop that influences their production. There is considerable circumstantial evidence to indicate that SPARC interacts with TGF-β1and/or affects proteins of the TGF-β1 signaling pathway.

It is known that SPARC binds to collagen, but the functional significance of the interaction of SPARC with collagen in tissues is not clear. Collagen may serve as a storage site for SPARC in the ECM or might directly modulate the activity of SPARC, e.g. its counteradhesive or anti-proliferative function. The fact that proteolytic

cleavage of SPARC results in a higher affinity for collagen indicates that collagen is a potentially important ECM ligand for SPARC.(Yan and Sage 1999): Interestingly, SPARC has been shown to increase the production and activity of MMPs (Shankavaram, DeWitt et al. 1997; Gilles, Bassuk et al. 1998):These results suggest that SPARC might participate in an autocrine or paracrine positive feedback loop. For example, SPARC stimulates the expression and activity of MMP-2 and in turn, MMP-2 proteolytically cleaves SPARC, which increases the affinity of SPARC for collagen and presumably its localization to the basement membrane, an efficacious site for an anti-proliferative and counteradhesive protein

1.5.4. Possible role of SPARC in the heart during stress and remodelling

The matricellular protein SPARC shows an increased mRNA level in the heart in response to injury or stress, which suggests a critical function of SPARC in wound hearling and ventricular remodelling (Masson, Arosio et al. 2000; Stanton, Garrard et al. 2000; Komatsubara, Murakami et al. 2003). SPARC may modulate matrix remodeling and wound healing in the heart by different ways. First, SPARC may alter activity of growth factors, including TGF-β, bFGF, PDGF and VEGF, which are involved in wound healing after cardiac injury (Brekken and Sage 2000). Yan and Sage 1999), Secondly, SPARC induced de-adhesion may be involved in stimulating invasion of wound healing cells including fibroblasts, but also facilitating myocyte slippage and cardiac dilatation.. Finally, SPARC may modulate angiogenesis (Sage and Vernon 1994; Reed, Bradshaw et al. 2005)and might thereby influence infarct healing after myocardial injury. SPARC has been involved in ventricular remodeling, this alteration may due to the different mechanisms: 1) SPARC may initiate de-adhesion between cardiomyocytes and the ECM, meaning the transformation from a strong cell–ECM adhesion to an intermediate cell–ECM adhesion, which allows cells to spread 2) SPARC might increase proteinases activity such as MMPs involved in cardiac remodeling and function in different cardiac diseases (Spinale 2002).

Whether osteonectin up-regulation after cardiac injury or during hemodynamic stress may be beneficial or detrimental for cardiac structure or function requires further investigation. The study of the role of SPARC in the heart during stress and remodeling is just at the beginning, more research is still behind us …

1.6 Aim of this study

1.6.1. The Matracellular protein SPARC has been shown to participate in a number of processes related to tissue repair, however, little is known about SPARC during myocardial remodeling. The present study was designed to clarify the contribution of SPARC in the remodeling process after myocardial infarction and aortic banding.

1.6.2. Integrines mediate cell-cell and cell-matrix interactions that lead to intracellular signal transduction and wound heading, processes important in tissue repair. Following our study of SPARC expression in myocardium after injury, by using integrin β1 knockout mice and integrin αv inhibited mice, we further investigate an interrelationship between SPARC and integrins in MI and aortic banding mice, which may identify the mechanism involved in the healing of the infacted myocardium.

1.6.3. Furthermore, SPARC can be secreted by a different type of cells including fibroblasts, but nothing was known about the expression of SPARC in cardiomyocytes.Therefore, the occurrence of SPARC expression in different cell types and the role of TGF will be studied.

1.6.4. Finally, the function of SPARC in injured myocardium is still speculative. As a main function SPARC modulate cell migration by binding to ECM proteins. The influence of SPARC on ECM –induced migration of fibroblasts will be investigated.

Chapter 2.

Characterization of Cardiac specific excision of the β1 integrin gene in mice -

2. Characterization of Cardiac specific excision of the β1 integrin gene in mice -

influence on the transcriptional response after transversal aortic constriction

Heart failure and pathological overgrowth of the heart often occur hand in hand. New data on a biomechanical sensor challenge the viewpoint that cardiac hypertrophy causes heat failure

(Barki-Harrington and Rockman 2003)

2.1. Introduction

Cardiac hypertrophy is an adaptive response to mechanical and hormonal stimuli. Arterial hypertension imposes the heart to work harder than under normal circumstances. Although the performance of the heart can be well-maintained in a wide range of physiological stressors increased biomechanical stress (from either exercise or disease) can drive morphological changes in the heart muscle, which is known as cardiac hypertrophy. Cardiac hypertrophy is an increase in mass of the heart primarily due to an enhanced cell size. This increase in heart mass and heart muscle strength is considered beneficial, because it allows the generation of greater contractile force, but -in parallel- it may result in activation of pathways that reduce the efficiency of structural adaptation, promoting the transition toward cardiac dilation and failure(Chien 1999). The molecular and cellular mechanisms, which drive the pathological transition from cardiac hypertrophy to cardiac failure has been the subject of intense investigation for over a half century.

Cardiac hypertrophic remodeling is triggered by a combined action of mechanical stretching of cardiac walls and activation of neurohumoral growth factors (Ruwhof and van der Laarse 2000). Signals originating from all these pathways

converge to promote cardiac hypertrophy, however, the mechanical sensor that initiates these responses is poorly understood. Transduction of mechanical stress into biochemical signals is usually mediated by a group of cell surface receptors called integrins, which link the extracellular matrix to the cellular cytoskeleton thus providing physical integration and signal transduction between the outside and the inside of the cell. This combination of properties allows integrins to play important roles in cell growth, differentiation, and survival. Also in the area of cardiovascular research, integrins perform essential roles in the developing and postnatal heart. Previous work *in vivo* and *in vitro* has provided a lot of evidence that integrins encompassing the β1 subunit are linked to the hypertrophic response. Ross et al demonstrated that ß$_1$ integrin function is involved in the α_1-adrenergic-mediated hypertrophic response of neonatal rat ventricular myocytes (Ross, Pham et al. 1998) whereas inhibition of β1 function and signalling reduced the adrenergically mediated hypertrophy (Ross, Pham et al. 1998).

Since the arrival of gene-targeting technology, not only can defined nucleotide changes be engineered into the genome of the mouse, but genetic switches can be designed to target expression or ablation of any gene to any tissue and any defined developmental period (Sauer 1998). Knockout mice models have proven to be elegant and powerful experimental models for answering questions about the function of individual gene products. However, ablation of many essential genes is lethal to mice, especially if the gene is needed early during development.As reported for β1 Integrin, the deletion of its gene in mice results in inner cell mass failure and peri-implantation lethality (Fassler and Meyer 1995; Stephens, Sutherland et al. 1995). To study the effects of knockout genes without the problem of embryonic lethality, a clever genetic control system (Cre/*lox*) has been devised, which made it possible to disrupt genes only in a particular cell or tissue type (Gu, Zou et al. 1993; Chen, Kubalak et al. 1998; Hirota, Chen et al. 1999). To evaluate the role of β1 integrins in hypertrophy development, we took advantage of Cre-loxP gene targeting system. This system is derived from bacteriophage P1 from E.coli (a circular lysogenic virus) and involves two components: the 38 kDa Cre site-specific recombinase and the 34 bp long Cre-specific recongnition sequences termed loxP (Hoess, Ziese et al. 1982; Abremski and Hoess 1984; Kilby, Snaith et al. 1993). The Cre enzyme catalyzes recombination between two loxP sites and, therefore, the gene of interest, in our case integrin β1, has to be flanked by two loxP sites and this

configuration is also referred to as a conditional "floxed" allele (Fassler and Meyer 1995). Because the loxP sequences lie within introns and are only 34 bp in length, the floxed allele is predicted to function normally and, therefore, the expression level of the floxed allele is expected to be the same as that of the wild type. Crossing of the mice encoding the floxed allele with transgenic mice carrying the Cre recombinase gene under the control of a cell type-specific promoter, in our case the cardiomyocyte-specific myosin light chain-2v*(MLC2v)* promoter leads to the generation of a ventricular-specific integrin β1 knock out. The *MLC2v* gene is expressed bilaterally in the embryo in the cardiac primordia. Because of the restricted cardiac expression of this gene to the ventricles at the earliest stages of ventricular specification, Cre recombinase are chosed under the control of *MLC2v* regulatory elements. *T*he Cre-loxP recombination system for the generation of conditional and tissue-specific knock-out mice is shown in Figure2.1.

Figure 2.1. Cre-loxP recombination system for the Generation of Regulated Knockouts (Sauer 1998).

Cell-type-specific gene knockouts using the loxP-Cre recombination system. Two loxP sites are inserted on each side of an essential exon (2) of the gene of interest (i.e., gene X) (blue) by homologous recombination. These sites do not disrupt gene function. The loxP-containing mouse is crossed to a transgenic mouse carrying a cell-type-specific promoter controlling expression of the Cre recombinase, which induces recombination between loxP sites. This mouse is heterozygous for a constitutive gene X knockout. In the resulting loxP-Cre mouse, Cre protein is produced only in those cells in which the promoter is active, and in those cells recombination therefore occurs between the loxP sites, leading to deletion of exon 2. Since the other allele is a constitutive gene X knockout, deletion between the loxP sites results in complete loss of function in all cells expressing Cre…………...........................
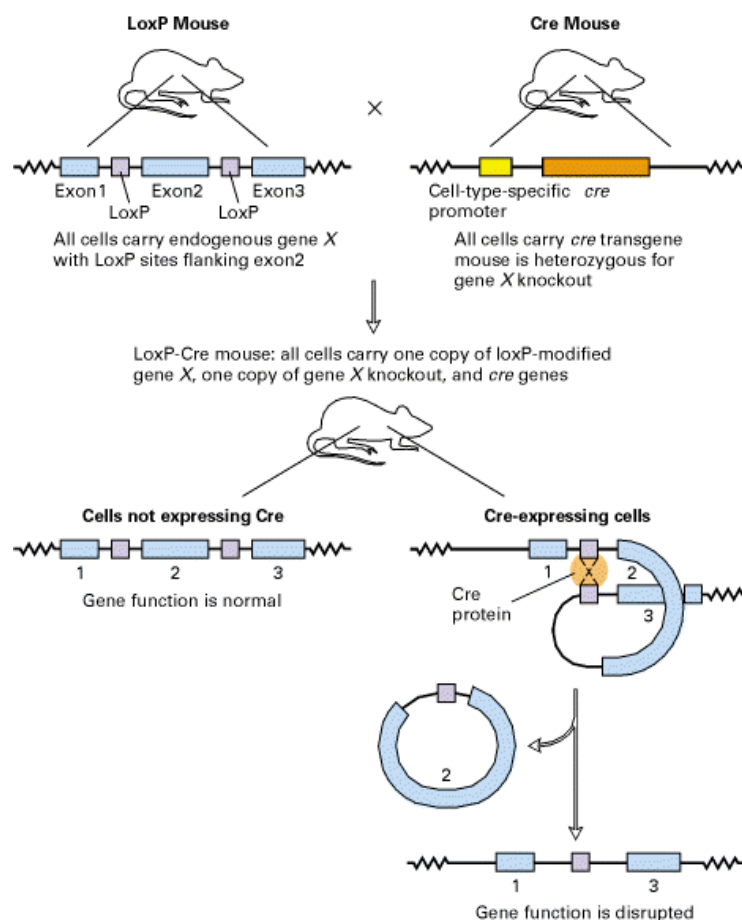
It is known that ECM proteins are involved in the tissue remodeling that is observed during cardiac hypertrophy. Activation of integrins by different ligands in the ECM (e.g., collagen, fibronectin and vitronectin) (Giancotti and Ruoslahti 1999; Laser, Willey et al. 2000) initiates singnaling transduction pathways through integrin-associated proteins that regulate gene expression, cell migration, growth and survival. However, knowledge concerning the function of Integrin β1 in the heart is far from complete. Little is known about the mechanisms how integrin β1 acts on ECM gene expression in heart after pressure overload, e.g. aortic banding. Integrin β1 is abundant in cardiac myocytes and is known to bind to collagen. In an effort to better understand the role of β1integrin in the pathogenesis of pressure overload-induced cardiac hypertrophy, the wild-type and β1 integrin knock-out mice were investigated 2 days, 7 days, and one month after aortic banding.

2.2. Results

2.2.1. Generation of heart-specific conditional β1-integrin knockout mice using the Cre-loxP system.

By using the Cre-loxP strategy (Marth 1996), a specific ventricular myocyte-restricted inactivation of the *β1 integrin* gene was achieved in mice. In particular, we mated the homozygous floxed β1 integrin mice to MLC2v ("myosin light chain 2v"-driven promoter for cardiac specificity) Cre reconbinase "knockin" mice, which have been characterized previously (Chen, Kubalak et al. 1998; Hirota, Chen et al. 1999). The sketch of the Cre-loxP strategy (Figure 2.2) shows that Cre reconbinase-mediated excision would delete exon 2 (containing the translational start codon) and exon 3 of the *β1 integrin* gene. This excision event would prevent expression of all known splice variants downstream of these exons.

In order to obtain the special heart conditional integrin β1 knock out mice two steps of interbreeding heterozygous mice were taken (shown in figure 2.4): firstly, we cross breeded the *Cre* reconbinase "knockin" mice (Cre+/-) and a conventional integrin β1 heterozygous knock out mice obtained from Dr.R.Fässler (Max-Planck- Institute of Biochemistry, Martinstried, Germany) as shown in figure 2.3 (Fassler and Meyer 1995) The offspring consisted four different genotypes. Mating the genotype mouse (Cre and integrin knock out double transgenic mouse: Cre+/-, β-/+) to the homozygous loxp-integrin mouse (Cre-/-, β c/c) will generate the final desired double-transgenic mouse in which the loxp-integrin genes will be deleted in ventricular myocyte in which the *cre* transgene has been expressed. The schematic figure was shown in figure 2.3, that is in our study transgenic mice containing integrin *β1 gene* surrounded by *loxP* sites are mated with transgenic mice that have the *cre* gene expressing only ventricular myocytes; The resulting integrin β1 knock out mice (β-/+) will contain both the *cre* gene and the *loxP*-flanked site In tissues with no *cre* gene the target gene with be present and function normally. In the ventricular myocyte where Cre is expressed, the target gene of *integrin β1* will be deleted.
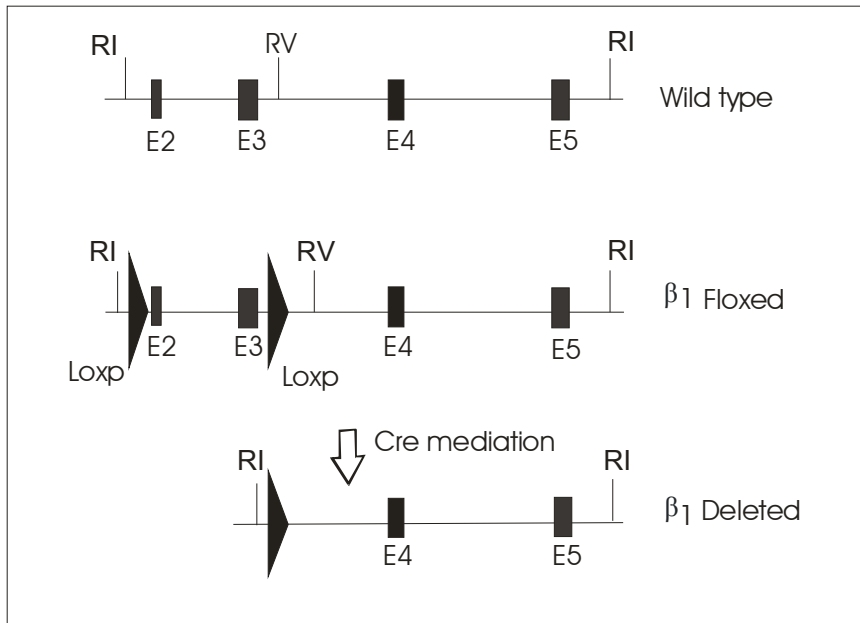
Figure 2.2. Schematic drawing of conditional *integrin β1* knock out. Restriction map of wild-type, floxed, and deleted allele of the *integrin β1* gene. Symbols are as in the figure. Triangles and rectangles present loxP sites and exons respectively. RI: EcoRI site, RV: EcoRV site. The recombined and non-recombined alleles could be discerned by EcoRI digestion-induced restriction length fragment polymorphism. Cre-mediated recombination leads to deletion of exons 2 and 3 of the *β1 integrin* gene.
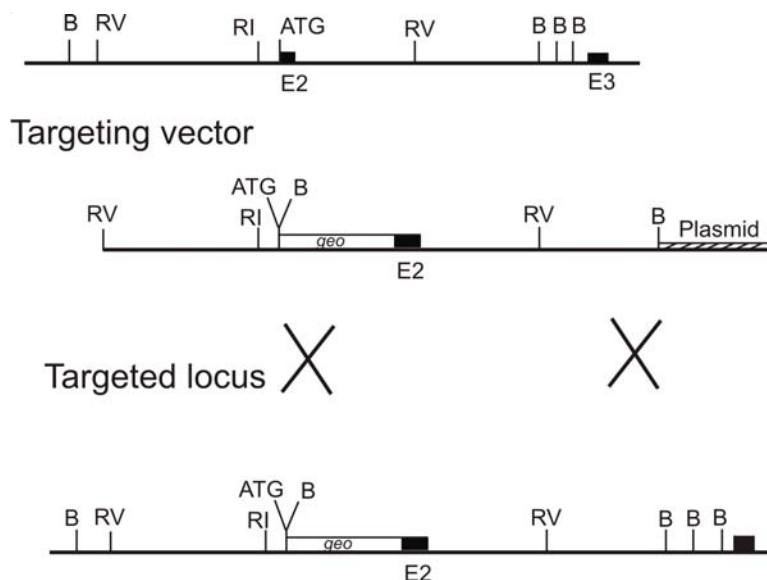
Figure 2.3. Schematic drawing of the conventional integrin β1 knock out: disruption of the second exon of the β1 integrin gene in ES cells. Restriction map of the wild type allele, the targeting vector and the mutated allele of the β1 integrin gene as indicated. The geo-cassette was inserted in frame with the ATG. Restriction sites: *B,* BamHI; *RI*, EcoRI; *RV, EcoRV.*

Figure 2.3 Cre/lox Mouse breeding. In the first step, Mice with the Cre protein expressing in a specific cell type (ventricular myocyte) are bred with heterozygous *integrin β1* knock out mice (Cre -/-, β+/-). The offspring with desired genotype'*'as indicated are further interbreeded with mice that contain a target gene *integrin β1* surrounded by *loxP* sites. When the mice are bred, the cells (ventricular myocyte) carrying Cre will cause those cells to lose the target gene in the second step of interbreeding of heterozygous mice. The symbol '*' as indicated is the desired mice, which is used for our study.

2.2.1.1. PCR analysis of genomic DNA

Genomic DNA from the offspring of crosses between homozygous integrin β1 floxed animals and Cre-transgenic mice (figure 2.3) were screened by PCR for the deletion event of integrin β1. (Figure 2.4) the PCR products were obtained from genomic DNA, using 3 primer sets to detect Cre recombinase, *integrin β1* knockout +/- and integrin β1 loxP(c/c). As expression of Cre recombinase was under control of the MLC -2v promoter, Cre expression and subsequent Cre-mediated excision only occurred in heart, whereas other organs such as liver, brain, spleen. Lung, kidney were not affected. This tissue and cell type specific action of MLC-2v-Cre was already demonstrated by a previous study (Shai, Harpf et al. 2002). Specially, in our study, by interbreeding, the conventional *integrin β1* knockout +/- mice contain transgenic gene cre+/- were cross bred with homogyous conditional integrin β1 loxP (c/c), the desired knock out mice are shown in the figure.
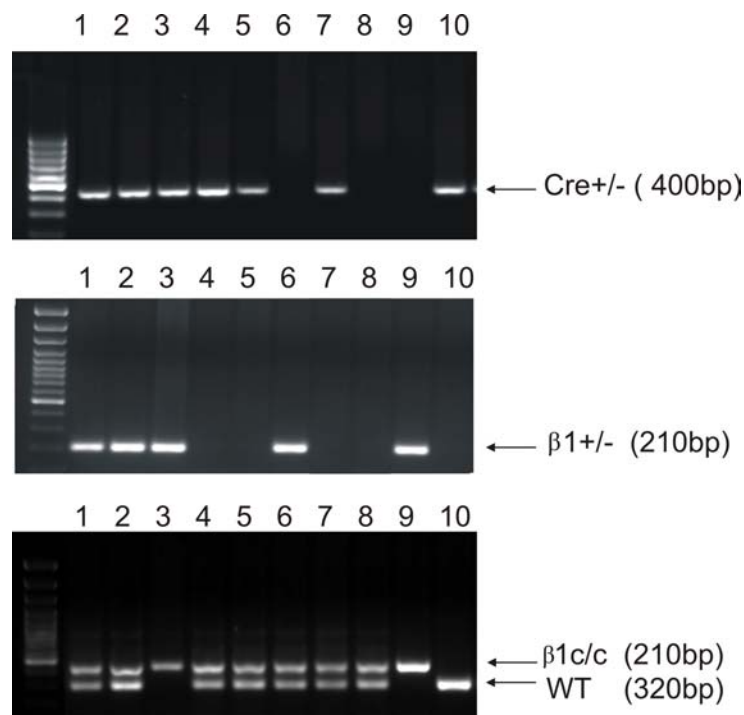
Figure 2.3   *β1 integrin* gene knock out detection by PCR analysis. Ethidium bromide visualization of PCR products generated with genomic DNAs isolated from 10 mouse tail biopsies. PCR reactions were performed using 3 sets of primers and separated on a 2% agarose gel. One set of primers detected a 419 bp fragment of the Cre transgene, Cre+/- (upper panel). A second set of primers detected a 210-bp band β1conventional heterozygous integrin gene (middle panel). The 400 bp and 320 bp bands indicated the conditional loxp (β1c/c) and wild type mice (WT) sequences respectively (lower panel). No abnormal sizes were detected.lane 3 indicated the desired *β1 integrin* gene knock out.

2.2.1.2. Detection of β1 Integrin protein level in knockout mice

The Integrin β1 subunit is expressed in multiple cell types, which are found in addition to cardiomyocytes in the ventricle. Indeed, only 14% of adult mouse ventricular cells are cardiomyocytes. However, muscle cells specifically express an isoform of β1, called β1D, which results from alternative splicing of the integrin β1 gene. To analyse the cardiomyocyte-specific deletion of the integrin β1 gene, we determined the levels of integrin β1D in the mouse heart by Western blot. Accordingly, hearts of β1 integrin knock out mice (MLC2v-Cre+/- β1 floxed c/-) at the age of one month, three months was extracted. As shown in Figure 2.4, Integrin β1D expression was reduced to about 35 %±3.4 and 12%±1.9 of the control levels, respectively (n=6 each group, p<0.001).

This result conformed *the integrin β1* Knock out mice at protain level expression.
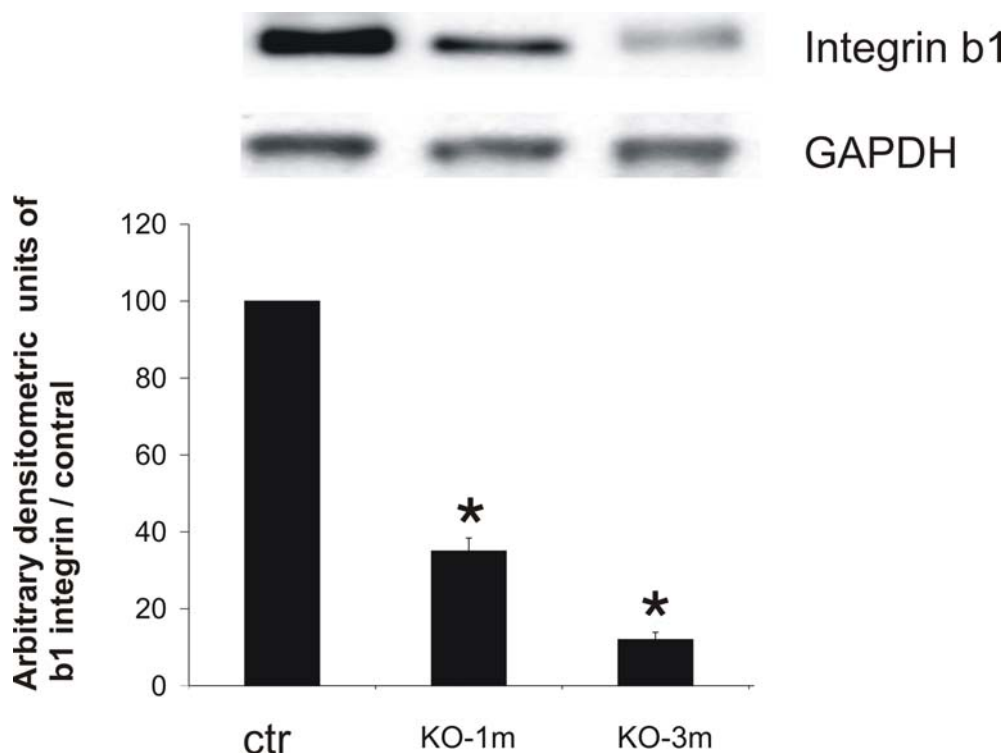
Figure 2.4 β1 integrin protein expression in knock out mouse. Densitometric analysis of Western blots showed that the normalized β1D Integrin protein (top panel) in heart of *β1 integrin* knock out mice (Cre+/-, β1-/C) at the age of one month or three months were reduced to 35 %±3.4 and 12%±1.9 of the control levels of wild-type animals (WT), Data are arbitrary densitometric units of β1 integrin protein normalized to GAPDH. (n=6 each group, *p<0.001)

2.2.2. Physiological alterations after aortic banding in mice

2.2.2.1. Enhanced mortality in integrin β1 knock out.

Mortality rate over one month observation period were higher in integrin β1 knock out than in wild type mice following aortic banding (AB) (knock out-AB 55% versus WT-AB 12% at day 2 after AB; knock out-AB 65% versus WT-AB 14% at day 7 after AB; knock out-AB 75% versus WT-AB 18% at one month after AB. Deaths in sham-operated mice (n=1 in KO sham. n=0 in WT sham group) occured in a single case during the surgery, which may due to lower anesthesia tolerance, but no post-surgical mortality was observed.
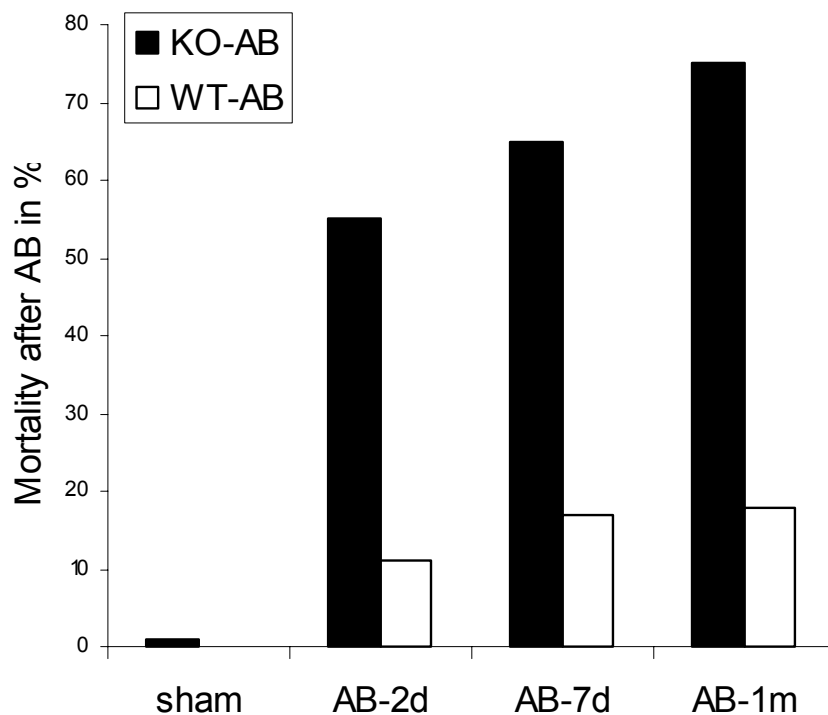
Figure2.5. Mortality after aortic banding (AB). Cumulative mortality rates of β1 integrin knock out and WT mice after AB or sham-operated as observed at day 2, day 7 and one month after surgery. Mortality rates were higher in group o f AB knock out mice than in WT-AB (n=12 for each group).

2.2.2.2. Morphometry

Tab1 Morphometric data

Parameter	WT		KO	
	sham (n=18)	AB (n=20)	sham (n=19)	AB (N=21)
Body weight, g				
AB-2d	27.1 ± 1.1	27.2 ± 2.8	28.2 ± 3.3	25.2 ± 2.2
AB-7d	28.3 ± 2.2	27.2 ± 3.3	27.8 ± 3.8	22.6 ± 3.4#
AB-1m	27.8 ± 3.2	28.1 ± 3.3	27.1 ± 3.4	23.1 ± 3.9#
Lung weight, mg				
AB-2d	148.8 ± 11.8	196.7 ± 23	168.9 ± 24.3	192.8 ± 24
AB-7d	149.8 ± 12.8	211.2 ± 21*	172.9 ± 34.3	246.0 ± 30*
AB-1m	148.6 ± 11.7	295.3 ± 45*	194.9 ± 14.3*	248.3 ± 36*
Lung weight/Body weight				
AB-2d	5.2 ± 0.5	8.6 ± 1.4	6.8 ± 0.9	7.8 ± 1.2
AB-7d	5.3 ± 0.5	7.4 ± 0.6	5.8 ± 0.8	11.2 ± 1.6*#
AB-1m	5.2 ± 0.4	10.2 ±1.6*	6.8 ± 0.6	11.0 ± 0.9*
Heart weight, mg				
AB-2d	135.1 ± 5.8	122.9 ± 3.8	140.2 ± 6.5	122.4 ± 9.9
AB-7d	137.1 ± 4.8	171.2 ± 10.3*	141.2 ± 5.5	155.6 ± 6.9
AB-1m	130.1 ± 5.7	203.8 ± 7.0*	139.2 ± 6.4	159.7 ± 9.6#
Tibia length, mm				
AB-2d	18.3 ± 0.1	18.1 ± 0.2	18.4 ± 0.4	18.1 ± 0.1
AB-7d	18.3 ± 0.1	18.1 ± 0.1	18.3 ± 0.2	18.4 ± 0.2
AB-1m	18.2 ± 0.1	18.0 ± 0.2	18.7 ± 0.2	18.5 ± 0.2
Heart weight/Tibia length				
AB-2d	7.3 ± 0.3	6.8 ± 0.3	8.1 ± 0.8	6.8 ± 0.6
AB-7d	7.2 ± 0.2	9.1 ± 0.5*	7.9 ± 0.3	8.3 ± 0.4
AB-1m	7.1 ± 0.1	10.9 ± 0.4*	8.2 ± 0.3	8.7 ± 0.5

Statistically significant differences between sham-operated and aortic banded mice of each group are indicated. All measurements were performed 2 days (2d), 7 days (7d) and 1 month (1m) after aortic banding or sham operation. The data were included after AB only when pressure gradients between left and right carotid are higher than 30 mmHg. *p< 0.05 AB vs sham; #P<0.05, KO-AB vs WT-AB.

Seven days after AB and after one month, body weight was significantly reduced in knock out mice as compared to wild-type control mice (7d:KO-AB 22.6±3.4 g vs. WT-AB 27.8±3.8 g, p<0.05; one month: KO-AB 23.1±3.9 g vs. WT-AB 28.1±3.4g, p<0.05). Lung weight and lung weight to body weight ratios were significantly increased in both groups and to a comparable extent after aortic constriction. The absolute gain in heart weight and heart weight to tibia ratios, which were significantly higher in AB-WT mice than in AB-KO mice at day 7 and one month after aortic banding (p<0.01). However, this increase was not observed in knock out mice after AB as compared to control group at any time point studied

.

2.2.2.3. Transthoracic Echocardiography in the beta-1 knock out Mouse

Echocardiograms, among the most widely applicable technologies in clinical cardiology, have been adapted for non-invasive physiologic studies in mice (Tanaka, Dalton et al. 1996; Pelzer, Loza et al. 2005). Echocardiograms are particularly useful because they can provide a generalized picture of the structure and function and of the heart throughout the life of the specimen. M-mode echocardiography provides quantitative data about contractile function. The analysis of echocardiograph is the procedure most often used in mouse studies. It is optimized for higher sample frequency and smaller heart size to accommodate the mouse´s diminutive size and resultant rapid heart rate. 2 days, 7 days and one month after AB, the consequences of the experimentally sustained pressure overload on LV morphology and function were non-invasively assessed using echocardiography. The data from these procedures provided a detailed and holistic view of cardiac function. Data comparisons from wild type and beta 1 knock out mouse with or without aortic banding were used to understand the effect of the genetic alteration in the heart pressure overload model in the context of the whole heart function. Data were shown in table 2.

Table 2

Echocardiography measurements after surgery

	WT n=20	KO n=19	AB-WT N=21	AB-KO N=18
HR, bmp				
AB-2d	445 ± 18	508 ± 49	401 ± 28	490 ± 21
AB-7d	455 ± 16	511 ± 49	440 ± 34	500 ± 43
AB-1m	438 ± 28	522 ± 24	450 ± 10	510 ± 39
IVS,mm				
AB-2d	0.80 ± 0.03	0.78 ± 0.09	0.79 ± 0.06	0.78 ± 0.05
AB-7d	0.81 ± 0.03	0.77 ± 0.04	1.38 ± 0.01*	0.72 ± 0.10#
AB-1m	0.80 ± 0.02	0.78 ± 0.07	1.63 ± 0.14*	0.91 ± 0.12#
PWTh,mm				
AB-2d	0.79 ± 0.08	0.85 ± 0.17	0.82 ± 0.08	0.86 ± 0.13
AB-7d	0.80 ± 0.06	0.84 ± 0.27	1.21 ± 0.17*	0.89 ± 0.09
AB-1m	0.79 ± 0.05	0.87 ± 0.19	1.38 ± 0.12*	0.90 ± 0.11
LV%FS				
AB-2d	37 ± 3.1	28 ± 2.9	33.2 ± 2.5	29.2 ± 3.5
AB-7d	38 ± 2.1	30 ± 2.7	44.1 ± 4.3	19.4 ± 4.2*#
AB-1m	35 ± 3.7	27 ± 3.0	30.2 ± 2.2	12.6 ± 4.8*#

All measurements were performed 2days (2d), 7 days (7d) and 1 month (1m) after aortic banding/ sham operation. HR, heart rate; IVS, interventricular septum; PWTh, end-diastolic posterior wall thickness; LV%FS, fractional shorting *p< 0.05 vs WT sham; # P<0.05 vs WT-AB
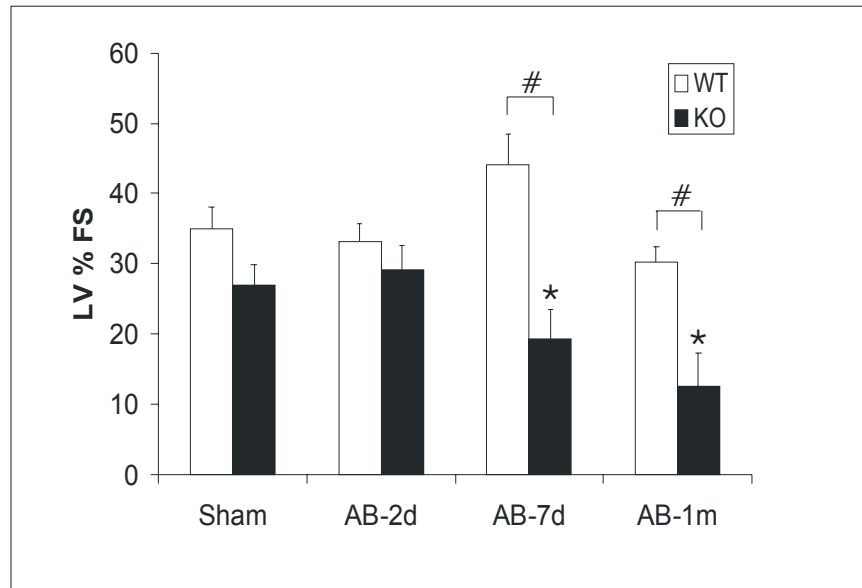
Fig 2.6. Value of LV fractional shortening (FS). FS in knock out and wild type mice after AB or sham operations at different time points. Bars represent the values of two independent experiments. Open bars and close bars indicate wild type and knock out mice, respectively. FS was significantly reduced in AB-knock out mice as compared to sham operated at day 7 and one month after AB. In both groups, no significant changes were observed two days after aortic banding as compared to sham-operated animals (n=6 for each group, *P<0.01 versus sham operated. # p<0.01 wild type versus knock out mice).

As compared to sham-operated mice, there were no significant changges of heart rates in both genotypes after AB. In contrast to corresponding sham-operated mice, LV fractional shortening (FS) was significantly reduced in knock out mice at day 7 and 1 month after AB, whereas, there were no significant changes in wild type mice at any of the time pointes tested in our study. The reduction of FS in AB-knock out mice was significantly reduced than that in AB-wild type mice (Fig 2.6) In both genotypes, IVS (interventricular septum), PWTh (end-diastolic posterior wall thickness) and FS (LV fractional shortening) did not differ significantly between sham-operated and AB 2 d post-surgery. 7 d and one month after AB, significant increases of IVS and PWTh were seen in wild type but not in knock out mice. Together with the morphometric data (no increase of heart weight to tibia ration in knock out mice after AB) showed that overload-induced heart hypertrophy occurs in wild-type mice but not in knock out mice (Fig 2.6).
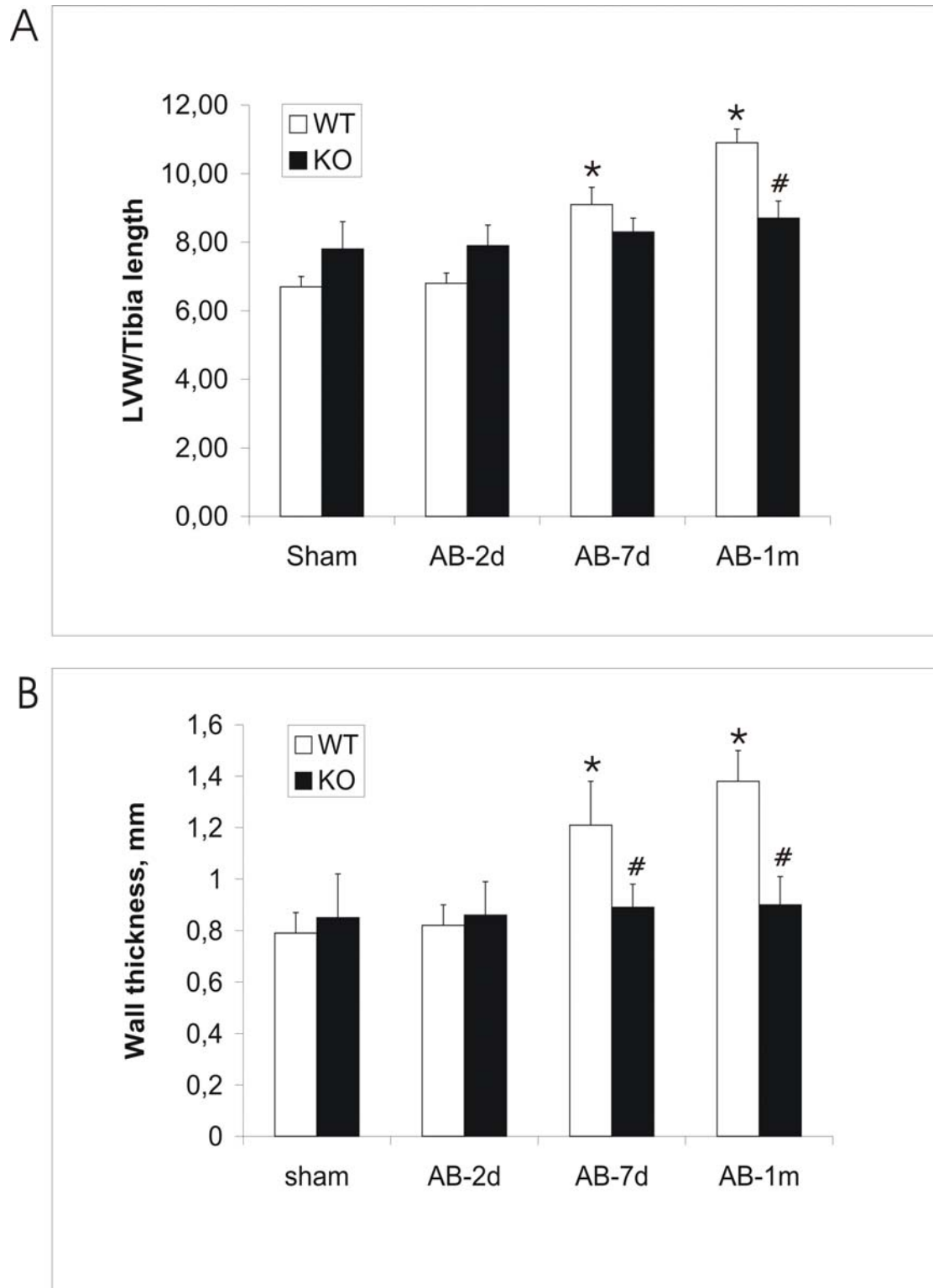
Fig2.7. Morphometry and Echocardiography. Parameters indicate a hypertrophic response induced by pressure overload (aortic banding) in mice. A: heart weight/tibia length ratio was significantly increased in AB-wild-type hearts vs. sham-operated hearts (n=12 for each group, *p<0.05.) B: After AB, wall thickness was statistically increased in wild type versus sham-operated hearts (n=5 for each group, *p< 0.05). Open bar indicated wild type and close bar indicated knock out mice.

2.2.2.4 Hemodynamic analyses

Table 3:

Hemodynamic data in WT and integrin beta-1 knock out mice.

	Ctr-WT n=20	Ctr-KO n=19	AB-WT n=21	AB-KO n=18
HR, bmp				
AB-2d	505 ± 12	526 ± 11	533 ± 28	478 ± 66
AB-7d	504 ± 23	532 ± 18	501 ± 26	482 ± 65
AB-1m	497 ± 33	551 ± 23	466 ± 21	475 ± 41
Systolic blood pressure, mmHg				
AB-2d	124 ± 10	122 ± 9	106 ± 14	117 ± 9
AB-7d	111 ± 11	112 ± 9	123 ± 10	109 ± 3
AB-1m	134 ± 12	132 ± 10	120 ± 14	128 ± 11
LVEDP, mmHg				
AB-2d	4.5 ± 0.5	4.0 ± 1.1	5.3 ± 0.6	6.1 ± 1.8
AB-7d	4.6 ± 0.5	4.5 ± 0.8	8.2 ± 0.6*	6.0 ± 1.7
AB-1m	4.8 ± 0.4	4.3 ± 1.1	10.6 ±1.6*	3.9 ± 1.0*#
dp/dt_{max}				
AB-2d	8041 ± 584	7980 ± 511	4266 ± 705	5800 ± 741*
AB-7d	7998 ± 465	7988 ± 415	9675 ± 442*	5239 ± 331#
AB-1m	8061 ± 345	8034 ± 389	10300 ± 452*	4001 ± 345#
dp/dt_{min}				
AB-2d	5418 ± 453	7244 ± 809	4800 ± 613	4806 ± 809
AB-7d	5423 ± 342	6987 ± 769	666 ± 518	4066 ± 731
AB-1m	5922 ± 453	6244 ± 812	4000 ± 339	4700 ± 454

Table 3. All measurements were performed 2days (2d), 7 days (7d) and 1 month (1m) after aortic banding/ sham operation. The data were included after AB only when gradients between left and right carotid are higher than 30 mmHg LVEDP indicates LV end-diastolic pressure, dp/dt_{max} velocity of systolic LV pressure devepment; dp/dt_{min} velocity of diastolic LV relaxation.*p< 0.05 vs WT sham; #P<0.05 vs WT-AB.

The consequences of the sustained pressure overload on LV morphology and function were also invasively assessed using a 1.4 F conductance catheter. No significantly differences in either systolic blood pressure or heart rate were detected in knock out and WT mice after AB. LV end-diastolic pressures (LVEDP) were increased at day 2 and elevated further one month after AB, whereas the LVEDP of knock out mice did not differ from the corresponding sham mice at day 2 and day 7 after AB. Furthermore, a reduction of LVEDP of knock out mice one month after AB was observed. Values for LV dp/dt_{max} were increased significantly in wild type mice after AB as compared to sham operated mice, on the contrast, the values were significant reduced in knock out mice after AB as compared to WT-AB. However, there were no significant differences in the values for LV dp/dt_{min} among the treated and untreated groups. There were no significant differences in these parameters among any of the time points of sham operated mice.

2.2.3. Effect of absence of β1-Integrin on SPARC gene expression after AB

2.2.3.1. SPARC gene expression was modulated

Most forms of cardiac hypertrophy are accompanied by changes in gene expression.(Stanton,L. W.,L.J. Garrrard, et al. 2000) Fig 2.8 shows that deletion of integrin β1 in mouse hearts modulated the expression profile of several genes following aortic banding. One of the strongly upregulated transcripts is coding for the matrix protein SPARC (secreted protein, acidic and rich in cysteine), also known as Osteonectin or MB-40). The location of SPARC is indicated by a circle in Figure 2.7. The expression of the employed positive controls β-actin (111,112), GAPDH (103,104), CyclophilinA (105, 106, 107,108) and ribosomal protein L13a (109,110) remained constant in both groups, independently of the presence or absence of Integrin β1. The total layout of the gene array is shown in Fig 2.8. In wild-type animals, the mRNA level of SPARC was significantly increased at day 2 and elevated further at day 7 and one month after AB, whereas the up-regulation was deprived in integrin knock out animals. Most of the genes of ECM were increased after AB as also shown previously (Tran, Lu et al. 2004), (Chen, Huang et al. 2004). Surprisingly, some well-characterized genes, such as MMP, were not detected in these analyses. The failure of detection by the microarray assay might be due to the limited sensitivity of the used cDNA microarray (Detisi, J 2000).
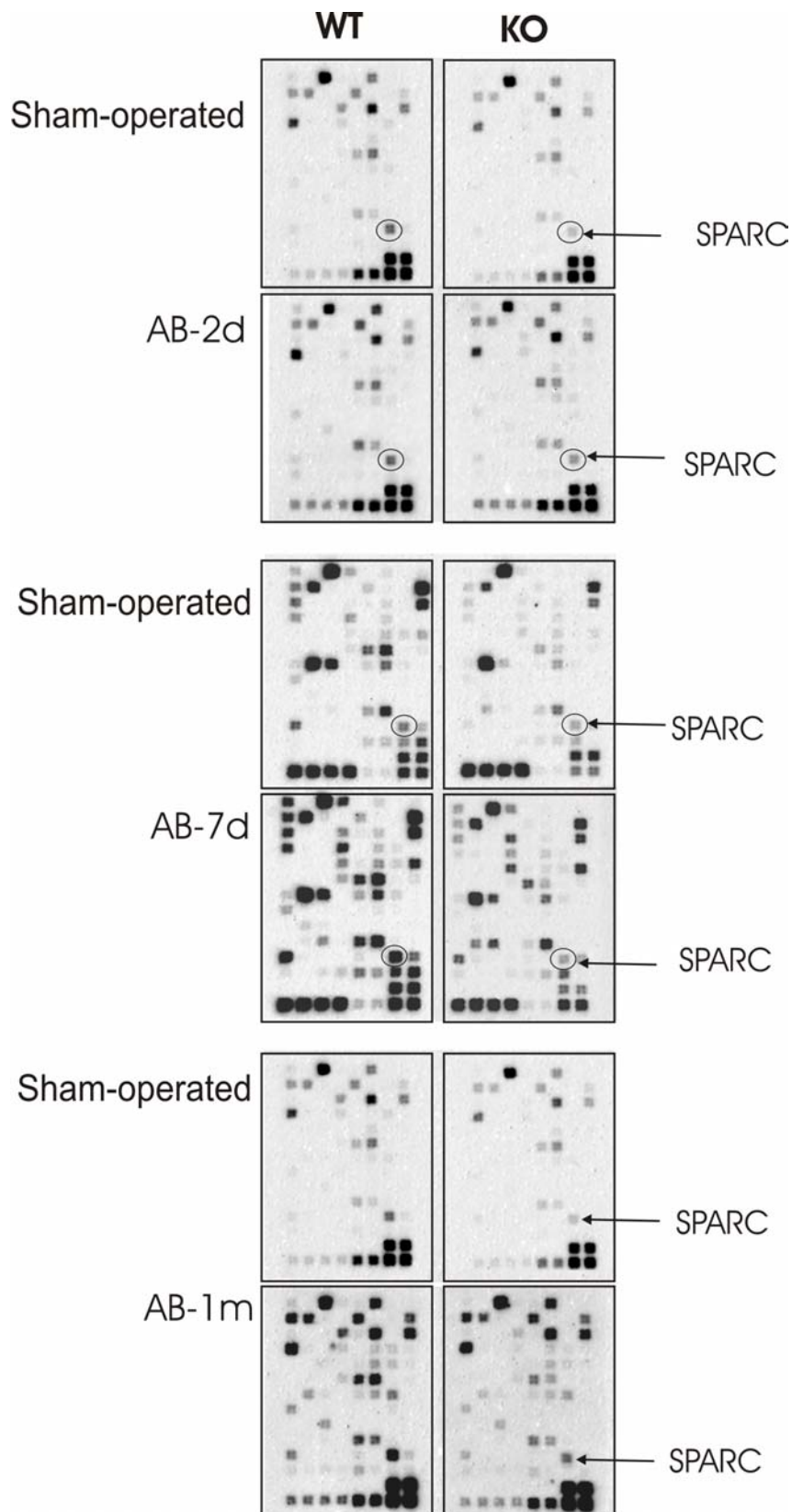
Figure 2.8 Representative expression profiles and comparison of ECM/integrin-related genes in mouse heart ventricle. Gene expression detected by cDNA

expression array system. Circle indicated *SPARC* gene. RNA was extracted from heart ventricles of the following groups of mice: sham-operated wild-type and knock out animals as control at different time point. Total RNA (5µg/membrane) was reverse-transcribed and labeled with biotin and gene expression levels were detected using Nonrad-GEArray Q series kit and LPR kit. All positive controls showed a clear hybridization signal, whereas blanks and negative controls consistently showed the absence of any hybridization signal. Membranes were hybridized with labeled RNA previously isolated from individual animals. Shown are representative membranes hybridized with RNA isolated from a sham operated animal or knock out animals at AB day 2, day 7 and one month as indicated.

Array layout table with gene symbol and position information

Adamts1	Adamts8	Bsg	Casp8	Casp9	Catna1	Catna2	Catnal1
1	2	3	4	5	6	7	8
Catnb	Cav	Cd44	Cdh1	Cdh2	Cdh3	Cdh4	Cdh5
9	10	11	12	13	14	15	16
Ceacam1	Cntn1	Col18a1	Col1a1	Col4a2	Cst3	Catnd2	Ctsb
17	18	19	20	21	22	23	24
Ctsd	Ctse	Ctsg	Ctsh	Dcc	Ecm1	Fn1	Icam1
25	26	27	28	29	30	31	32
Itga2	Itga2b	Itga3	Itga4	Itga5	Itga6	Itga7	Itga8
33	34	35	36	37	38	39	40
Itgae	Itgal	Itgam	Itgav	Itgax	Itgb1	Itgb2	Itgb3
41	42	43	44	45	46	47	48
Itgb4	Itgb5	Itgb6	Itgb7	F11r	Lamb1-1	Lamc1	Mmp1a
49	50	51	52	53	54	55	56
Mgea5	Mmp10	Mmp11	Mmp12	Mmp13	Mmp14	Mmp15	Mmp16
57	58	59	60	61	62	63	64
Mmp17	Mmp19	Mmp2	Mmp20	Mmp23	Mmp24	Mmp3	Mmp7
65	66	67	68	69	70	71	72
Mmp8	Mmp9	Ncam1	Ncam2	Pecam	Plat	Plau	Plaur
73	74	75	76	77	78	79	80
Sele	Sell	Selp	Serpinb5	Serpine1	Serpinb2	Sparc	Thbs1
81	82	83	84	85	86	87	88
Thbs2	Thbs3	Thbs4	Timp1	Timp2	Tnc	Vcam1	Vtn
89	90	91	92	93	94	95	96
PUC18	PUC18	PUC18	Blank	Blank	Blank	Gapd	Gapd
97	98	99	100	101	102	103	104
pia	Ppia	Ppia	Ppia	Rpl13a	Rpl13a	Actb	Actb
105	106	107	108	109	110	111	112

Figure 2.9. Distribution of genes in mouse heart chip. The chip encompasses 96 genes that encode cell adhesion and extracellular matrix proteins. These proteins play key roles in mediating cell-cell, cell-tissue and cell-extracellular matrix interactions. The PCR fragment of each gene was printed on a Nytran+ membrane with rectangular area of 23x35 mm.There are 96 spots including blanks: (100-102), negative control: PUC18DNA (97-99), positive control genes: glyceraldehyde-3-phosphate dehydrogenase (103,104); cyclophilin A (PPIA) (105-108), ribosomal protein L13a (109,110) and beta-actin (111, 112).

2.2.4. Altered protein expression

2.2.4.1. Increased integrin β1expression

Previous data have shown that Integrin β1 participate in the hypertrophic response of rat ventricular myocytes. Our study (Figure 2.10) demonstrated that in wild-type animals, integrin β1 is significantly increased at day 2 following aortic banding (1.8±0.08-fold, $p<0.05$ and was further elevated at day 7 (2.4±0.1-fold, $p<0.05$) as compared to sham-operated animals. In contrast, only sparse integrin β1 expression) was observed in knock out mice.

2.2.4.2 Induction of SPARC

Because up-regulation of *SPARC* gene was observed on the mRNA level and this induction was abolished in knock out mice, we further investigated the regulation of SPARC protein level by Western blotting. SPARC protein expression was investigated in mouse hearts following aortic banding at day 2 and day 7. Following a pattern very similar to that observed for integrin β1, SPARC protein levels were increased at day 2 (1.6±0.14-fold) and reached a significant difference at day 7 (2.2±0.18-fold, $p<0.05$) after AB. This induction was abolished in integrin β1 knock out mice (Fig 2.9).

2.2.4.3.Pro-ANP Expression in the left ventricle

Furthermore, the amount of atrial natriuretic peptide (ANP), a marker for the severity of heart dysfunction and predictive for patients survival (Daugaard, Lassen et al. 2005; Pelzer, Loza et al. 2005) were investigated by Western blots. In wild-type mice, a significant increase of pro-ANP was observed 2 d and 7 d after AB (2.8±0.15-fold, $p<0.05$ and 4.4±0.21-fold, $p<0.05$) as compared to sham-operated control mice. Interestingly, ANP expression was already significantly up-regulated in sham-operated knock out mice as compared to sham-operated wild-type mice but aortic banding did not strongly influence the ANP expression in these animals.
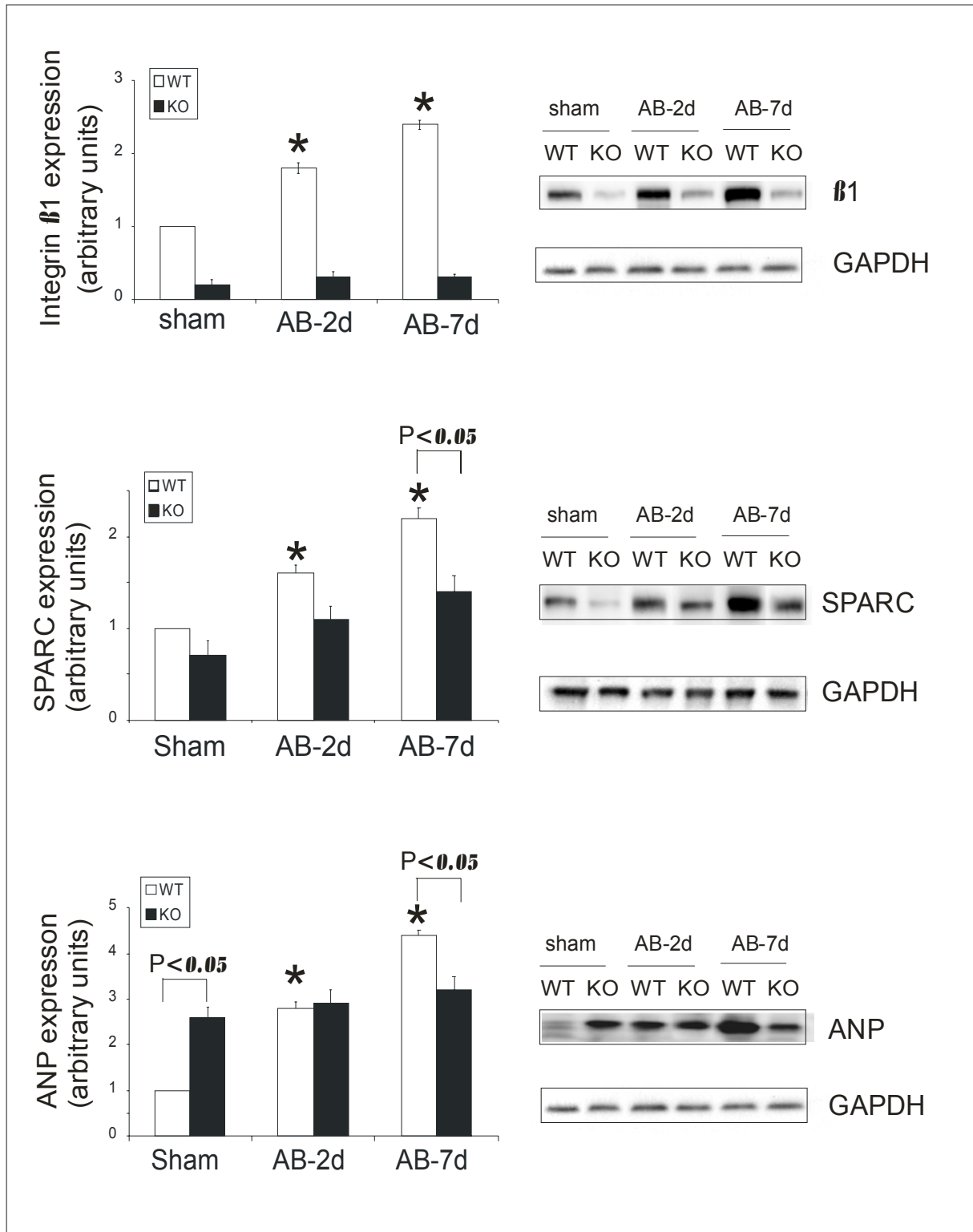
Figure 2.10 Modulated protein expression following aortic banding. The expresson of integrin β1, SPARC and ANP was analysed by Western blot. Detection in cardiac protein extracts from mice hearts was performed using specific antibodies for Integrin β1 SPARC and ANP. Open bars and close bars represent wild-type and knock out mice as indicated. The intensity of the bands from total of 5 mice per group was measured and relative intensity was calculated. *P<0.05 versus sham-operated.

2.3. Discussion

The investigation reported here support the hypothesis that integrin β1 is necessary for the development of heart hypertrophy in response to pressure overload in mice. This is the first study to suggest interplay between integrin and SPARC in heart remodeling. The major mew findings of this study are that mice with a ventricle-specific integrin β1 knock out exhibit impaired hypertrophic response after chronic pressure onveload (compared with WT), and that the lack of integrin β1 is associated with decreased induction of the ECM protein SPARC.

To circumvent the early embryonic lethality of the conventional integrin β1 gene deletion strategy (Fassler and Meyer 1995), we have generated the mice by using the Cre loxP-system. As the Cre expression was restricted to the heart by the myosin light chain-2v promoter (Chen, Kubalak et al. 1998). the mice survived to adulthood. Soon after birth, some Integrin β1 was still present, because of incomplete Cre-mediated recombination in the hearts of these mice. However, most of the knock out mice could not survive longer than 6 months, due to a heart failure which is in agreement with another work, in which another strategy to achieve heart-specific deletion of the β1 gene has been used (Shai, Harpf et al. 2002). It might be that further reduction of Integrin β1 protein in the cardiac myoctes (reduction of integrin β1 in our knock out mice was shown in figure 2.4) below a "not yet identified limited level", could lead to an abnormal cardiac development and a final heart failure.

Compensatory hypertrophic response, as measured by increased either HW-to BW ratio or HW-to tibia ratio was increased after aortic banding in wild-type mice and differed significantly at day 7and after one month, whereas this response was not observed in integrin β1 knock out mouse. Similar results were obtained by echocardiography showing as well that left ventricular wall thickness significantly increased at day 7 and after one month after aortic banding in wild type but not in knock out mice (data shown in Figure 2.7). The findings in our knock out mice are similar to melusin (a muscle-specific β1 integrin-interactin protein, that interacts with the integrin β1 cytoplasmic domain, has been demonstrated that response to mechanical overload) null mice, in which lack of melusin resulted in blunted hypertrophic response to pressure overload (Keller, Shai et al. 2001). In line with our results, which indicated that Integrin β1 is necessary to the development of hypertrophy in response to hemodynamic overloading. In addition, ANP,regarded as

"a hypertrophic maker" (Holtta, Happonen et al. 2001), the induction of Pro-ANP expression (linear regression analysis revealed a significant correlation between ANP serum levels and ventricular pro-ANP expression (Pelzer, Loza et al. 2005)) after aortic banding was observed in wild-type mice, consistent with the activation of ANP gene expression as described previously (Abbate, Biondi-Zoccai et al. 2002). However, the difference of ANP expression was abolished in integrin β1 knock out mice. Interestingly, although no significant difference of pro-ANP expression levels between sham-operated knock out and aortic banding knock out mice, a significant up-regulation of pro-ANP in sham-operated knock out mice was observed as compared to sham-operated wild type mice. In our study, no evidence of hypertrophy in β1 integrin knock out mice was observed. The data presented here suggested that cardiac hypertrophy and an increase in ventricular expression of ANP are not necessarily correlated. However, up-regulation of ANP in knock out mice pointed towards an existing chronic cardiac abnormality in their hearts. This was supported by the observation that the β1 KOs did not reach their normal life-span and died due to a heart failure.

Interaction of ECM proteins with Integrins is proposed to play an important role in cardiac myocyte interaction and myocardial hypertrophy. β1 Integrin is a critical component of the linkage between the extracellular matrix and cytoskeleton. In the heart, the dominant postnatal isoform of β1 integrin is β1D, it is 5-10 times more strongly expressed in the heart than in skeketal muscles. Because the myocardium is subject to continuous mechanical stress, we analysed heart integrin β1D expression after aortic banding. Data showed an up-regulation at day 2 and day 7 in wild-type mice, suggesting an association of this protein with hemodynamic pressure overloading. In parallel with integrin β1 expression, we observed the same pattern of increased SPARC expression at day 2 after aortic banding, and further elevated at day 7 and one month. The increased RNA levels of SPARC has been shown in response to β-adrenergic stimulation of cardiac hypertrophy in hearts of rats (Masson, Arosio et al. 2000). Interestingly, the induction of SPARC in our knock out mice was abolished either on RNA level or on protein levels. SPARC is a multifunctional protein belonging to extra cellular proteins. (Sage, Vernon et al. 1989) It has been found to be expressed after tissue injury, to modulate ECM deposition and to inhibit cellular adhesion and spreading on collagen matrix (Sage and Bornstein 1991; Lane and Sage 1994). The role of SPARC in the injured adult heart is still speculative, but its

anti-adhesive properties may contribute to a loosening of ECM organization, facilitating the migration of immune cells to the site of injury, Cardiomyocyte hypertrophy, and matrix re-arrangement. Our data suggests an Integrin-dependent SPARC induction and function in the remodeling after heart injury.

What could be the function of the Integrin β1 in the development of hypertrophy? Ventricular hypertrophy is an important adaptive mechanism to maintain the heart`s output. Investigators have shown an altered modulation of Integrin expression and extracellular matrix proteins in the hypertrophied myocardium (Pelouch, Dixon et al. 1993; Farhadian, Contard et al. 1995; Nebe, Rychly et al. 1995; Yamazaki, Komuro et al. 1995). This is particularly noteworthy and indicated that Integrins work as mechanotransducers, translating mechanical signals to biochemical signals (Ingber 1991; Nebe, Rychly et al. 1995). Thus Integrin might play a role in the translation of increased mechanical stress into the cardiac cell in response to stress. Interestingly, hypertrophic response to Angiotensin II was not different in WT and Melusin (Integrin β1-interacting protein) null mice (Kim, Dalal et al. 2000). This indicated that biomechanical stress attribution to pressure overload is different from that of neurohumoral-induced cardiac hypertrophy. Additionally, in light of our study, the interplay of Integrin β1 and SPARC was involved in the remodelling of heart injury. It was known that SPARC induces matrix metallo-proteinases (MMPs) such as Gelatinase B, sStromelysin, and Collagenase, which support immune cell invasion. MMPs are linked to the remodelling that occurs during the development of hypertrophy, and thus, it is possible that alterations in these molecules may also be present in our knock out mice. Appropriate linkage of ECM and cytoskeleton through β1 Integrins is essential for the development of compensatory hypertrophy. When β1 integrin is reduced at the cell surface, this linkage is disrupted.

In summary, we have produced a hemodynamic overload model with cardiac-specific Integrin β1 deficiency resulting in abnormal response to pressure overload. Using this knock out model, we demonstrated the modulation of SPARC in different genotype mouse. However, the direct roles, which β1 Integrin and SPARC play in the hypertrophic response pathways in myocytes is presently unknown and needs to be explored further.

Chapter 3

Transient expression of SPARC in response to myocardial infarction in mice

3. Transient expression of SPARC in response to myocardial infarction in mice

Myocardial infarction is the most common cause of cardiac morbidity and mortality in many countries, and left ventricular remodeling after myocardial infarction is important because it causes progression to heart failure

(Harada, Qin et al. 2005)

3.1. Introduction

Following myocardial infarction, the injured heart tissue undergoes a process of wound healing and scar formation, which is necessary to maintain structural and functional integrity of the organ. The preservation of cardiac function depends in part on the invasion of cardiac fibroblasts as well as restructuring of the extracellular matrix (ECM). In particular, deposition of ECM proteins such as collagen, fibronectin, and vitronectin at the infarcted area is thought to replace necrotic myocytes and leads to scar formation.

In addition to classical ECM proteins, a number of so-called matricellular proteins has been described. Their role in cell adhesion and extracellular matrix remodeling is less well defined, but they seem to act as modulators of cell-ECM interactions. Prototype examples of matricellular proteins include thrombospondin (TSP)-1,TSP-2, tenascin C, osteopontin and also SPARC (secreted acidic protein and rich in cysteine) (Schellings, Pinto et al. 2004). Studies in SPARC knockout mice indicate that these proteins influence the wound healing response and play critical regulatory roles in tissue renewal(Bradshaw, Reed et al. 2002). SPARC, also known as osteonectin or BM-40, is an extracellular Ca^{2+}-binding glycoprotein that promotes de-adhesion of cells from the matrix and influences migration, proliferation, shape and motility of cultured cells(Funk and Sage 1993) High levels of SPARC expression are observed during tumor growth(Bornstein and Sage 2002) and after tissue injury(Lane and Sage 1994)our recent studies using hemodynemic overload animal model in a heart specific integrin β1 knock out mice have indicated an

increased expression of SPARC in the myocardium after injury or stress, this is in line with other studies (Masson, Arosio et al. 1998; Komatsubara, Murakami et al. 2003; Simkhovich, Kloner et al. 2003). Furthermore, this increased expression depending integrin β1 function was observed in our study. Integrins are the main family of cell surface receptors that sense the composition and structure of the ECM (Shai, Harpf et al. 2002). The cross talk of integrin and SPARC studied in some investigate showed that SPARC is able to promote prostate cancer cell migration and this activity of SPARC is functionally connected to integrins $α_vβ_3$ and $α_vβ_5$(De, Chen et al. 2003). SPARC protein induction through $β_3$ integrin expression has been reported (Sturm, Satyamoorthy et al. 2002). These findings suggest that wound repair are influenced by an interplay between integrins, including $α_v$ and the matricellular protein SPARC. However, the potential role of SPARC in the myocardium is still speculative and how SPARC expression and function are integrated into the ECM remodeling events following myocardial infarction is currently unknown.

In the present study we investigated altered gene expression of ECM proteins and SPARC in response to experimental myocardial infarction in the mouse. We followed the hypothesis that SPARC is involved in ECM remodeling and myocardial infarction

3.2. Results

2.2.1. Gene expression events following experimental myocardial infarction

Remodeling of the extracellular matrix and scar formation at the infarcted area is the key to compensate for lost cardiomyocytes and to sustain proper heart function. To analyse gene expression events concerning extracellular matrix proteins and the respective cellular receptors and regulators, we compared heart muscle transcript levels of sham operated animals to the RNA levels observed after experimental myocardial infarction by the help of GEArray^{TM} cDNA macroarrays. Gene expression profiling was performed on the ligation of the descending branch of the left coronary artery (LAD)-induced myocardial infarction and sham-operated mouse heart. (figure3.1). The distribution of the gene fragments, positive, negative controls and the complete gene list are available at www.superarray.com.The use of Ampolabeling-LPR derived probes provides more accurate and sensitive gene

expression profiling results in our cDNA macroarrays. The expression levels were analyzed and shown as -fold intensity in comparison with sham operated samples displayed in Table 1 and Table 2. The used arrays encompass 96 cDNAs encoding cell adhesion molecules, extracellular matrix proteins, and additional proteins that play central roles in cell-extracellular matrix interactions as well as tissue remodelling. Upon total RNA isolation from individual heart tissues at 2 or 7 days after the intervention, mRNA was reverse transcribed using gene specific primers in the presence of biotin-labeled UTP before hybridization to the array and signal detection. Following normalization of individual hybridization experiments, the expression levels in infarcted hearts were compared to sham operated samples. Whereas none of the analysed 96 genes showed significant down-regulation during the course of the study, a total of 14 genes were found to be induced more than 1.8-fold after myocardial infarction two days (Table 1) and 23 genes were increased more than 1.8-fold at day 7 of myocardial infarction. (Table2). As indicatiors for successful myocardial infarction and induction of cardiac remodeling, collagen and fibronectin were strongly up-regulated. Beside several ECM genes, a prominent induction was observed for the matricellular protein SPARC (secreted protein acidic and rich in cysteine; also known as osteonectin and BM-40). Expression of SPARC was significantly increased after 2 days (2.65 ± 0.24 fold, $p<0.01$) and 7 days (3.78 ± 0.11 $p<0.01$) following myocardial infarction.
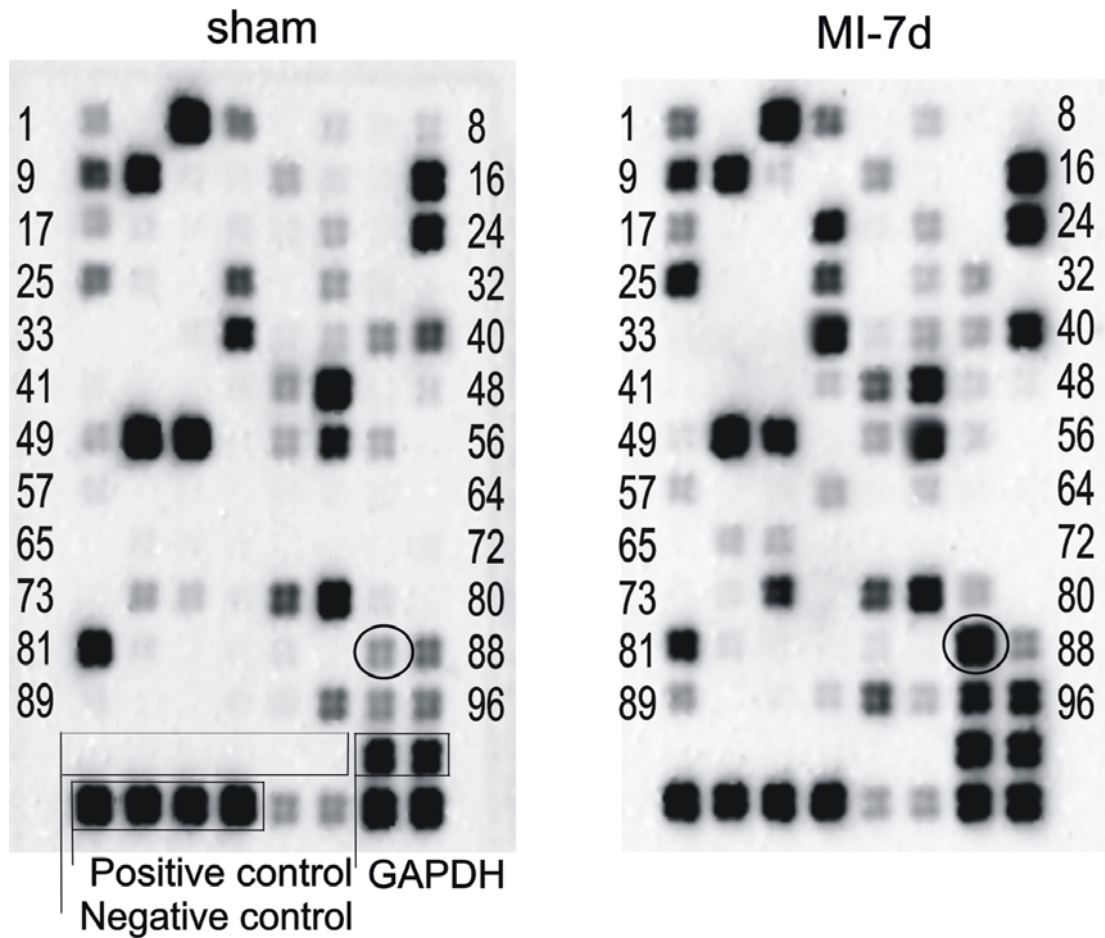
Figure 3.1 Representative gene expression profile in mice heart after myocardial infarction 7 days. . A total of 112 cDNA fragments (400bp in length) were arrayed in an 18x16 format including 96 spots representing extracellular matrix proteins, integrins, proteases and related genes. 6 spots (Negative control including blanks), 4 spots (positive control), and the 2 spots encoding the house-keeping gene glyceraldehyde-3-phosphate dehydrogenase (GAPDH) used for normalization are indicated. All positive and house-keeping genes show a clear hybridization signal, All bland spots and negative controls consistently show the absence of any hybridization signal. Glyceraldehydes-3-phosphate dehydrogenase (GAPDH) were chosen as positive controls and spotted on the bottom of the chip GAPDH were chosen as house-keeping genes. Membranes were hybridized with RNA isolated from individual animals. For the full layout of the array see fig 2.9.

.

Table 1: Differential expression of genes in mouse hearts 2 days after experimental myocardial infarction (MI).

Spot location	Gene name	fold induction (MI versus sham operated) n=6
Cell adhesion molecules		
39	Integrin alpha 7	1.88 ± 0.26
75	NCAM	3.77 ± 0.71
95	VCAM-1	2.31 ± 0.30
Extracellular matrix proteins		
20	Collagen 1a1	5.59 ± 1.45
31	fibronectin	2.01 ± 0.45
87	SPARC	2.65 ± 0.24
96	vitronectin	1.82 ± 0.44
Proteases		
4	caspase-8	2.35 ± 0.34
25	Cathepsin D	1.80 ± 0.26
57	Hyaluronidase	2.05 ± 0.45
60	MMP12	1.88 ± 0.23
79	uPA	2.88 ± 0.46
Protease inhibitor		
92	Timp1	9.83 ± 1.57
93	Timp2	2.25 ± 0.54*

The listed genes displayed on average a more than 1.8-fold difference between the sham-operated and the infarcted animals 2 days after the intervention. The expression levels are shown as -fold increase compared to sham operated samples after normalization using the internal control (GAPDH). Values represent mean ± SEM of independent hybridizations of RNA isolated from 6 animals for each treatment for each time point

Table 2, Differential expression of genes in mouse hearts 7 days after experimental myocardial infarction (MI)..

Spot location	Gene name	fold induction (MI versus sham operated) (n=5)
Cell adhesion molecules		
17	CEACAM 1	4.73 ± 0.51
36	Integrin alpha 4	6.90 ± 1.97
38	Integrin alpha 6	2.03 ± 0.30
39	Integrin alpha 7	3.69 ± 1.12
40	Integrin alpha 8	3.36 ± 0.05
45	Integrin alpha x	3.05 ± 0.39
81	ELAM-1	4.26 ± 0.20
75	NCAM	4.40 ± 1.57
95	VCAM-1	2.95 ± 0.35
Extracellular matrix proteins		
20	Collagen 1a1	21.73 ± 2.27
31	fibronectin	6.15 ± 1.04
54	Laminin B1	2.51 ± 0.35
87	SPARC	3.72 ± 0.11
94	Tenascin C	1.87 ± 0.20
96	vitronectin	1.94 ± 0.68
Proteases		
1	Adamts 1	4.19 ± 0.46
25	Cathepsin D	1.92 ± 0.36
57	Hyaluronidase	2.31 ± 0.58
60	MMP12	5.91 ± 1.20
67	MMP2	4.15 ± 1.77
79	uPA	3.03 ± 0.58
Protease inhibitor		
92	Timp1	6.43 ± 1.78
93	Timp2	4.71 ± 1.39

The listed genes displayed on average a more than 1.8-fold difference between the sham-operated and the infarcted animals 2 days after the intervention. The expression levels are shown as -fold increase compared to sham operated samples after normalization using the internal control (GAPDH). Values represent mean ± SEM of independent hybridizations of RNA isolated from 6 animals for each treatment for each time point

3.2.2. SPARC protein levels strongly, but transiently increase during myocardial remodelling

Having identified SPARC as a gene up-regulated in response to MI, we next wanted to test whether the induction of SPARC at the mRNA level also reflected an increase in expression of SPARC protein. Because the correlation between mRNA and protein expression for a particular gene is highly variable, proteins are the actual effectors of most cellular processes, mRNA changes not accompanied by corresponding alterations in protein levels may not be mechanistically meaningful. The biological activity of many proteins is regulated by sub-cellular localization and post translational modifications, neither of which is addressed by transcriptional analysis. To our knowledge, there are no investigations of SPARC protein levels following MI in the mouse. We analyzed the expression of a 43 kDa glycosylated form of SPARC by Western blot at the time points 2 days, 7 days, 1 month, and 2 months after MI. In line with the observed changes in mRNA levels, SPARC protein levels were strongly increased upon myocardial infarction with a maximal induction at day 7. Within the next 2 months, SPARC protein levels returned to the background levels of sham-operated animals. Probing of the membranes with antibodies against GAPDH demonstrated equal loading of the samples. Quantification of the Western Blot signals indicated a significant increase in SPARC protein expression at day 2 (2.58 ± 0.21 fold, $p<0.01$, $n=12$), day 7 (3.72 ± 0.28 fold, $p<0.01$, $n=12$) and 1 month (1.9 ± 0.16 fold, $p<0.01$, $n=12$) following the infarction, respectively (Fig.3.2). Furthermore, the kinetic of SPARC expression indicates that this protein presumably plays a transient role during the remodeling of the infarcted heart tissue.
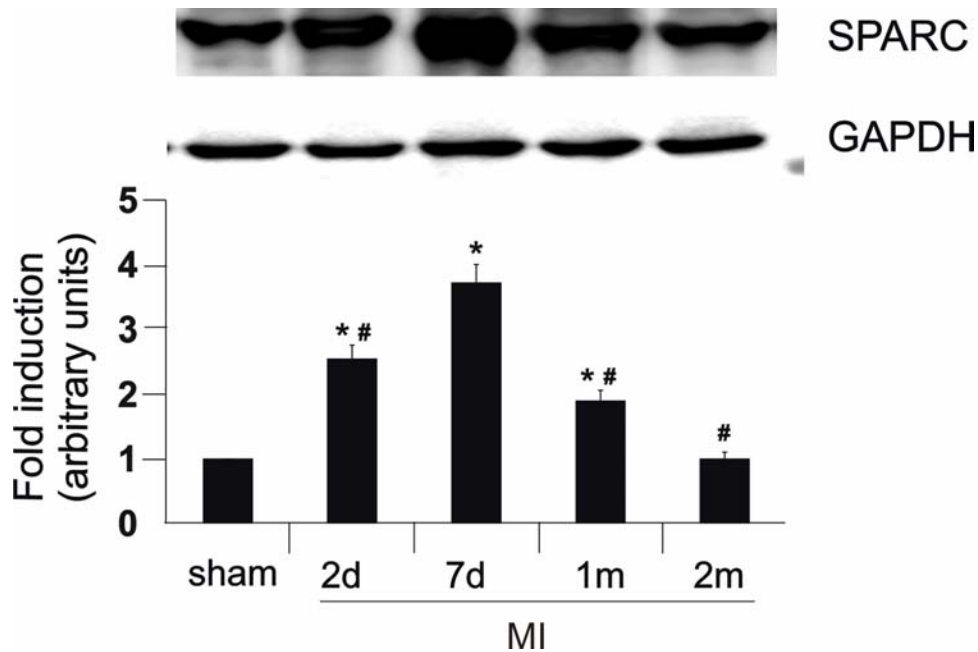
ig 3.2 Changes in SPARC protein levels following myocardial infarction. Western Blot of sham-operated mice (Ctr) or infarcted animals (MI) at the indicated times after the procedure (upper panel). Each lane was loaded with 15µg protein of the tissue extract. for GAPDH. The bar diagraph indicates the quantification of SPARC expression Following Semi-quantitative analysis of SPARC in mouse hearts at different times after MI as indicated. Data are expressed as fold changes from corresponding sham-operated mice after normalization. Values are mean ± SEM; n=12 *P< 0.01 vs. corresponding sham –operated animals; # P < 0.05 vs. MI-7d. One way ANOVA test.

3.2.3. Enhanced SPARC expression occurs predominantly in the infarcted area

To analyze the tissue distribution of SPARC after myocardial infarction, frozen sections of infarcted tissue or control mouse hearts were stained with anti-SPARC antibodies and detected with fluorescence-labeled secondary antibodies. To identify both cardiomyocytes and non-myocytes, cellular actin and nuclei were also labeled with phalloidin-rhodamine and DAPI, respectively (Fig. 2). To test for specificity of the SPARC antibody used, either the SPARC antibody was omitted (data not shown) or a blocking peptide (encompassing the region used to generate the SPARC antibody) was included. No significant SPARC staining could be observed in the negative controls ("blocking peptide" in Fig. 2). Importantly, the expression of SPARC was low in normal heart tissue (Fig. 2). However, 2 days after infarction, significant increases in SPARC expression could be observed in the infarcted area. In parallel, a decrease in

the phalloidin staining, suggestive of actin degradation in the infarct zone, together with an increased number of nuclei, suggestive of invasion of inflammatory cells and fibroblasts, could be observed. Moreover, 7 days after the infarction, strong SPARC staining was evident with further reduction in the actin signal and a strongly increased number of nuclei (presumably non-myocytes). SPARC deposition was localized dominantly to the infarcted area surrounding the invaded fibroblasts and inflammatory cells. Strikingly, 2 months after the experimental infarction, SPARC immunoreactivity in the infarcted area was decreased again to the background levels seen in normal heart tissue, while an organized scar tissue without actin staining and elevated nuclear signal from fibroblasts and other non-myocytes could be seen. These data demonstrated that enhanced expression of SPARC is transient in the remodeling tissue. Furthermore, up-regulation of SPARC coincides with the invasion of fibroblasts and the induction of scar formation in the injured heart tissue.
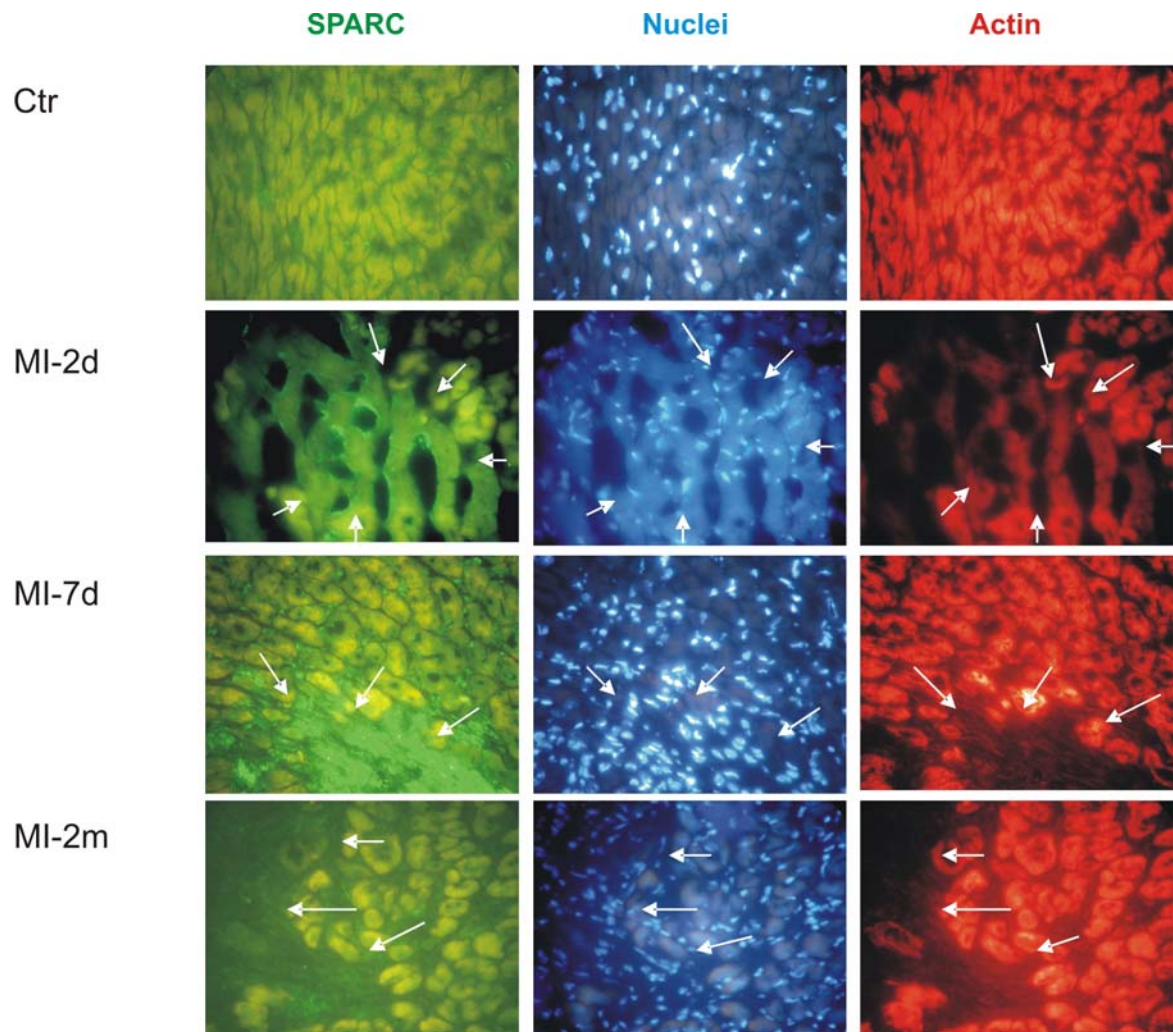
Figure 3.3 Immunofluorescence studies of mouse frozen myocardial tissue sections for SPARC, nuclei and actin after MI. Tissue sections were stained with goat anti-SPARC IgG, Alexa 546-Phalloidin (actin), DAPI (nuclei) and, followed by Cy2-anti goat secondary antibody. A, the signal of SPARC, the corresponding nuclei and actin staining in the Sham-operated group, SPARC is diffusely observed in normal myocardium section, the nuclei of cells and actin is clearly to be seen. B, after MI-2d immunostaining for SPARC is enhanced along the margin of the infarcted area, while the actin signal is reduced. C, after 7 days of MI, the SPARC staining is increased at sites of the infarcted area (arrows). DAPI staining noted a large number of nuclei in the infarcted area, while the corresponding actin staining is hardly found .D, After 2m of MI the signal of SPARC remains present in non infarcted myocardium but not in the infarcted area as seen after 7d.

2.2.4. Induction of SPARC depends on integrin α_v function

3.2.4.1.Regulated SPARC gene expression

Previously, we have observed a prominent role of integrins in modulating tissue remodeling events upon myocardial infarction.Therefore, mice that underwent myocardial infarction were simultaneously treated with a specific integrin α_v inhibitor or the vehicle control. Gene expression events observed in infarcted animals treated with the vehicle control were identical to those observed previously upon myocardial infarction and the same set of genes was found to be up regulated after 7 days (Fig. 3.4). Importantly, upregulation of SPARC expression following myocardial infarction was dependent on integrin α_v function as the inhibitor blocked the increase in SPARC mRNA at day 2 (1.42±0.37 fold) and day 7 (1.64±0.29) after myocardial infarction. This was in contrast to the 2.58±0.24 fold and 3.78±0.11 fold induction of SPARC mRNA after 2 days and 7 days after infarction in the vehicle control group, respectively.
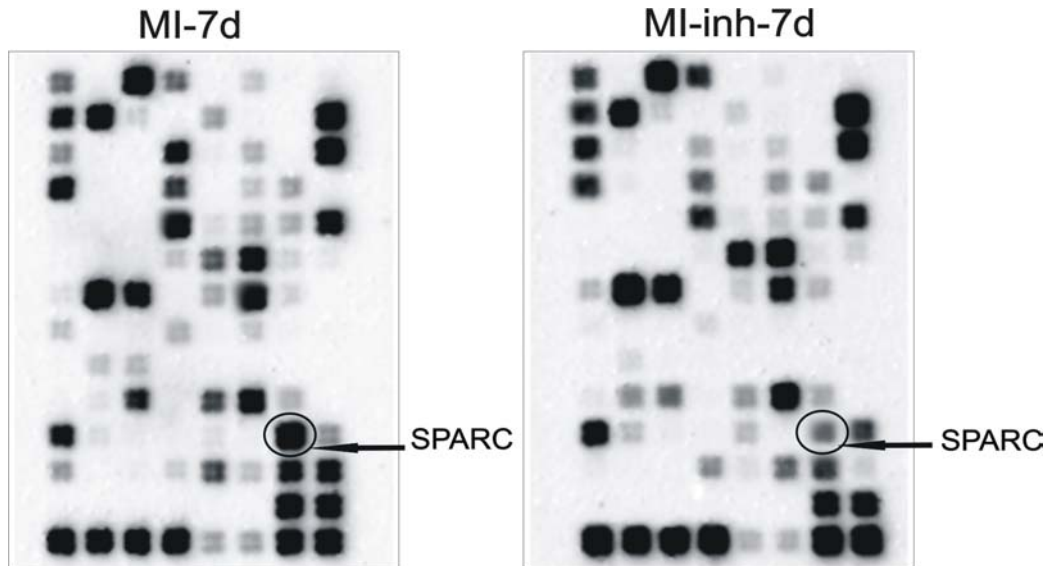
Fig 3.4 Representative gene expression profile of the effect of integrin αv on ECM gene expression. gene expression analysis in mouse myocardium 7 days after experimental myocardial infarction and sham-operated detected by cDNA expression array system. RNA was extracted from mouse heart after myocardial infarction or sham-operated. Total 5μg was reverse-transcribed and labelled in labelled with biotin, and gene expression was detected using Nonrad- GEArray Q series kit as described in method. The intensity of the data by first subtracting the average background (mean blank intensity) and then comparing intensity levels with the average intensity of the hybridization signal of the house keeping gene,

3.2.4.2. Modulation of SPARC protein level

To verify the result from the gene array, the protein level of SPARC was detected by Western blots. Again, the upregulation of SPARC protein expression was closely followed by similar increases in SPARC mRNA levels. Inhibition of integrin α_v severely blocked the increase in SPARC protein 2 days (1.58±0.24 fold vs. 2.58±0.21 fold, p>0.01, n=12) and 7 days (1.63±0.22 fold vs. 3.72±0.28 fold, p>0.01, n=12) after infarction (Fig. 3.5).
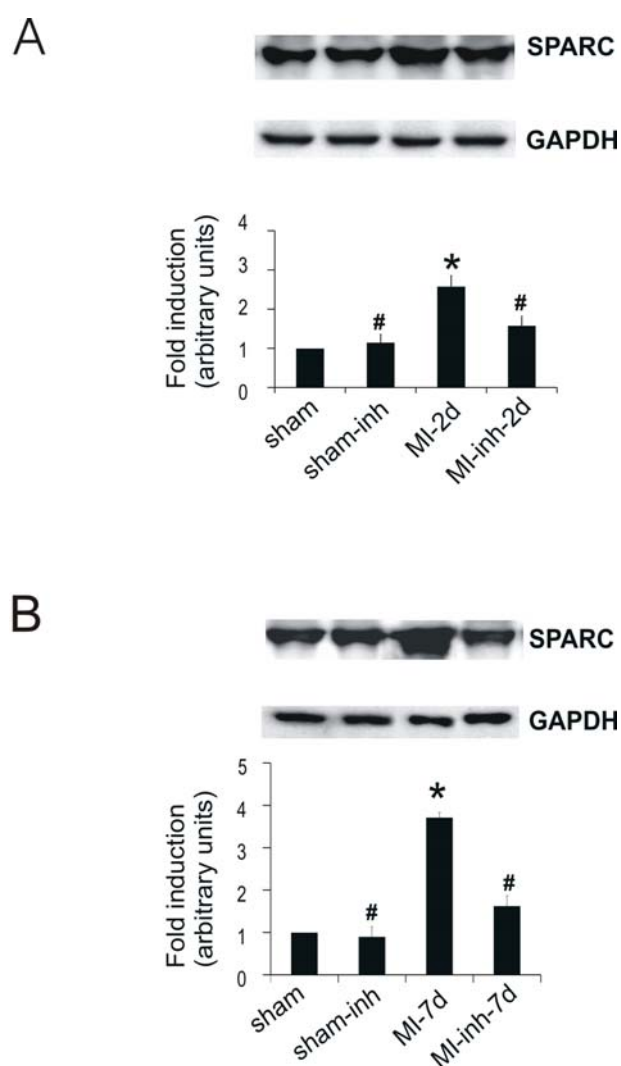
Figure 3.5 SPARC protein expression in mouse hearts 2 and 7 days after MI. Application of the α_v integrin inhibitor via mini-pumps blocked the increase in SPARC protein expression. Data are expressed as fold changes from corresponding sham-operated mice, normalized to GAPDH. Values are mean ± SEM; n= 12; * = p< 0.01 ctr vs. sham operated animals; # = p < 0.05 MI vs. MI-Inh.

3.3. Discussion

Expression and abundance of extracellular matrix proteins and their cellular receptors undergoes dramatic changes following myocardial infarction to keep up organ function. In the present study, we analyzed gene expression changes upon experimental myocardial infarction in the mouse and followed these changes in the course of the healing response up to 1 month after infarction. Most strikingly, we observed a transient and locally confined increase in SPARC expression in response to myocardial infarction. Induction of SPARC depended in part, on $_v$ integrin function and localized to the infarcted heart tissue undergoing active remodeling. our results pointed to an important role of SPARC in the transient healing response after myocardial infarction.

Several studies have indicated that SPARC expression is high during embryonic development, but usually low during normal postnatal life. However, SPARC can be induced in various tissues such as bone, gut mucosa and skin during healing responses (Holland, Harper et al. 1987; Sage, Decker et al. 1989) and enhanced SPARC expression is associated with malignant tumors (Porter, Sage et al. 1995). In these contexts, SPARC may contribute to the reorganization of connective tissue and stimulate angiogenesis (Sage, Vernon et al. 1989; Reed, Puolakkainen et al. 1993). With respect to heart tissue, SPARC is abundantly expressed in this organ during early development. In contrast, its expression in the heart is very low during adulthood (Holland, Harper et al. 1987; Sage, Vernon et al. 1989). Importantly, increased mRNA levels of SPARC have been detected in the myocardium following myocardial infarction.(Stanton, Garrard et al. 2000; Komatsubara, Murakami et al. 2003) indicating a role for SPARC in matrix remodeling during wound healing in the heart.

One of the important properties of SPARC is its anti-adhesive effect. Accordingly, SPARC can modulate the interactions between cells and their surrounding matrix by inhibiting adhesion and spreading on a collagen matrix (Sage and Bornstein 1991). In the process of repair after myocardial infarction, necrotic cells in the infarcted area are gradually resorbed and being replaced by scar tissue. Scar formation is already evident within a few days after infarction and the scar tissue is characterized mainly by a collagen- and fibronectin-rich extracellular matrix and the presence of fibroblasts. Our gene expression analysis demonstrates that SPARC is co-regulated together with several extracellular matrix proteins including collagen, fibronectin, and laminin and their enhanced transcription is detectable within 2 days after infarction. By immunostaining,

the increased SPARC protein levels were localized to the margin of the infarcted, necrotic tissue during the initial healing response. These results indicate that during the acute phase after myocardial infarction, cardiomyocytes and interstitial fibroblasts in the border zone between intact and damaged heart tissue synthesize SPARC. This early increase in SPARC might help to loosen the strong adhesive connections between surviving cardiomyocytes and connective tissue, thereby allowing the influx of fibroblasts, facilitating tissue reorganization and scar formation.

Direct SPARC induction through integrin α_v subunit has been reported in human melanoma cells. However, the molecular mechanism that connects myocardial infarction with increased SPARC expression in vivo is currently unknown. Our results established an important role for integrin α_v in the regulation of SPARC in vivo, as SPARC mRNA levels were severely compromised in infarcted animals receiving a specific integrin α_v inhibitor.

Together, our data suggest an important role for the matricellular protein SPARC in the healing response following myocardial infarction. Deposition of SPARC in the infarcted zone seems to be intimately involved in scar formation. Additionally, we suggest that SPARC has an impact not only in the direct scar area, but also in the remote regions with regard to collagen incorporation.

Whether the transient up-regulation of SPARC after myocardial infarction is essential for the maintenance of cardiac structure and function requires further investigation.

Chapter 4

Fibroblast migration is modulated by SPARC

4. Fibroblast migration is modulated by SPARC

Migration is an important process involved in development, wound healing and angiogenesis. During migration cells are required to spatially coordinate polarization, adhesion to the substratum, and actin polymerization to move the membrane in the direction of migration.

(Edin, Howe et al. 2001)

4.1 Introduction

SPARC (secreted protein, acidic and rich in cysteine) is a 43 KD matricelluar protein which is also known as BM-40 or osteonectin. The best- characterized matricellular proteins include the tenascins, thrombospondin-1 and -2 and SPARC. These proteins are secreted by numerous cell types and have multiple functions. SPARC is a secreted Ca^{2+}-binding glycoprotein, which can interact with several extracellular matrix molecules and cytokines.(Sun and Weber 2000). The protein was first purified as a major non-collagenous component of bovine bone, with binding affinity to collagenI-I(Termine, Kleinman et al. 1981; Murphy-Ullrich 2001; Wang, Fertala et al. 2005) SPARC is expressed at high levels in many different tissues and cell types in both embryonic and adult mice The precise functions of SPARC are unclear, but it appears to counter cellular adhesion when it is in solution or incorporated into a substrate (Murphy-Ullrich 2001). SPARC is believed to exert its anti-adhesive effects on many cell types, resulting in cell rounding and partial detachment from the cell substrate. Furthermore, SPARC is expressed by tissues undergoing morphogenesis and modulates the attachment and spreading of various cell types on extracellular matrixes (Paulsson, Deutzmann et al. 1986; Sage and Bornstein 1991). Recently, upregulation of gene expression in injured heart was reported (Stanton, Garrard et al. 2000). Importantly, a transient increase of SPARC protein levels after myocardial infarction was observed in our study. SPARC could be secreted by a several cell type present in the mouse heart, such as fibroblasts, endothelial cells or macrophages, but the precise cellular origin of SPARC during the remodeling of the injured heart is still speculative.

SPARC is known to bind to certain growth factors. SPARC could modulate PDGF activity during inflammation and tissue repair by limiting the availability of dimers containing the PDGF–B subunit (Raines, Lane et al. 1992). Transforming growth factor beta1 (TGF-β1) is well known as a cytokine involved in wound healing and it is also found to be up-regulated after MI mediating tissue repair (Thompson, Bazoberry et al. 1988). TGF-β1 is a distinct TGF-β isoform which is capable to stimulate the production of ECM components in a variety of cell types. TGF-β1 and SPARC have been reported to be associated with the rapid remodeling of connective tissue that occurs in wound healing and developmental processes (Wrana, Overall et al. 1991). SPARC and TGF-β1 can engage one another in a reciprocal relationship, previous studies have shown that TGF-β1 increases SPARC expression at mRNA and protein levels in fibroblasts and osteoblasts, whereas, SPARC induces TGF-β1 expression in Mv1Lu and R1B cells (Wrana, Overall et al. 1991). These data suggest that the link between SPAR and growth factors like TGF-β1 and PDGF-BB play a role in wound healing.

SPARC protein induction through β_3 integrin expression has been reported (Sturm, Satyamoorthy et al. 2002). SPARC is able to promote tumor cell migration and this activity of SPARC is functionally connected to integrins $\alpha_v\beta_3$ and $\alpha_v\beta_5$ on cancer cells (De, Chen et al. 2003). These findings suggest that tissue remodeling processes during tumor growth or wound repair are influenced by an interplay between integrins, including α_v containing receptors, and the matricellular protein SPARC. Recent studies have also indicated an increased expression of SPARC in the myocardium after injury or stress

Adequate wound healing and scar formation is an essential response to myocardial infarction (MI). Following myocardial infarction, dead tissue is necrosed and replaced by a scar composed primarily of type 1 collagen. Fibroblasts are primary cellular components regulating the process. Myofibroblasts (MyoFb) first appeared at these sites of repair on day 3 and remained abundant thereafter at all time points examined; Fibroblast migration to infracted area and proliferation is critical to the scar formation. The process of wound healing after myocardial infarction begins with clearance of necrotic myocytes and other cell debris and is closely followed by migration of myofibroblasts into the infarct zone where these cells proliferate synthesize new extracelluar matrix proteins. and mediate wound contraction to form the mature scar.Our study in chapter 3 results suggest that

SPARC, as expressed in post-MI heart, predominately in the scar area may play an important role in ongoing remodeling of the scar. SPARC's properties to interact with extracellular matrix and to promote de-adhesion of cells from the matrix, contribute to a cellular state conducive to migration.

In this study, we further investigated the expression and regulation of SPARC in isolated cell types in vitro and followed the hypothesis that SPARC expression might be induced by integrins and increased SPARC levels may account for scar formation after myocardial infarction via fibroblasts invasion.

4.2. Results

4.2.1. Induction of SPARC by TGF-β1 and PDGF in fibroblasts and cardiomyocytes

The local distribution of SPARC in the infarcted heart could result from its expression by either cardiomyocytes or invading fibroblasts. To investigate the cellular origin of SPARC and the role of integrin α_v in this process, we compared SPARC secretion by isolated mouse fibroblasts and neonatal rat cardiomyocytes. Cardiomyocytes were isolated as described in Material and Methods and stained for the cardiomyocyte-specific protein troponin. Cultures of primary cells contained more than 95% of troponin-positive cells (Figure 4.1). To analyse SPARC expression by different cell types, fibroblasts and isolated neonatal rat cardiomyocytes were preincubated in serum-deprived medium for 12 h and then incubated for 72h with TGF-β1or PDGF in the serum-free medium. Due to the limited viability of cells in serum-free medium, we could maintain cardimyocytes and fibroblasts under the serum-starved condition for only a maximum of 72 h. Faint levels of accumulated SPARC protein after 36 –h incubation under non-stimulus conditions were detected. However, there are no significant different between the TGF-β1 stimulated cells and untreated cells. (data is not shown) This weak protein expression may indicate that SPARC was able to be slowly released from the intracellular pool after serum-starvation (Gooden, M.D. et al.,).SPARC protein in the culture medium was detected by western blots (Figure 4.2). By using an anti-SPARC antibody, obvious immuno-staining for SPARC was observed in myocardial cells of rat neonatal cardiac tissue (Figure 4.1). In both cases, basal SPARC secretion in serum-free medium was low, but could be strongly induced upon treatment of the cells with either platelet-derived growth factor (PDGF-

BB) or TGF-β1. Interestingly, plating of fibroblasts or cardiomyocytes onto vitronectin, a well characterized ligand for integrin α_v, had no effect on SPARC expression in cardiomyocytes or fibroblasts However, SPARC expression in isolated cardiac myocytes could be strongly stimulated by TGF-ß1 (2.8±0.1fold, p<0.01) and PDGF (2.3±0.3 fold, p<0.01)(Fig. 4.2A). Similarly, treatment of fibroblasts with either TGF-ß1 (3.9±0.26 fold, p<0.01) or PDGF (3.2±0.30 fold, p<0.01) significantly increased SPARC expression as compared to untreated cells (ctr) (Fig. 4.2 B). Consistent with the failure of VN to stimulate SPARC expression, inhibition of integrin α_v did not interfere with TGF-β1 or PDGF stimulated SPARC secretion as determined by ELISA assays (Fig 4.3.A and 4.3.B). SPARC secretion by fibroblasts in response to TGF-β1 or PDGF was considerably higher (TGF-β1: 855ng/ml±46; PDGF: 721ng/ml±44) than the levels of SPARC secreted by cardiac myocytes (TGF-β1: 220ng/ml±33; PDGF: 189ng/ml±25) (Fig. 4.3 A and 4.3 B). These results suggested that the effect of integrin α_v on SPARC expression in vivo might be indirect and integrin α_v might function upstream from growth factor mediated stimulation of SPARC expression.

Induction of SPARC by TGF and PDGF in cardiomyocytes
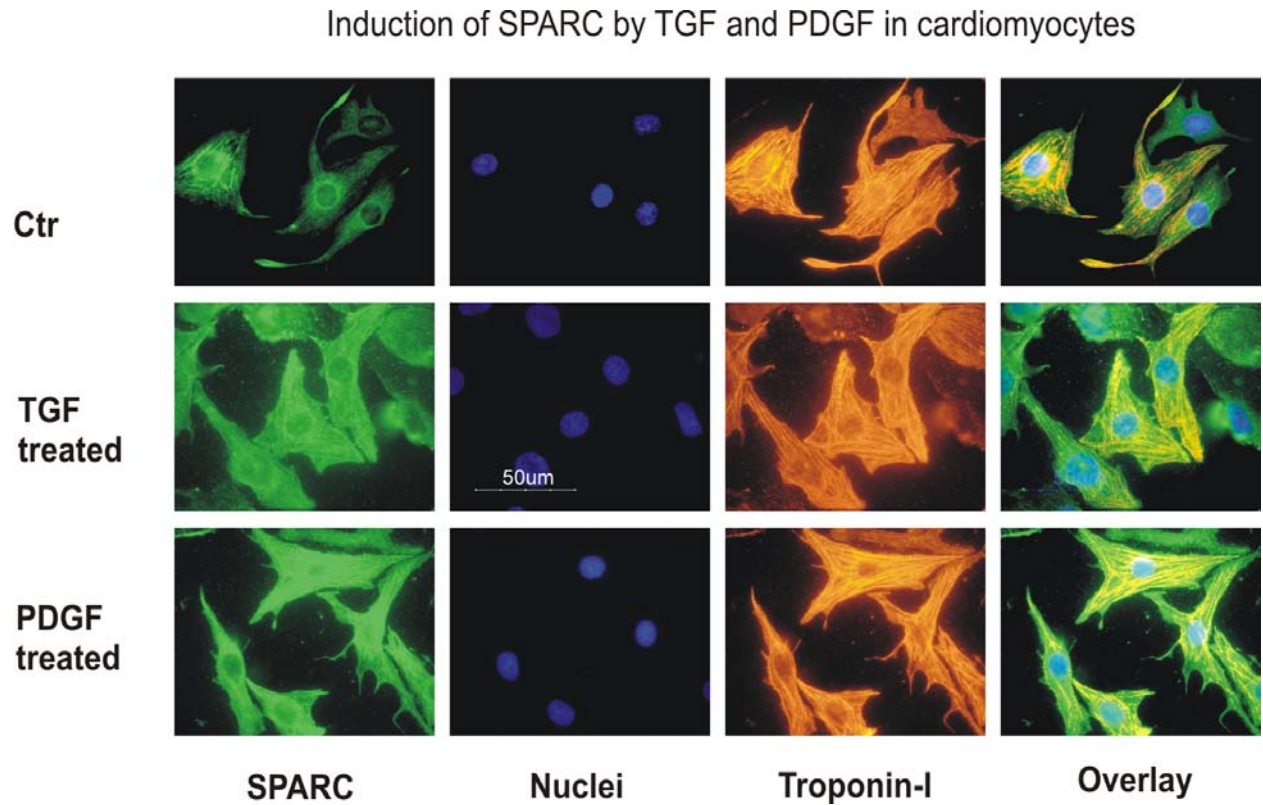
Troponin-I staining for cardiomyocytes
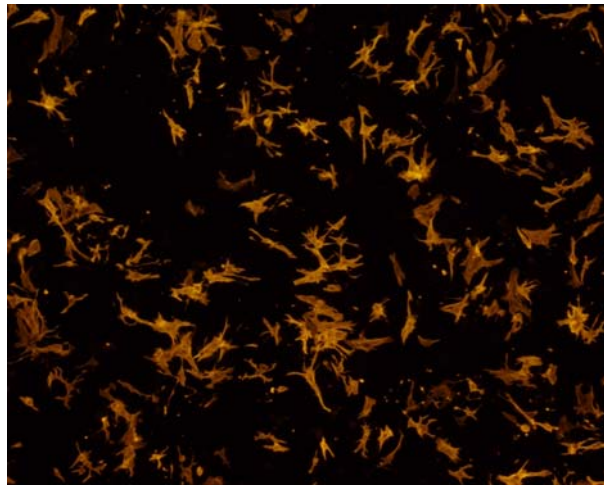
Figure 4.1. .Induction of SPARC expression in neonatal rat cardiomyocytes. Cardiomyocytes were isolated from neonatal rats, cultured and serum starved cells were treated by adding TGF-ß 1 (5µg/ml) or PDGF-BB (5µg/ml) for 72 hours before fixation. Immunofluorescence was performed with anti-SPARC, anti-troponin-I and DAPI as indicared. Cardiomyocytes were identified by troponin-I staining which is only expressed in cardiomyocyte. SPARC expression in untreated cardiomyocytes is predominantely perinuclear. After Growth factor stimulation there was a clear increase in SPARC immunoreactivity in the cytosol of cardiomyocytes. All figure s are of the same magnification. Scale bar =50um as indicated,
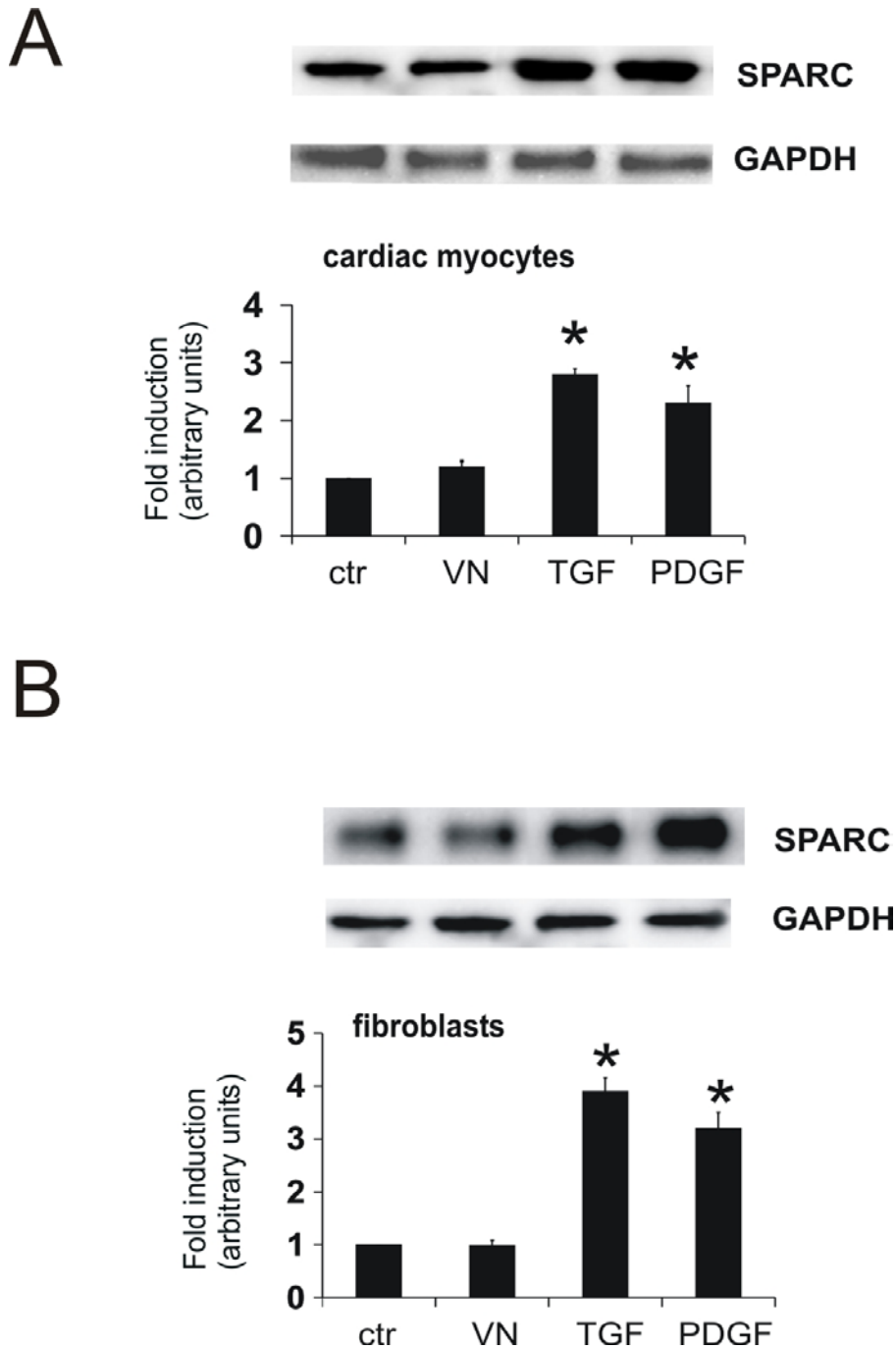
Figure 4.2 SPARC expression in cardiac myocytes and fibroblasts. Cultured cardiac myocytes (A) or fibroblasts (B) were stimulated with TGF-ß1 (5ng/ml) PDGF-BB (5ng/ml) or vitronectin (1µg/ml) respectively. Expression of SPARC was analysed by Western blotting of conditional medium from cultured rat neonatal myocardial cells with a anti-SPARC antibody (upper panel). Culture medium from equal amounts of cells (2x10 [5]) was loaded in each lane. In parallel, GAPDH was detected in the same samples with a monoclonal/polyclonal antibody (middle panel). Bar graphs depict mean values of the fold induction of SPARC expression in cardiomyocytes (A) or fibroblasts (B) ± sem compiled from three separate experiments. * $p<0.05$ vs untreated myocardiocytes or fibroblasts, respectively.
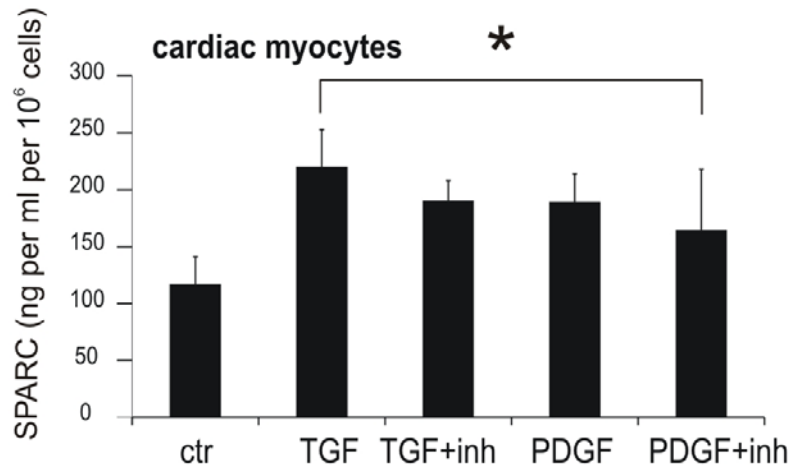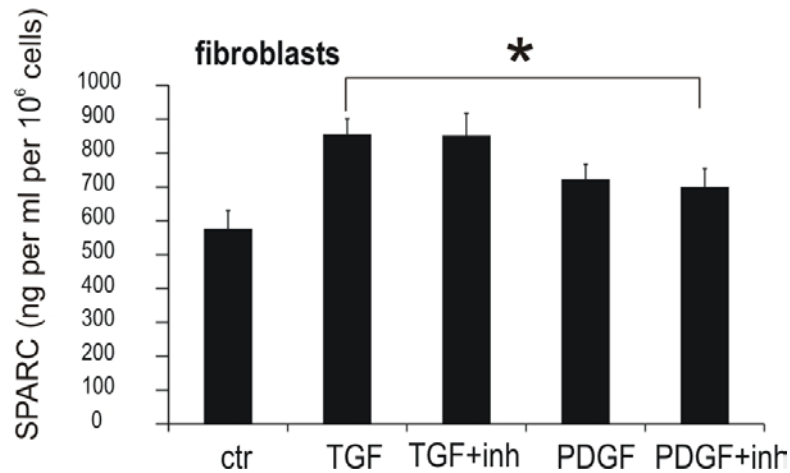
Figure 4.3 SPARC secretion by neonatal rat cardiac myocytes and mouse fibroblasts as measured by enzyme-linked immunosorbent assay. Cardiac myocytes (A) or fibroblasts (B) were treated by TGF-ß1 (5ng/ml) or PDGF-BB (5ng/ml) with or without integrin α_v inhibitor (10mM) for 72 hours. SPARC secretion (ng/10^6 cells) was determined in conditioned culture medium using the SPARC ELISA kit according to the manufacturer's protocol. Bars represent the concentration of SPARC in different samples. Values are the mean ± SEM, *p<0.05 vs. untreated cells (n=12)..

4.2.2. Vitronectin stimulates TGF-β1 and PDGF expression in cardiac myocytes

To investigate if integrin α_v engagement might indirectly impact on SPARC gene expression by modulating the secretion of growth factors, we studied TGF-β1 and PDGF-BB expression in cardiac myocytes after stimulation with vitronectin. Vitronectin is a major ligand for the vitronectin receptors integrins $\alpha_V\beta_3$ or $\alpha_V\beta_5$. We observed that incubation of isolated cardiac myocytes with vitronectin (1µg/ml) significantly increased the secretion of TGF-β1 (423 ±115 pg/ml; n=12, p<0.05) as well as PDGF (84±17pg/ml; n=12, p<0.05) as compared to untreated cells (Fig.4.4 A and B). This increase was completely abrogated by addition of an integrin α_v inhibitor. Interestingly, no significant stimulation of TGF-β1 and PDGF expression by vitronectin was observed in fibroblasts (figure 4.5).

Together, the data obtained with isolated cells suggested that in vivo a cross-talk between different cell types might finally lead to SPARC secretion and that the initial VN-induced and integrin α_v-mediated growth factor release from cardiac myocytes might promote strong SPARC expression predominantly by fibroblasts (Figure 4.6)
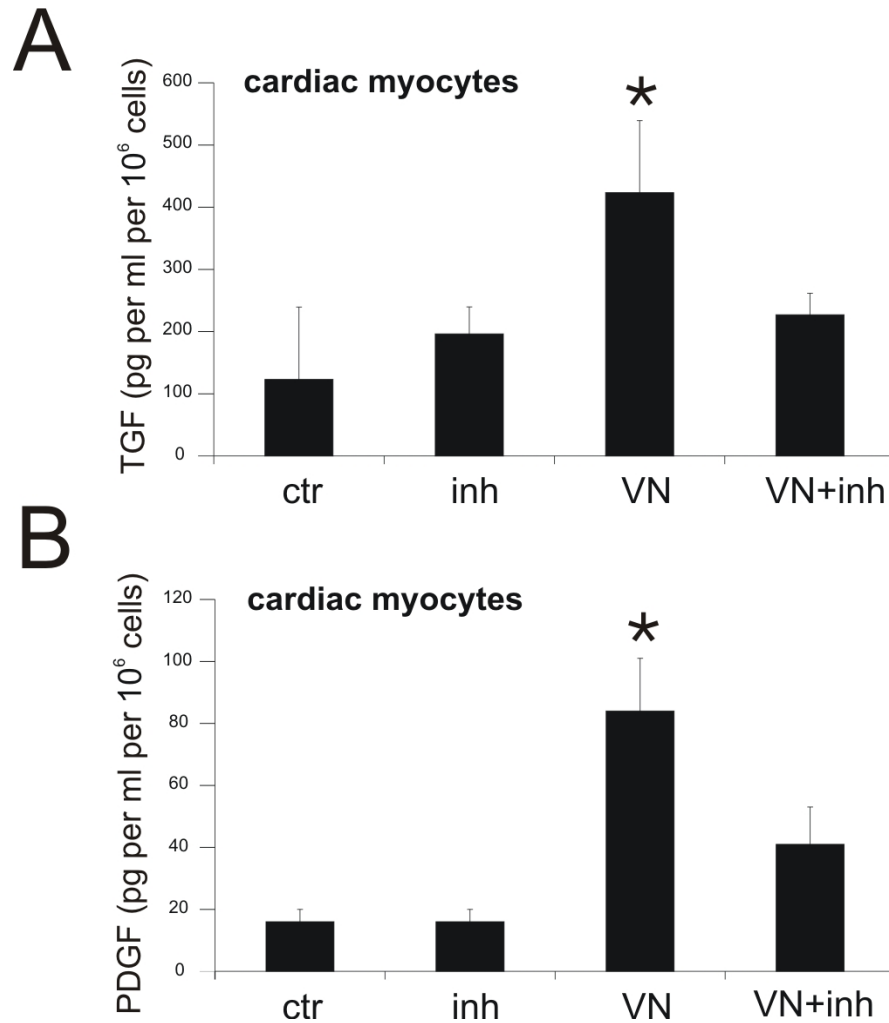
Figure 4.4 Induction of growth factors by vitronectin in neonatal rat cardiac myocytes. Vitronetin treated of cardiac myocytes increase A) TGF-β1and B) PDGF-BB protein levels in cardiac myocytes. The increase was abrogated by addition of Integrin αv inhibitor. Serum staved neonatal cardiac myocytes were treated by either vitronectin (1ug/ml) or PBS (ctr) with or without integrin α_v inhibitor (10mM) for 72 hours. TGF-β1 and PDGF-BB content (pg/10^6 cells) was derermined in conditioned medium using the TGF-β1 and PDGF-BB ELISA kit respectively according to the manufacturer's protocol. Bars represent the concentration of SPARC in different groups. Each treatment was performed in triplicate. Cell numbers were determined and protein values were normalized to cell number. Values are the mean ± SEM, *P<0.05 vs. untreated cardiac myocytes (n=12).
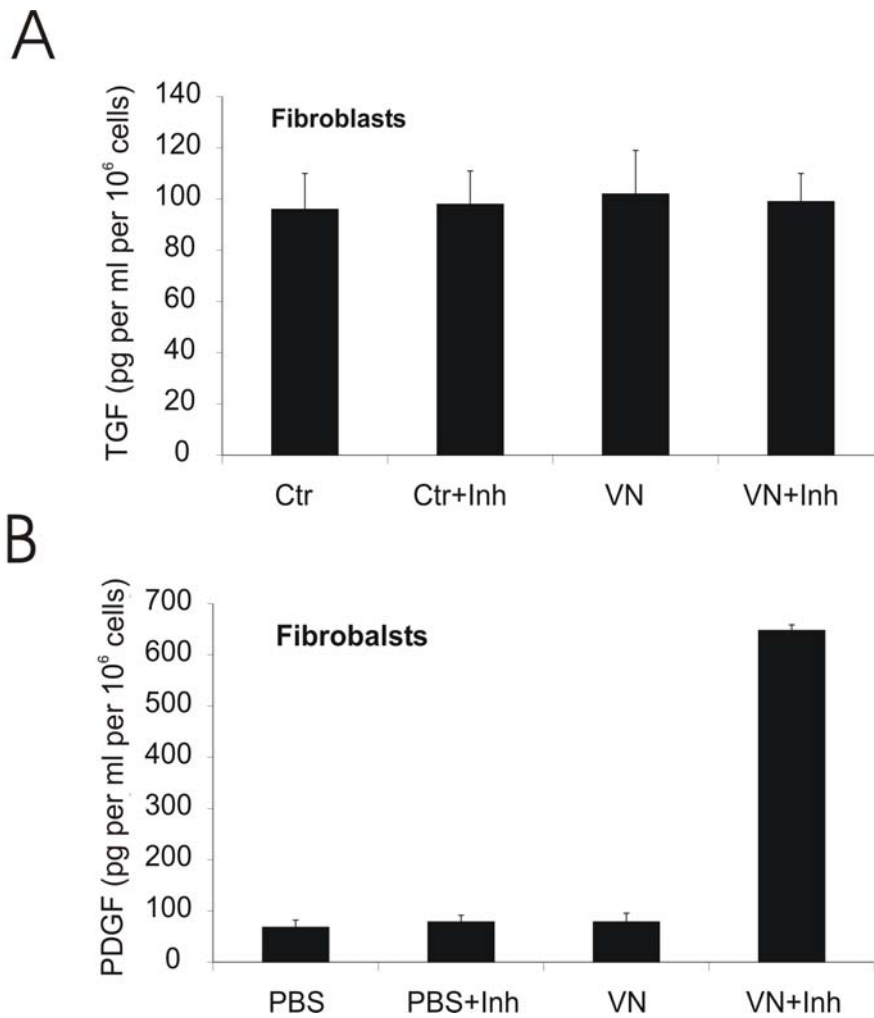
Figure 4.5 Induction of growth factors by vitronectin in fibroblasts. Serum staved neonatal cardiac myocytes were treated by either vitronectin (1ug/ml) or PBS (ctr) with or without integrin α_v inhibitor (10mM) for 72 hours. TGF-β1 and PDGF-BB content (pg/10^6 cells) was derermined in conditioned medium using the TGF-β1 and PDGF-BB ELISA kit respectively according to the manufacturer's protocol. Bars represent the concentration of growth factorsin different groups. A) Treatment fibroblasts with either vitronetin or integrin αv inhibitor did not impact on TGFβ1 expression as indicated in the figure. B) PDGF-BB protein levels in fibroblast were not influenced by treatment of either vitronectin or inhibitor alone. But there is a induction of PDGF-BB by treatment of combinations of vitronectin and integrin αv.. Each treatment was performed in triplicate. Cell numbers were determined and protein values were normalized to cell number. Values are the mean ± SEM, *P<0.05 vs untreated fibroblasts.
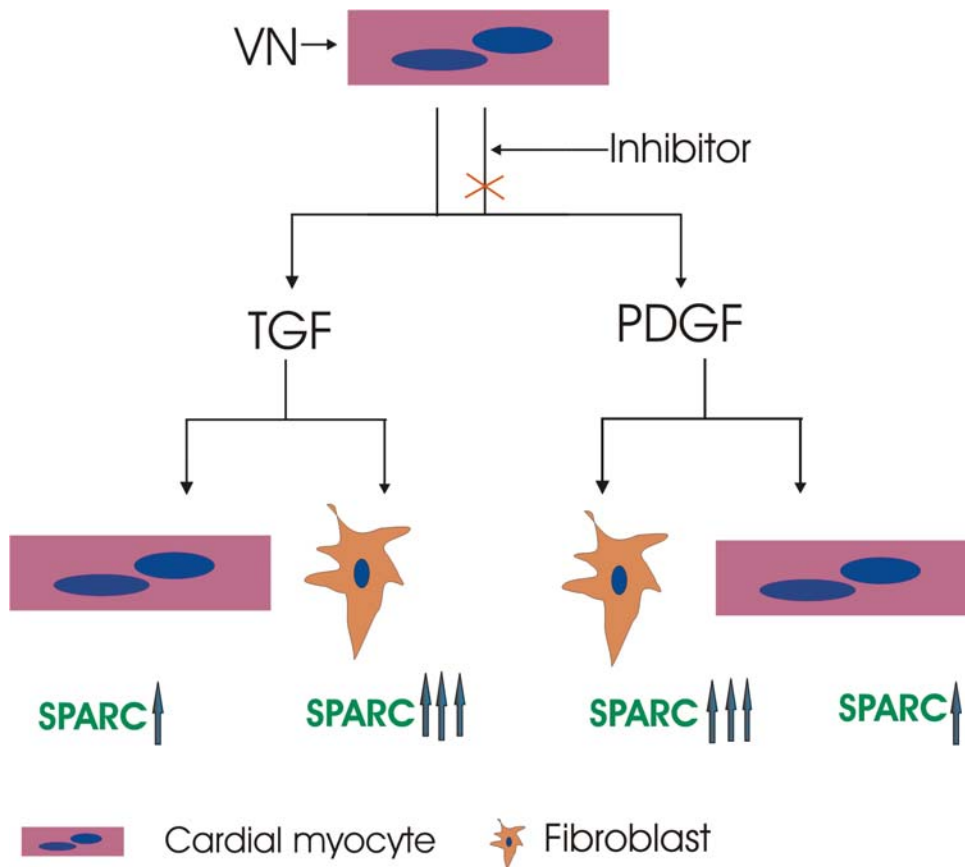
figure 4.6 Schematic drawing of induction of SPARC expression. Treatment with vitronectin increases the expression of growth factors (TGF-β1 and PDGF-BB) by cardiac myocytes. Secreted growth factors promote strong SPARC expression predominantly by fibroblasts. Induction of SPARC expression by the growth factors could not be interfered by integrin αv inhibitor directly in the same cells, but expression of the growth factors itself by cardiac myocytes could be abrogated by addition of integrin αv inhibitor .Symbols present cardiac myocyte and fibroblast are indicated.

4.2.3. Behavior of SPARC in FN inducted migration of fibroblasts

4.2.3.1.SPARC modulates the haptotaxis response of fibroblasts towards fibronectin

The experiments described in chapter 2 and chapter 3 demonstrated a transient up-regulation of SPARC during the remodeling of the injured mouse heart in vivo. Furthermore, increased ECM gene expression after aortic banding or myocardial infarction was observed in our study. Fibronectin (FN) is involved in many cellular processes, including tissue repair, embryogenesis, blood clotting, and cell

migration/adhesion. Fibronectin sometimes serves as a general cell adhesion molecule by anchoring cells to collagen or proteoglycan substrates. FN also can serve to organize cellular interaction with the ECM by binding to different components of the extracellular matrix and to membrane-bound FN receptors on cell surfaces(Farhadian, Contard et al. 1995).To get an idea about the functional significance of SPARC during wound healing, we analyzed the haptotaxis response of fibroblasts on a fibronectin (FN) matrix in the presence or absence of SPARC. Haptotaxis is the directed movement of cells induced by a gradient of an immobilized stimulus such afrom chemotaxis that is induced by soluble stimuli.

To this end, modified Boyden migration chambers were coated on the underside of the membrane with different combinations of FN and SPARC and fibroblasts seeded into the top compartment were allowed to migrate for 7 h. Clearly, FN-coated chambers stimulated a dose-dependent migratory response, whereas in control chambers, where the membrane had been coated with BSA, fibroblasts did not migrate from the top to the bottom compartment (Fig.4.7). Interestingly, coating with a combination of FN and a constant amount of SPARC (1 µg/ml) led to an increased haptotaxis response for each FN concentration tested as compared to the response towards FN alone. In an attempt to specifically abrogate the effect of SPARC, a SPARC antibody was used, whose specificity was demonstrated in previous experiments (chapter 3). The effect of SPARC could be blocked by adding a polyclonal anti-SPARC antibody (Santa Cruz) at 1ug/100ml (anti SPARC 100 ul and SPARC 1µg incubated at RT for half an hour) demonstrating the specificity of SPARC-mediated enhancement of FN-stimulated migration.
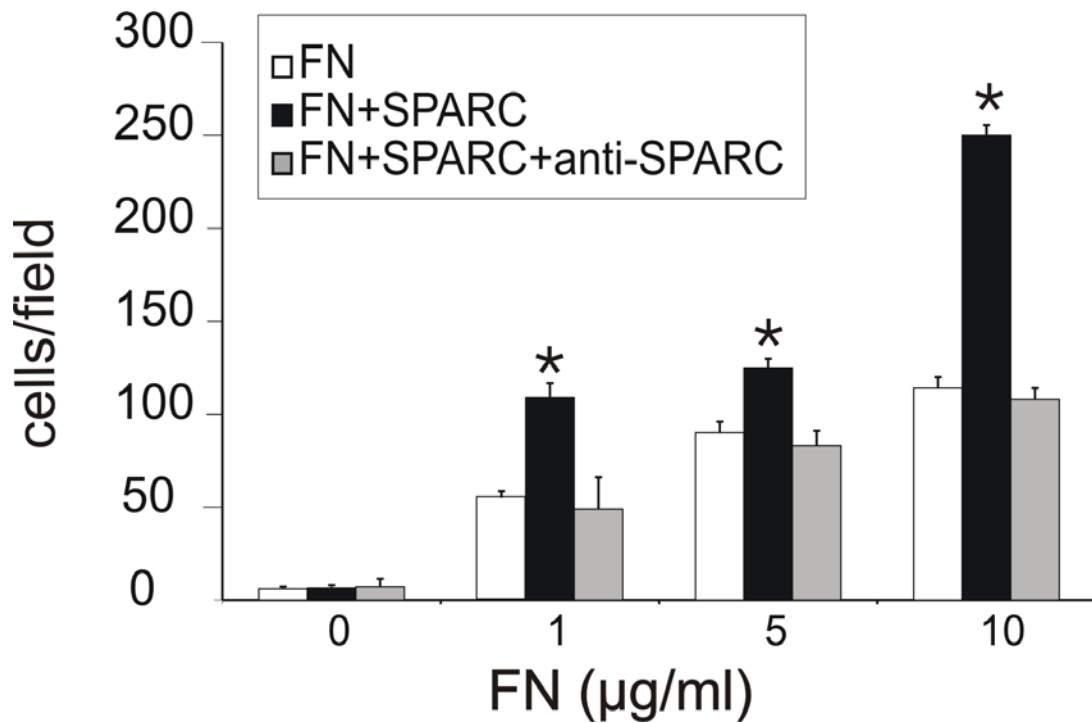
Figure 4.7 Effect of SPARC on FN-induced fibroblasts migration. The migration behaviour was assessed in haptotaxis assays using modified Boyden migration chambers coated with fibronectin (FN) at the indicated concentrations in the absence (open bar) or the presence of SPARC (1µg/ml; closed bar) and the combination (FN and SPARC) with a specific SPARC antibody for two hours (gray bars) The results are expressed as numbers of migrated cells in 8-10 random fields/chamber at 20x power. Serum starved fibroblasts were employed in the migration chambers. After migration 7 h, cells on the lower side of the membrane were fixed, stained, and counted. ''0'', ''1'', ''5'',''10'' were the respective concentration of FN (µg/ml) as indicated in the figure, diluted in EMDM media only. No migration was observed when absence of FN. There is an elevated fibroblasts migration with rising fibrometin concentration. The combination of FN and SPARC further promotes the migration with a significant difference as compared to that FN used alone Addition of an anti-SPARC antibody abolishes effects of SPARC on FN-induced cell migration. Bars represent means ± S.D. from three independent experiments. Error bars represent the standard error of the mean. *$P<0.05$ vs absent SPARC

4.2.3.2. Effect of SPARC on haptotaxis response of fibroblast is concentration dependent

The effect of SPARC on FN –stimulated cell migration have been studied previously in other cell types. However, whereas in some cases a negative effect of SPARC on cell migration has been observed (hagan, S 2003), other results have found a supporting role of SPARC on cell migration. These contrasting results might be due to the use of different concentrations of SPARC, as dependent on the concentration SPARC exerted either a promotive or a counteracting effect on cell migration. Interestingly, SPARC on its own at concentrations ranging from 1 to10 µg/ml did not influence cell motility (Fig.4.8). Again, a combination of fibronectin (1 µg/ml) and low concentrations of SPARC (1 µg/ml) enhanced FN-stimulated fibroblast migration. In contrast, when higher SPARC concentrations (5 – 10 µg/ml) were combined with a given concentration of fibronectin (1 µg/ml), the promigratory activity of SPARC was reversed and an inhibitory effect of SPARC was observed This inhibitory effect of SPARC at higher concentrations could be overcome by addition of 0.5% FBS demonstrating that the used commercial preparation of SPARC was not contaminated by general inhibitors of cell migration (Fig 4.8).

To further provide evidence for the purity of the used SPARC preparation we separated the commercial SPARC preparation by SDS-PAGE and performed silver staining of the resulting gel (Figure 4.9). Whereas low concentrations from 1 µg of SPARC could be easily observed, no additional protein bands in the size range from 10 – 80 kDa could be detected. In addition, 500 ng or 1 µg of the growth factors TGF and PDGF, respectively, were readily detected by the silver staining. From this experiment we conclude that the SPARC preparation we used was not only devoid of TGF and PDGF but also devoid of other protein contaminations.

Finely, our results provide evidence that SPARC can modulate ECM-triggered haptotaxis of fibroblasts. Furthermore, these data are in line with the idea that SPARC acts as a switch to first promote and then at higher concentrations to shut off fibroblast migration during tissue remodeling events. (Figure 4.11)
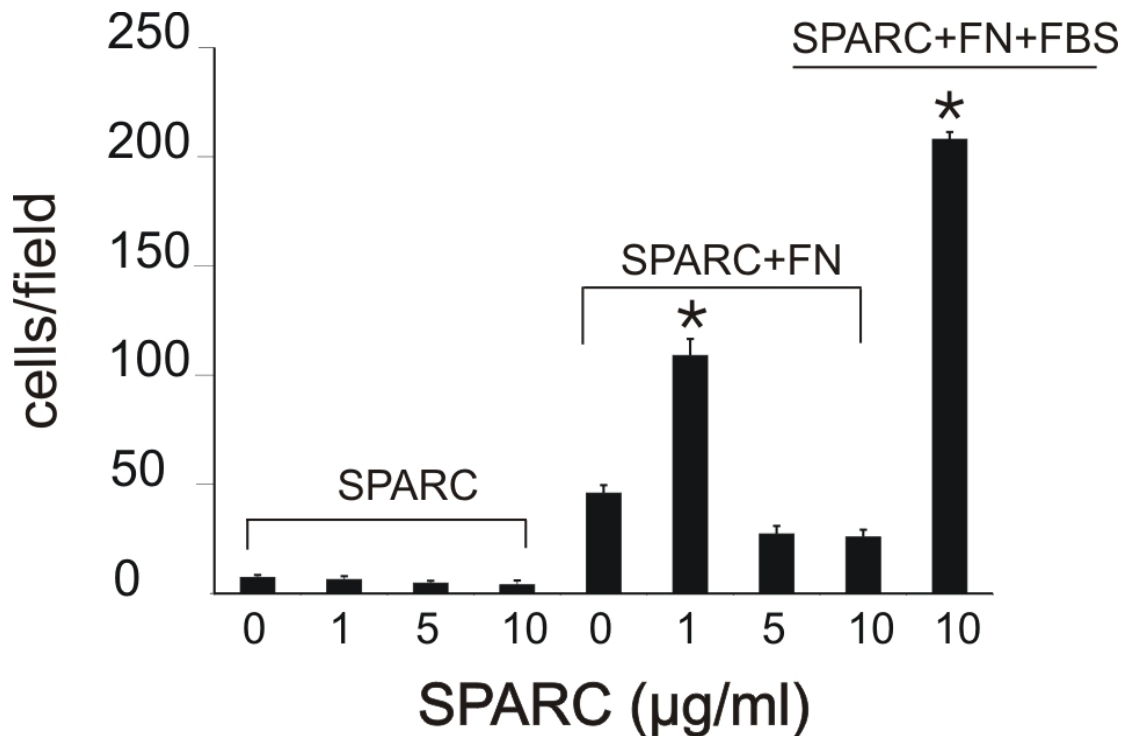
Figure, 4.8 Concentration dependent effect of SPARC on Haptotaxis of fibroblasts. The haptotaxis was analysed in Boyden chambers coated with SPARC at the indicated concentrations in the absence or the presence of FN (1µg/ml) Results are expressed as counted migrated cells in 8-10 random fields/chamber at 20x power. Serum starved fibroblasts were employed in the migration chambers. After migration 7 h, cells on the lower side of the membrane were fixed, stained, and counted. ''0'', ''1'', ''5'',''10'' were the respective concentration of SPARC (µg/ml) as indicated in the figure, diluted in EMDM media only. No migration was observed when SPARC at concentrations ranging from 1 to10 µg/ml used alone. Whereas low concentrations of SPARC enhance FN-initiated haptotaxis, higher SPARC concentrations have an inhibitory effect. Addition of FBS (0.5%) overcomes the inhibitory effect of high amounts of SPARC, demonstrating that purified SPARC is not contaminated with general inhibitors of migration. Bars represent means ± S.D. from three independent experiments. Error bars represent the standard error of the mean *P<0.05 vs absent of SPARC
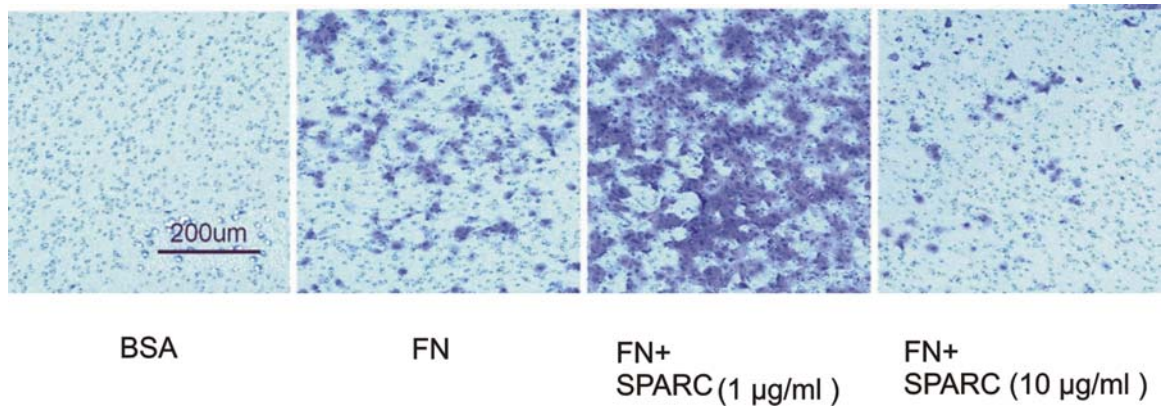
Figure 4.9 representative fields of view from migration. Millicell modified Boyden chambers were employed in haptotaxis assays, the lower surface of the Millicell polycarbonate membrane was coated on the underside of the membrane with 0.1% BSA, 1µg FN and different combinations of FN and SPARC respectively. SPARC increased FN-stimulated fibroblast migration at a low concentration (1µg/ml). the migration towards a source of combination of FN and SPARC was diminished at a high level of SPARC (10µg/ml)
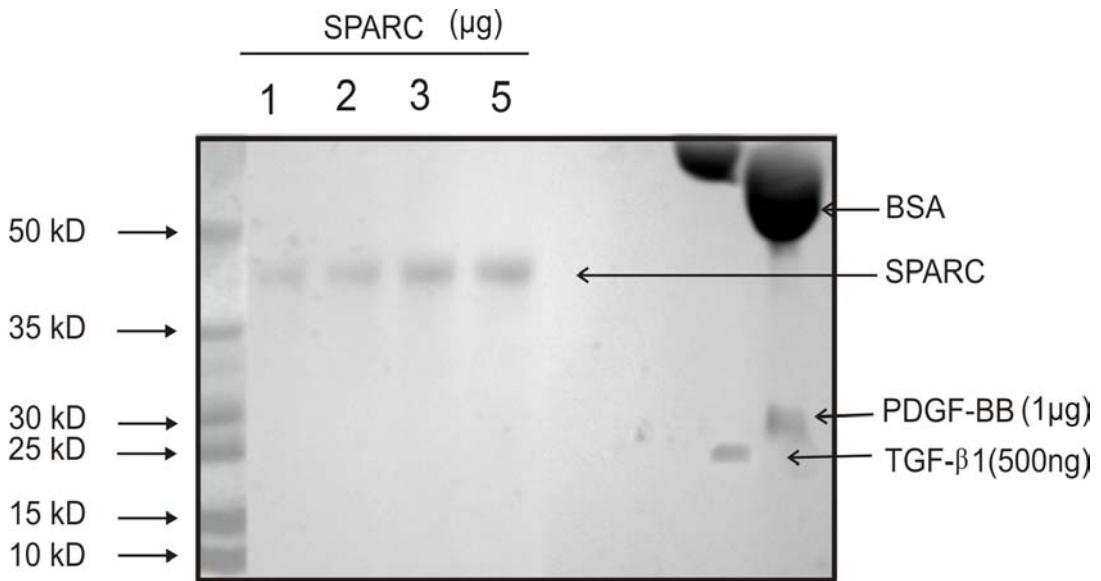
Figure 4.10 SPARC Silver staining of a SDS gradient gel (4-12%). Different amounts of the commercial SPARC preparation were separated by SDS-PAGE. 500 ng TGF and 1 µg PDGF (in 0.5% BSA solution) were used as growth factor standards. After silver staining low concentrations of SPARC (1 µg) or of the growth factors (500 ng) could be easily detected. No contamination of the SPARC preparation with addlitional proteins was observed.
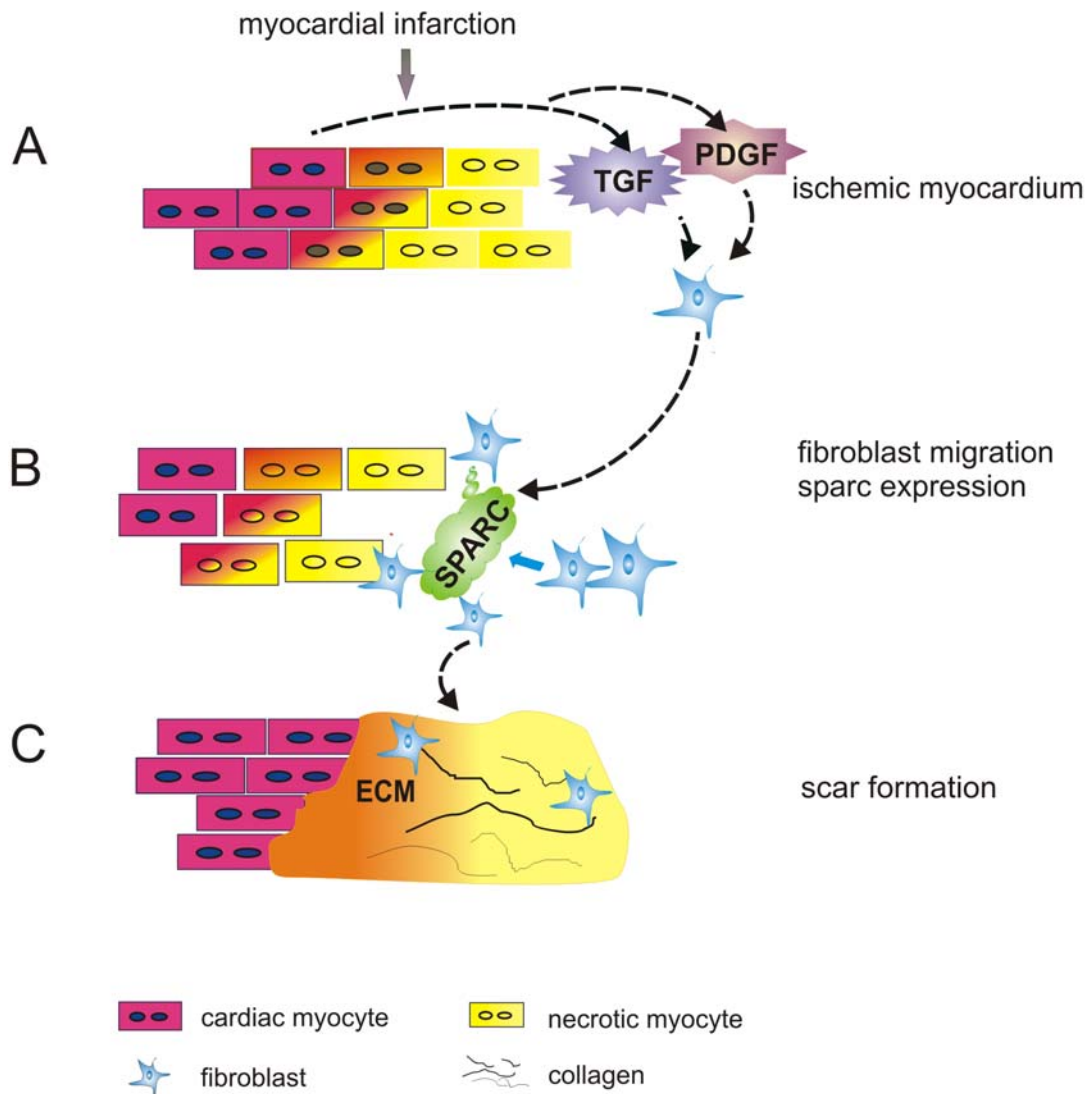
Figure.4.11. Schematic drawing summarizing wound healing processes after myocardial infarction (MI) with special regard to SPARC expression and fibroblast migration. A) As a result of myocardial ischemia there is an increased expression of growth factors (e.g. TGF and PDGF), These growth factors mainly act on fibroblasts. B) SPARC expression from fibroblasts may open up spaces for the invading fibroblasts (activated by TGF/PDGF) and simultaneously act as haptotactic stimulus to promote further fibroblast migration. C) Fibroblasts eventually cause wound healing and scar formation after myocardial infarction with deposition of collagen. In our model, especially SPARC causes fibroblast migration to the resulting scar area.

4.3. Discussion

The molecular mechanism that connects myocardial infarction with increased SPARC expression in vivo is currently unknown. To this point, our results clearly establish an important role for integrin α_v in the regulation of SPARC in vivo, as SPARC mRNA levels were severely compromised in infarcted animals receiving a specific integrin α_v inhibitor.

However, stimulation of isolated cardiac myocytes or fibroblasts with vitronectin, a well characterized ligand for integrins $\alpha_v\beta_3$ and $\alpha_v\beta_5$, failed to induce SPARC secretion in vitro suggesting that integrin α_v has an indirect role in the upregulation of this matricellular protein. Our further experiments point to growth factors such as TGF-β1 and PDGF that moderately induce SPARC secretion in isolated rat neonatal cardiac myocytes, but very strongly in fibroblasts. In addition, these growth factors have been shown to increase SPARC expression in human gingival fibroblasts, rabbit articular chondrocytes, and human pulp cells (Wrana, Overall et al. 1991; Zhou, Hammonds et al. 1993; Reed, Vernon et al. 1994; Shiba, Fujita et al. 1998).

Although growth factor cDNAs were not included on the GEArray and therefore, their regulation was not examined after myocardial infarction in the present study, the level of TGF-β1 is strongly enhanced in infarcted compared to non-infarcted myocardium within 2 days after coronary artery ligation in the rat (Thompson, Bazoberry et al. 1988; Deten, Holzl et al. 2001). The measurement of TGF, PDGF and SPARC secreted from isolated cells in vitro suggests a coordinated sequence of events, where in a first step integrin α_v engagement on cardiac myocytes causes an upregulation of TGF and PDGF. Inhibition of integrin α_v can abrogate this vitronectin-mediated increase in growth factor secretion. In a second step, we envision that SPARC expression is increased moderately after TGF and PDGF stimulation of cardiac myocytes in an autocrine manner. At the same time, the growth factors secreted by cardiac myocytes promote a strong increase in SPARC expression by fibroblasts. Such a two step process that requires communication between different cell types would also help to explain, why specific integrin α_v inhibition, though severely interfering with SPARC expression in vivo, did not block growth factor induced SPARC expression in vitro. Furthermore, it is also key to understand the failure of vitronectin to directly stimulate a significant level of SPARC expression by isolated cardiac myocytes or fibroblasts.

Together, these observations indicate a complex interplay between growth factors, integrins and the induction of ECM and matricellular proteins that mediate the healing response in the infarcted heart. Recent work has also demonstrated, that SPARC itself can upregulate TGF-ß1 and this upregulation accounts for the secretion of collagen I in different cell types(Schiemann, Neil et al. 2003; Francki, McClure et al. 2004). Most importantly, to understand how SPARC exerts its counteradhesive effect in MI remodeling, the modulation of SPARC in fibroblast was investigated. Our results provide novel insight into the functional role of SPARC in cell migration induced by immobilized ECM proteins. Clearly, SPARC alone did not serve as a haptotactic stimulus for fibroblasts. However, in combination with fibronectin, low concentrations of SPARC (1 µg/ml) consistently elevated the pro-migratory effect of fibronectin. These results are in line with previous reports that have indicated a positive effect of SPARC on fibronectin-induced cell migration (Rempel, Golembieski et al. 2001) Surprisingly, increases in SPARC concentration in the context of constant amounts of fibronectin resulted in an impairment of fibronectin-stimulated haptotaxis. These data suggest that the balance between SPARC and fibronectin determines the effect of these proteins on cell migration. Indeed, cell migration on extracellular matrix substrates requires an optimum balance between adhesion and detachment to allow efficient movement of adherent cells. The coexistent effects of SPARC on promotion and inhibition of migration has been also observed in a glioma cell line (Rempel, Golembieski et al. 2001). As SPARC modulates cellular adhesion to the ECM by direct interaction with several ECM proteins (Brekken and Sage 2000), the concentration of SPARC and more importantly the ratio between SPARC and its binding partners in the ECM might influence fibroblast migration in a positive or negative way. It is interesting to speculate in this context, that the transient accumulation of SPARC in the infarct zone might initially contribute to enhanced fibroblast migration into this area, whereas later, with higher SPARC concentrations, further fibroblast migration will be diminished. Clearly, studies with SPARC-deficient mice have demonstrated that this protein is required for a proper wound healing response and efficient cell migration in skin (Basu, Kligman et al. 2001) and this is consistent with our findings in the mouse heart after experimental myocardial infarction.

Together, our combined in vivo and in vitro data suggest an important modulatory role for the matricellular protein SPARC in the healing response following myocardial

infarction. Deposition of SPARC in the infarcted zone seems to be intimately involved in scar formation presumably by promoting the migration of fibroblasts. Whether the transient up-regulation of SPARC after myocardial infarction is essential for the maintenance of cardiac structure and function requires further investigation.

Materials /Methods

5. Materials

5.1. Animals

Wild type adult male and female C57/black mice (Charles River, Sulzfeld, Germany, weighing 22-25 g., at the beginning of the study) ; Pregnant rats were from Charles River, Sulzfeld, Germany; Adult ß1 knockout mice were obtained from Dr. R. Fässler (Max-Planck-Institute of Biochemistry, Martinsried, Germany). Cre-knock out mice with a myosin light chain 2v driven promotor for cardiac specificity were obtained from Dr. Ken Chien (University of San Diego, CA, USA). All the animals were closely monitored for clinical signs of heart failure until echocardiographic, hemodynamic, and molecular analyses, which were performed 2days, 7 days, and one month after MI. All procedures were approved by the institutional animal research committee and kept under conventional conditions in the animal facilities in 'Medizinische Universitätsklinik' University of Würzburg. Experimental were performed in according to the animal care guidelines of the American Physiological Society.

5.2. Cells:

Mouse fibroblasts

Neonatal rat cardiac myocytes

5.3. Antibodies

Primary antibldy	Application	Size (kDa)	Dilution	Ig	Company
Biotinylated-SPARC	WB	42	1:500	Steptavidin-peroxidase	B&D System Inc. MN ,U.S.A. BAF 941
SPARC	Immuno		1:100	Goat polyclonal	Santa-Cruz-Biotechnology,Inc., Santa Cruz, U.S.A. Sc-13326

Troponin I	Immuno		1:500	Rabbit polyclonal	Santa-Cruz-Biotechnology,Inc., Santa Cruz, U:S.A. Sc-15368
Integrin αV	WB	25 and 27	1:500	Rabbit polyclonal	Chemicon Inernational, Inc., Temecula, U.S.A. AB1930
Integrin β1	WB	130/140	!:1000	Armenian hamster monoclonal I	Santa-Cruz-Biotechnology,Inc., Santa Cruz, U:S.A.
Timp2	WB	24	1:1000	Mouse anti-human	Chemicon Inernational, Inc., Temecula, U.S.A. MAB3310
GAPDH	WB	37	1:4000	Anti-mouse	Chemicon Inernational, Inc., Temecula, U.S.A. MAB 374

5.4. Proteins

SPARC   (CALBIOCHEM, Merck, Schwalbach, Germany);
TGF   (Sigma , ST.Louis. Missouri. USA)
PDGF   (Sigma , ST.Louis. Missouri. USA)
FN   (Sigma , ST.Louis. Missouri. USA)

5.5. Primer

Cre 5:   5'-TTC GGA TCA GCT ACA CC-3'
Cre 3:   5'-AGG TGC CCT TCC CTC TAG A-3'
T 56:   5'-AGG TGC CCT TCC CTC TAG A-3'
L1:   5'-GTG AAG TAG GTG AAA GGT AAC-3'
L26:   5'-TAA AAA GAC AGA ATA AAA CGC AC-3'

5.6. Solution and buffer

5.6.1. Cardiomyocyte preparation

CBFHH (Calcium and bicarbonat-free Hanks with Hepes)

$$8g\ NaCl$$

0.4g KCl

$0.2\ MgSO_4.7H_2O$

1g Dextrose

$0.06g\ KH_2PO_4$

$0.048g\ Na_2HPO_4$ anhydrogenous

4.77g HEPEA

H_2O to 1L

Adjust PH to 7.4

T&D

CBFHH 100ml

150mg Trypsin

1ml DNAse (2mg/ml ub 0.15MNacl)

MEM/5 and 2% CPSR1:

1LMEM

5ml BrdU (20 mM stock solution)

1ml Vitamin B12(2mg/ml stock solution)

1ml Penicillin (782g dissolved in 25 ml)

50 ml Charcoal -stripped FCS (for MEM/5)

20 ml CPSR1(for 2% CPSR1 medium)

5.6.2.Fibroblasts cells culture

Starvation medium

100 DMEM

0.5% FCS (Fatal calf serum)

anti trypsinization solution

100 ml DMED

0.25 mg BSA

Thoy bean trpsin inhibitor 25mg

PBS (1x)

0.2 g KCl

$0.2\ g\ KH_2PO_4$

$0.1\ g\ MgCl_2H_2O$

8g NaCl

$2.16\ g\ Na_2HPO_47H_2O$

pH 7.4

5.6.3 For DAN electrophoresis

Agarose gel	Agarose Ultrapure 2%
	1x TAE
	Ethidum bromide (0.5 µg/ml)
6x loading Dye (Agarose gel)	0.25 % bromphenol blue
	30 % glycerol in water
	0.25 % xylen cyanol
TAE (50x)	242 g Tris base
	57.1 ml Acetic acid
	100ml 0.5M EDTA
	Add H2O to 1 liter ,adjust pH to 8.5.

5.6.4. RNA

MOPS running buffer (10x)	41.86 g MOPS
	6.8 g $NaOAc.3H_2O$
	3.8 g Na_4EDTA
	H_2O to 1L
RNA electrophoresis	1 g Agarose
	88 µml H_2O DEPC
	10 ml 10x MOPS buffer
	2.3 µl EtBr
	1.87 ml Formaldehyde
RNA loading dye	720 µl Formamide
	160 µl 10xMOPS buffer
	260 µl Formaldehyde
	193 µl H_2O
	267 µl 6x Bromophenol blue DAN loading dye

5.6.5. cDNA Array

10 x Dnase 1 Buffer	400 mM Tris-HCl (pH 7.5)
	100 mM NaCl
	60 mM $MgCl_2$

20 X SSC	175.3 g NaCl
	88.2 G $Na_3Citrate.2H_2O$

5.6.6. <u>Western blot</u>

2% Tris-Triton Lysis Buffer	2 ml Triton-x 100
	10 mM EGTA
	200 µl NaVO3 (1000 x)
	Tris-HCL (100mM)
	H2O up to 100 ml
	Adjust pH to 7,4

PBS (10x)	2 g KCl
	2 g KH_2PO_4
	80 g NaCl
	11.5 g Na_2HPO_4

Western Blot Buffer 10x TBST	100 ml 0.5 M EDTA
	12.1g Tris-Base

Running Buffer	24 g Tris-Base
	116 g Glycine
	20 ml 20% SDS
	4L sterile H2O

RIPA Buffer:	1x PBS
	1% Igepal CA-630
	0.5% Sodium deoxycholate
	4 L sterile H_2O

Transfer Buffer	12g Tris-Base
	28 g Glycine
	800 ml Methanol
	Sterile H_2O up to 1 liter pH 7,5
	57.1 ml Glacial acetic acid

20% SDS	200 g SDS

PBST	1xPBS with 0.05% Tween 20

Stripping Solution   67g Guanidine-HCl (7M)

370mg Glycine (50 mM)

374mg Glycine (50 mM)

1.86mgEDTA (0,05)

740mg KCL (0,1 M)

156mg 2 (beta)-Mercaptoethanol (20 mM)

Sterile H2O up to 100 ml

adjust pH to 10,8 with 10 M NaOH

SDS Gels:

Buffer   1,5 M Tris-Base:

0,5 M Tris-Base

Ammoniu Persulfate (APS) 10 %

SDS 20%

Acrylamide 40% (premade solution)

Bisacrylamide 2% (premade solution)

Seperating SDS Gels

Buffers /%	7.5% (ml)	10% (ml)	12.5% (ml)
H20	16	13.8	10.9
1.5 M Tris-Base	11.3	11.3	11.3
20 % SDS	280µl	280 µl	280 µl
40 % Acryl	10.5	14	17.5
2 % Bis	4.1	2.7	2.2
TEMED	14µl	14 µl	14 µl
APS 10%	315 µl	315 µl	315 µl

4 % Stacking gels:

H$_2$O	9 ml
0.5 M Tris	1.75 ml
20% SDS	90 µl
40% Acryl	1.8 ml
2% Bis	1.05 ml
TEMED	14 µl
10% APS	210 µl

5.6.7. Immunoflurencence

Triton	0.5% Trion in PBSA
PBSA	137 mM Nacl
	3 mM KCl
	1.5 mM KH2PO4
	PH 7.4
Goat serum	10% serum diluted in TBSA
Donkey serim:	10% serum diluted in TBSA
2% PFA	Paraformaldehyde 4g
	disstlled water 180 µl
	10x PBS 20 µl
	PH 7.4

5.7. Chemical and Kits

Chem Glow	Alpha Innotech corporation CA, USA
Formaldehyde	Merck
Isopropyl alcohol,	Sigma (St. Louis, MO)
trypsin	Sigma (St. Louis, MO)
2 (beta)-Mercaptoethanol	Sigma (St. Louis, MO)
ABS (albumin bovine serum)	Sigma (St. Louis, MO)
Acrylamide	Sigma (St. Louis, MO)
Agarose	Sigma (St. Louis, MO)
Ammoniu Persulfate	Sigma (St. Louis, MO)
Ammoniu Persulfate	Sigma (St. Louis, MO)
Bisacrylamide	Sigma (St. Louis, MO)
BrdU	Sigma (St. Louis, MO)
BSA	Sigma (St. Louis, MO)
Charcoal -stripped FCS	C.C.Pro
chemiluminescence (ECL	Sigma (St. Louis, MO)
Chloroform, agarose were from Sigma	Sigma (St. Louis, MO)
CPSR1	Sigma (St. Louis, MO)
Dextrose	Sigma (St. Louis, MO)
DMEM	Sigma (St. Louis, MO)
DNAse	Sigma (St. Louis, MO)

DEPC	Sigma (St. Louis, MO)
EDTA	Sigma (St. Louis, MO)
EtBr	Sigma (St. Louis, MO)
Ethanol	Merck
FCS	Sigma (St. Louis, MO)
Formaldehyde,	Sigma (St. Louis, MO)
Formalin	Sigma (St. Louis, MO)
Formamide	Merck
Glacial acetic acid	Sigma (St. Louis, MO)
Glycine	Sigma (St. Louis, MO)
Guanidine-HCl	Sigma (St. Louis, MO)
H2O DEPC	Sigma (St. Louis, MO)
HEPEA	Sigma (St. Louis, MO)
KCl	Sigma (St. Louis, MO)
KH2PO4	Sigma (St. Louis, MO)
Lab-Tek chamber slides	Nunc Inc., Naperville, IL, USA
Methanol	Sigma (St. Louis, MO)
MgSO4.7H2O	Sigma (St. Louis, MO)
MOPS	Sigma (St. Louis, MO)
NuPAGE LDS Sample Buffer	Invitrogen, (Carlsbad, CA)
NuPAGE 4-10% Bis-Tris Gel	Invitrogen, (Carlsbad, CA)
NuPAGE MOPS SDS Running Buffer	Invitrogen, (Carlsbad, CA)
NuPAGE Transfer Buffer	Invitrogen, (Carlsbad, CA)
Na2HPO4 anhydrogenous	Sigma (St. Louis, MO)
Na2HPO47H2O	Sigma (St. Louis, MO)
Na4EDTA	Sigma (St. Louis, MO)
NaCl	Merck
NaH2PO4	Sigma (St. Louis, MO)
NaN3	Sigma (St. Louis, MO)
NaOAc.3H2O	Sigma (St. Louis, MO)
NaOAc.3H2O	Sigma (St. Louis, MO)
Nitrocellulose ECL Membranes	Sigma (St. Louis, MO)
PVDF Membran filter paper	invitrogen
Penicillin	Sigma (St. Louis, MO)
RnaseZAP	Ambion Inc.
PAP pen	Daido Sangyo Co., Ltd., Tokyo, Japan
Plolyvinylidene Fluoride.membranes	Gelman Laboratory
Sodirmazide	Sugma
Tissue.tec	Sakura Finetek Europe B.V., Zoeterwoude, The Netherlands

Tris base	Sigma (St. Louis, MO)
Tween 20	Sigma (St. Louis, MO)
Vitamin B12	Sigma (St. Louis, MO)
LPR Kit	Supper Array Bioscience Corporation
Taq PCR Master Mix kit	QIAGEN (Hilden ,Germany
DANfree Kit	Ambion Inc.)
Bio-Rad protein Assay	Bio-Rad (munic Germany)
Protease inhibito cocktail set	Calbiochem (Darmstadt, Germany.)
Mouse/Rat PDGF-BB ELISA kit	R&D systems (Inc. MN ,U.S.A)
Mouse/Rat TGF-β1 ELISA kit	R&D systems (Inc. MN ,U.S.A.)
Osteonectin ELISA kit	US Biological (Swampscott, USA)
PCR SuperMix	Invitrogen, (Carlsbad, CA)

6. Methods

6.1. Animal experiments

6.1.1. Myocardial infarction model in mouse

6.1.1.1. Experimental design

the experimental protocol for left coronary artery ligation has been previously described (Li et al., 1997; Harada et al., 1999) and is routinely performed in our laboratory. Mice are sacrificed 2d. 7d, one month and two months after to analyze immediate responses Hearts are excised and the infarct size calculated and expressed as a percentage of left ventricular surface area. Animals with less than 30% of infarct size will be excluded from the studies, as they generally do not show typical left ventricular remodeling. Ventricles are isolated and snap-frozen in liquid nitrogen for gene-expression analyses. Part of the herats is used for histopathological analysis.

6.1.1.2. Operational Procedure

After an adequate depth of anesthesia is attained the mouse is fixed in a supine position with tape. A 5-0 ligature is placed behind the front upper incisors and pulled taut so that the neck is slightly extended. The tongue is retracted and held with forceps, and a 20-G i/v catheter is inserted into the trachea. The catheter is then attached to the mouse ventilator via the Y-shaped connector. Ventilation is performed with a tidal volume of 200ul and a respiratory rate of 133/min. 100% oxygen is provided to the inflow of the ventilator. Prior to the incision the chest is disinfected with betadine solution and 70% ethyl alcohol. The chest cavity is opened by an incision of the left fourth intercostal space. Chest retractor is applied to facilitate the view. The heart is exposed, the pericardial sac is opened and pulled apart, and the left anterior descending (LAD) artery is visualized. Ligation is proceeded with a 7-0 silk suture passed with a tapered needle underneath the LAD artery about 1-2 mm

lower than the tip of the left auricle. Occlusion is confirmed by pallor of the anterior wall of the left ventricle. A drop of 1% lidocaine is placed on the apex of the of the heart to prevent arrhythmia. Lungs are overinflated, and the chest cavity, muscles, and skin are closed .
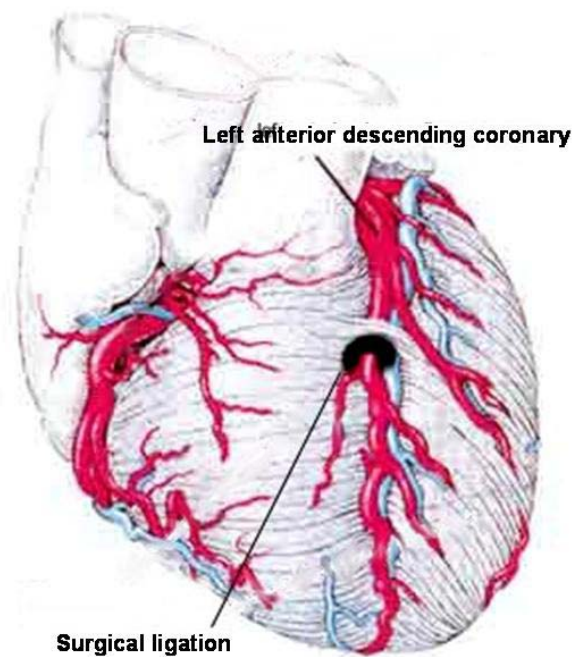
Fig. 6.1 Induction of myocardial infarction. Myocardial infarction was induced by surgical ligation of proximal left anterior descending coronary artery. Sham operated animals under went the same procedure except that no ligation was performed.

6.1.2. . Pressure overload hypertrophy model in mice-

Chronic pressure-overload LV hypertrophy was induced by aortic banding (AB) in wild-type (WT) and integrin beta 1 knock mice. Aortic banding was maintained for two days, 7days and one month. Mice were anesthetized with tribromoethanol / amylene hydrate (Avertin; 2.5% wt/vol, 6 µL/g body weight IP). A topical depilatory agent was applied to the neck and chest, and the area was cleaned with betadine and alcohol. Mice were placed supine, A horizontal skin incision 0.5–1.0 cm in length was made at

the level of the suprasternal notch. The thyroid was retracted, and a 2- to 3-mm longitudinal cut was made in the proximal portion of the sternum. This allowed visualization of the aortic arch under low-power magnification. A wire with a snare on the end was passed under the aorta between the origin of the right innominate and left common carotid arteries. A 6-0 silk suture was snared with the wire and pulled back around the aorta. A bent 27-gauge needle was then placed next to the aortic arch, and the suture was snugly tied around the needle and the aorta. After ligation, the needle was quickly removed. The skin was closed, and mice were allowed to recover on a warming pad until they were fully awake. The sham procedure was identical except that the aorta was not ligated.
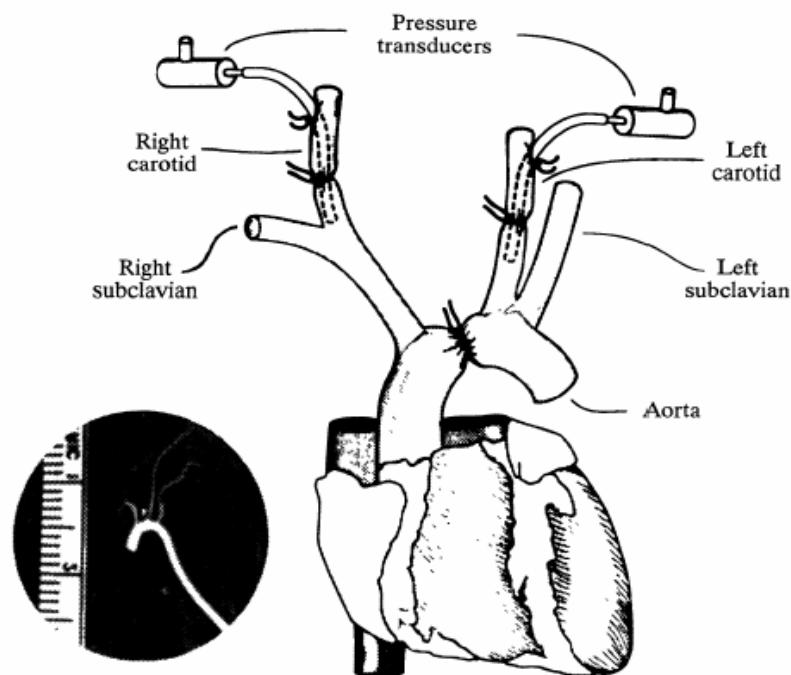
Fig. 6.2. Induction of hypertrophy Left ventricular pressure overload hypertrophy in these mice was induced by partial banding of the aorta. As a control, a thoracotomy was performed on the sham-operated mice without hemodynamic interventions. Under this condition, systemic arterial ressure remained unaltered for one week to two months.

6.1.3. In vivo inhibitior of integrin αv-

Mice were treated in vivo with a specific integrin α_v inhibitor 1 day prior to myocardial infarction. Alzet osmotic mini pumps were implanted subcutaneously. The release rate was 1μl/hour/animal of either a solution of 100 mg/ml of the integrin α_v inhibitor in 50% DMSO/PBS or DMSO/PBS alone (vehicle control).

6.1.4. β1 knock-out mice -

6.1.4.1. Inducible knockouts: The Cre/lox system
Adult ß1 conventional knockout mice were obtained from Dr. R. Fässler (Max-Planck-Institute of Biochemistry, Martinsried, Germany). Cre-knockin mice with a myosin light chain 2v driven promotor for cardiac specificity were obtained from Dr. Ken Chien (University of San Diego, CA, USA).The myosin light chain 2v (MLC2v) gene is expressed bilaterally in the embryo in the cardiac primordial (around E7.5 in the mouse), and is restricted to ventricular precursors and definitive ventricular tissue from the linear heart tube stage throughout the entire postnatal time window (O'Brien, Lee et al. 1993) Because of the restricted cardiac expression of this gene to the ventricles at the earliest stages of ventricular specification, it is chosen to express cre recombination under the control of MLC2v regulatory elements. The method for conditional gene KO makes use of the site specific recombinase Cre, a 38kDa protein from bacteriophage P[29]. This enzyme can be used to generate tissue-specific or inducible knockouts in the genome of mice. Cre is a member of the integrase family of recombinases, which can perform an efficient site specific recombination at its target site loxP. LoxP sites are 34bp long and contain a 13 bp inverted repeat flanking a core region that determines the orientation of the site. The function of Cre is to ensure that only monomers of the plasmid are maintained by resolving plasmid dimers by site-specific recombination into monomers[30]. The recombination occurs precisely and the loxP sites after recombination are still functional. Thus, the recombination is a reversible process. The use of Cre for both site specific mutations in ES cells that can be passed into the mouse germline and for conditional KO in vivo The most promising aspect of the Cre-loxP System is its application for conditional KOs. With the system, it is possible to knock out a gene only in certain cell types or tissues. If a gene is needed early in development of the mouse, eliminating it in all

tissues could be lethal, as reported for beta.1-integrin. With a tissue –specific knockout this problem can be avoided.

6.1.4.2. Induction of heart ventricular integrin β1 knock out in mouse.

1). To engineer the knockout, loxP sites are inserted so they flank the gene of interest and introduced into one mouse strain.

2). Transgenic mice are also prepared that carry the Cre gene linked to a cell-type specific promoter (region on DNA that controls transcription).

3). Mating of the two strains of mice gives progeny that carry the loxP sites flanking the gene of interest and the Cre gene controlled by a cell-type specific promoter. Recombination will only occur in the cells where the promoter is active, so the gene is only knocked out in certain tissues.

4.) The mice containing the loxP mutant allele can be crossed with different mouse strains with Cre under control of different tissue-specific promoters to look at phenotypic effects in different tissues.

Adult ß1 conventional knockout

6.1.5. Hemodynamic Measurements and Left Ventricular Volume-

Hemodynamic studies were performed either 2days, 7 days and one month after coronary artery ligation of MI model or aortic banding mice model according to published protocols under light isoflurane anesthesia and spontaneous respiration (isoflurane 1.5 vol% supplemented by 0.5 L of oxygen per minute).LV pressure curves were recorded after catheter placement in the LV cavity; systolic and diastolic blood pressure measurements were obtained on catheter withdrawal in the thoracic aorta All measurements were performed by a single trained investigator blinded to genotypes and treatment. Animals with small infarcts (<10% of LV circumference; BERKO n=6, WT n=8) and nonphysiological heart rates below 400 bpm (BERKO n=2, WT n=3) were excluded from morphometric, hemodynamic, echocardiographic, and molecular analyses. r(Hu, Gaudron et al. 1998).

6.1.6. Transthoracic Echocardiogram (M-mode)
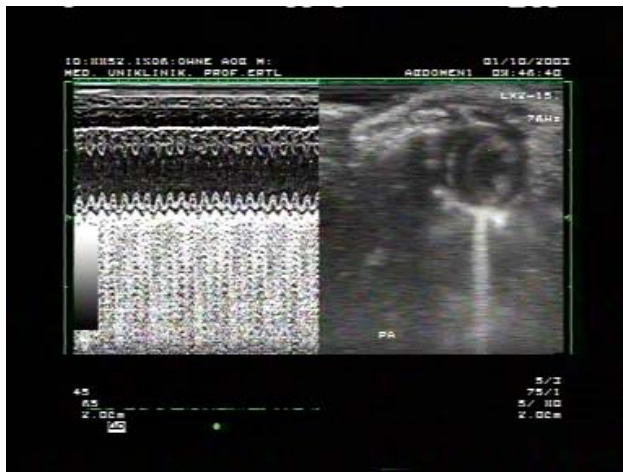
Fig .6.3 Transthoracic Echocardiogram (M-mode) The echocardiograph used a Toshiba Power Vision 6000 system with a 15-MHz frequency ultrasound probe under general anesthesia with tribromoethanol/amylene hydrate (Avertin; 2.5% wt/vol, 6 µL/g body weight IP) under spontaneous respiration at a minimum depth setting of 3 cm for 2D (on the right of the figure) and M-mode imaging.(In the left of the figure, from the same mouse in the parasternal short-axis view.)   The 2D images were obtained in white-on –black format with M-mode imaging and the spectral Doppler tracings in black-on white format.

6.1.6.1. Echocardiography

Transthoracic echocardiography is the echocardiogram that is performed by positioning a probe, called a transducer, on the outside of the chest wall while the mouse is lying down. Sound waves lack the ability to travel through air, so a clear, gel-like substance is placed between the chest and the transducer to provide a medium through which sound waves can travel. The gel also helps to improve the contact between the transducer and the skin. The transducer is placed in various positions on the chest to obtain different images of the heart.

6.1.6.2. Measurements.

Observatons were made in 47 intact, anesthetized mice. Mice were weighed and general anesthesia with tribromoethanol/amylene hydrate under spontaneous before the echocardiogram was performed. In later studies, a specially transducer was used. With the mouse in the left lateral decubitus position, the transducer was placed on the left hemithorax. The correct transducer placement was judged by the round appearance of the left ventricular (LV) cavity after angulation and cranio-caudal transducer movements. Need to be careful that avoid excessive pressure, which can induce bradycardia. LV end-systolic and end-diastolic areas were calculated by manual tracings of the endocardial border followed by planimetry with the Nice

software package (Toshiba Medical Systems).and transversal M-mode tracings were recorded with the cursor placed in the middle of the LV cavity. Taken the guide of the 2D parasternal short-axis imaging plane, the LV M-mode tracing was obtained close to the papillary muscle level Measurements are taken for anterior and inferior wall-thickness, left ventricular and end-diastolic dimension..

6.1.7.Ventricular mass calculation

In normal mice and knock out mice with or without transverse aortic constriction after echocardiography the experiment was terminated with an overdose of intraperitoneal sodium pentobarbital, the heart was excised, the atria and vessels were dissected free, and the ventricles are weighed. For normalizing the dates, body weight and the tibia are measured as well

6.2. RNA isolation

RNA was extracted from mouse heart with different treatments using TRIzol (Invitrogen) as described previously (Knepp, Geahr et al. 2003)Total RNA from 5-6 each groups of mice 2d or 1 wk after MI and sham-operated mice Total RNA from 4 groups of mice 2d or 1 wk after MI with or without integrin alphv with or without integrin alphv. 1ml of TRIZOL was added per tube containing 50-100 mg of heart tissue before homogenization. Then, homogenate was mixed well with 0.2 ml of chloroform per 1 ml of TRIZOL, and incubated at room temperature for 2-3 min. Following centrifugation (12000g for 15 min at 4 ºC), lower phase, interphase and upper phase of sample appeared in the tube. The upper phase was removed carefully and transferred to a new tube. RNA was precipitated by adding 0.5 ml of Isopropanol per 1ml of TRIZOL and incubated at room temperature for 10 min then centrifuged at 12000 g for 10 min at 4 ºC. After removing the supernatant, RNA pellets were mixed with 75% ethanol and then centrifuged at 7500g $\times$ 5 min at 4 ºC. After the supernatant was removed, the pellets were permitted to stand for air drying. RNA was dissolved in 20 μl of DEPC water and incubated at 55 ºC for 10 min.
To remove contaminating DNA 0.1 volume of 10X DNase 1 Buffer and 1ul of DNase 1 were added to the RNA (DNAfree, Ambion Inc.). The RNA solution was mixed

gently and incubated at 37ºC for 20-30 min. The DNase Inactivation Reagent was resuspended by vortexing the tube and 0.1volume or 5ul was added to RNA solution. The tube was incubated for 2 min at room temperature and centrifuged at 10,000x g for 1 min to pellet the DNase Inactivation Reagent . The RNA was stored at -80˚C for later use.

RNA quality was analysed by electrophoresis in formaldehyde containing 1% agrose gels using a MOPS buffer. The integrity of the 18 s and 28 s rRNA bands are an incication of RNA quality. The concentration is md under UV light by using spectrophotometer. Only the ratio at (280nm/ 260 nm) more than 1.8 are considered pure RNA and used for further gene array.
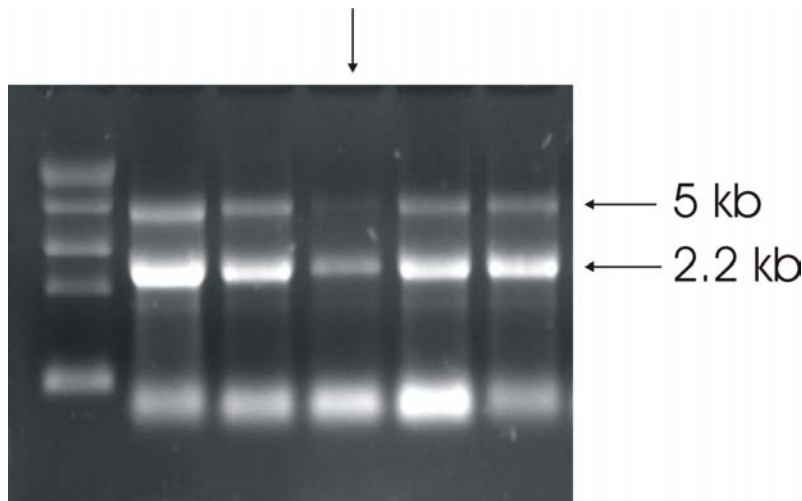
Figure 6.4, RNA electrophoresis Total RNA (5-10 ug) containing ethidium bromide are separated electrophoretically using a 1% formaldehyde agarose gel   with a circulating running buffer of 1X MOPS for 2 hours .The two bands, upper 28S (5 kb), and the bottom 18S (2.2 kb), suggested a good quality of RNA. The RNA in the third lane indicated that the RNA was degraded.

6.3. cDNA gene micro Array

6.3.1 RNA preparation and Gene Chip hybridization

 RNA was extracted from mouse hearts with different treatments using TRIzol (Invitrogen) as described before. Total RNA from 4 groups of mice 2d or 7d after MI with or without integrin alphv was used as starting material and hybridized to the non-radioactive GEArray TM Q series cDNA array (SuperArray Inc.,USA). This array contain 96 sets of biotin deoxyuridine triphosphate (dUTP)-labeled cDNA probes (ECM-integrin related gene-specific cDNA fragments).These known genes encoding

cell adhesion and extracellular matrix proteins were specifically generated in the presence a designed set of gene-specific primers Intensity differences > 2-fold in gene expression are considered significant and selected gene were further analyzed through Western blot analysis and immunofluorescence.

SouperArray Extracellular matrix Gene Array was using total RNA (5ug per membrane) as template for probe synthesis. The dUTP labeled cDNA were specifically generated by following protocols of Ampolabeling (LPR kit; Cat#:L-03N) The RNA was reverse-transcribed by gene-specific primers with biotin-16-dUTP. Biotinylated cDNA probes were denatured and hybridized to the ECM-integrin related gene-specific cDNA fragments spotted on the membranes at 60C for 17 h. The GEArray membranes were then washed and blocked with GEA blocking solution, and incubated with alkaline phosphatase-conjugated streptavidin (washed twice with 2x saline sodium citrate buffer (SSC) 1% sodium dodecyl sulfate (SDS) and then twice with 0.1 x SSC/1% SDS at 60 C for 15 min each.) Chemiluminescent detection steps were performed by subsequent incubation of the membranes with alkaline phosphatase-conjugated streptavidin and CDP-Star substrate. The results were analyzed using ScanAlyze 2 software. All cDNA microrray experiments were performed twice with new filters. The positive and negative spots were identified and matched by at least two experiments are presented. Each array membrane comprised 96 marker gees, four positive controls including beta-actin, glyceraldehyde-3-phosphate dehydrogenase (GAPDH), cyclophilin A, and ribosomal protein L13a; and a negative control, bacterial plasmid pUC18. The relative expression levels of different genes were estimated by comparing its signal intensity with that of internal control GAPDH.

6.3.2 Post-Hybridization Data Analysis

The gene expression profile could easily distinguish during 4 different independence experiments. To quantify the results, we normalize the intensity data by first subtracting the average background (mean blank intensity) and then comparing intensity levels with the average intensity of the hybridization signal of the house keeping gene.
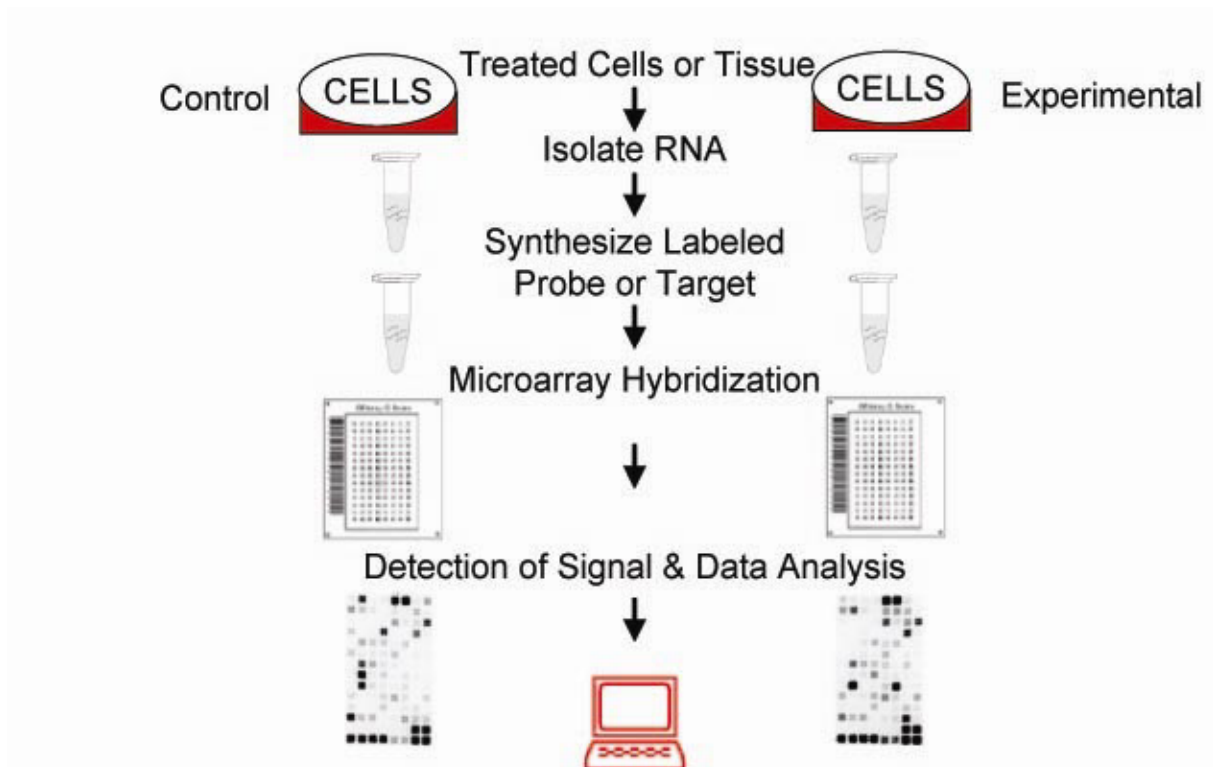
Figure 6.5. Process of cDNA gene array was shown as indicated.(from SuperArray Inc.,USA)

6.4. Cell isolation and cell culture

6.4.1.Isolation of rat neonatal cardiomyocytes

Cardiac myocytes were isolated and cultured from neonatal rat hearts based on the method reported previously (Tamamori-Adachi, Hayashida et al. 2004; Burkard, Becher et al. 2005). Experiments were performed according to Institutional Animal Care and Use Committee and NIH guide lines. Hearts were removed from 1- to 2-day-old neonatal wistar rats after decapitation and kept in CBFHH (137 mM NaCl, 5.36 mM KCl, 0.1 mM MgSO$_4$ H$_2$O, 5.5 mM Dextrose, 0.44 mM KH$_2$PO$_4$, 0.4 Na$_2$HPO$_4$, Hepes, pH 7.4) with 0.3% Heparin. Ventricles were trimmed free and minced with dissecting scissors (minced ventricles). Cells were washed one time by T&D (1ml Dnase per 100ml trypsin) and then dissociated at room temperature using a magnetic stir bar at the lowest speed (100-150rpm) with 15 ml T&D 15 min at 37 °C. Transfer supernatant to 3.75% FBS, observe a drop of the supernatant under microscope every time till there no more cardiomyocytes left. Cells were pelleted by centrifugation at 1600 r.p.m for 5 minutes at room temperature. The supernatant was

discarded and cells were resuspended in complete medium [MEM (Minimum Essential Medium from Sigma), plus 0,1mM BRdU, penicillin G streptomycin 0,01% vintaminB (Sigma)] with 5%FBS (Sigma), then filtered through a metal sieve to filter out large material. The resulting mixture was pre-plated for 1.5h in 37 °C, 0.1% CO_2 incubator. Cells still in suspension were enriched with myocytes and were plated on 6-well dishes at high density (600,000 cells each well and 200,000 cells each chamber slide) and maintained in MEM with 5 % fetal bovine serum for 24 hours. Following 12 h serum starvation (0.5% FBS) cells were treated by adding TGF-β_1 (10ng/ml) or PDGF-BB (10ng/ml) for 72 h. The Condition medium was assessed the expression of SPARC by Western blotting. When the expression was assessed immunohistochemically, the isolated cells were cultured under the same conditions on Lab-Tek chamber slides (Nunc Inc., Naperville, IL, USA). Non-myocyte contamination of primary cultures 46h after isolation consisted of approximately 5% of the total cell population. Myocardial cells were morphologically distinguished by a coarse, granular cytoplasm containing small, dense nuclei, whereas non-myocytes were readily distinguished by a phase-lucent cytoplasm.

6.4.2. Cell culture of fibroblasts

Mouse fibroblasts were maintained on cell culture dishes in DMEM supplemented with 10% fetal bovine serum (FBS), non-essential amino acids for MEM, penicillin (50U/ml), streptomycin (50μl/mi) at 37^0C, 5% CO_2. Cells were grown to confluence and passaged with 0.25% trypsin and 0.02 % EDTA in sterile PBS, for 2 min. Detached cells were mixed with serum and centrifuged for 3 min at 600 rpm. Cells were employed in the experiments of migration assay at between fourth and sixth passage.

6.5. DNA Isolation from mice tail.

DNA from mouse tails was isolated according to the protocol of the manufacturer (QIAGEN). 0.4-0.6 cm of mouse tail was cut into a 1.5-ml microcentrifuge tube. 180 μl Buffer ATL was added to the tube. The tail tissue was digested by 40 μl of proteinase K at 55°C. The tube was vortexed occasionally during digestion. Lysis

was usually complete in 6-8h. 4ul of RNase A (100mg/ml) was added to the sample, mixed by vortexing, and incubated for 2min at room temperature. After vortexing for 15sec, 400 µl Buffer AL-ethanol was added to the sample and mixed vigorously by vortexing. The mixture was then pipetted into the mini column sitting in a new 2-ml collection tube and centrifuged at 6000 g for 1 min. Flow through was discarded. The mini column was placed in a new 2-ml collection tube and 500 ul of Buffer AW1 was added to the column. After centrifugation (6000 *g* x 1min), flow through was discarded. The mini column was placed in a new 2-ml collection tube and 500 µl of Buffer AW2 was added to the column. After centrifugation (6000 *g* x 1min), flow through was discarded. The column was re- centrifuged for 1 min at full speed. The mini column was placed in a clean 1.5 ml or 2-ml microcentrifuge tube and 200 µl Buffer AE was directly pipetted onto the membrane. The column was incubated at room temperature for 1 min, and then centrifuged for 1 min at 6000 *g* to elute the DNA.

6.6. PCR

A Cre5' primer (5'-AAC ATG CTT CAT CGT CGG), a Cre3' primer (5'-TTC GGA TCA TCA GCT ACA CC-3'), a primer L26 (5'-TAA AAA GAC AGA ATA AAA CGC AC-3') a primer T56 (5'-AGG TGC CCT TCC CTC TAG A-3')and a primer L1(5'-GTG AAG TAG GTG AAA GGT AAC-3 ') were used for genotyping of the KO mice. The Taq PCR Master Mix (+ Q-solution) from Qiagen was mixed on ice with template DNA (0.5 to 1.0 µg /reaction) and specific primers (0.25 µl/reaction from 100 µM stock final conc. 0.4 µM). The final volume of the PCR reaction was 50 µl. For beta.1 heterozygous KO (beta.1 +/-) the primer combination L26 and T56 was used to detect the neomycin cassette in the KO allele, which yielded in a 210 bp product. For beta.1 conditional KO (beta.1 c/c) the primers T56 and L1 were used and showed a 400 bp product for homozygous conditional KO (beta.1 c/c), a 320 bp product for WT (beta.1 +/+) or both products for heterozygous conditional KO (beta.1 c/+). For detection of mice heterozygous for Cre-recombinase (Cre +/-) the primers Cre 5' and Cre 3' were used and yielded in a 419 bp product. The thermal cycler was programmed for 1 cycle 4 min at 94˚C followed by 20 cycles of 0.5 min at 94 ˚C, 1 min at 63 ˚C with touchdown (0.5°/cycle) to 53°C, 1 min at 72 ˚C, followed by 20

cycles of 0.5 min at 94 ˚C, 1 min at 53°C, 1 min at 72 ˚C and a final extension of 4 min at 72°C. The PCR product was confirmed by agarose gel electrophoresis.

6.7. Protein methods

6.7.1. Protein extraction for Western blotting

Proteins are extracted from tissue or cultured cells by lysis of cells in RIPA buffer or homogenisation of tissue in 2% Tris-Triton Lysis Buffer. Detergent soluble fractions were prepared from the supernatant, after 14000 g centrifugation for 10 min at 4°C to remove nuclei and the insoluble fraction then stored at- 80° C. Protein concentration was determined by the Bradford protein assay using a BSA standard curve.

6.7.2. Preparation of Conditional medium for Western blotting

Proteins in CM were precipitated by adding 3 volumes of precooled ethanol for each volume of CM and the mixture was stored at -20°C for 20 h. Proteins were separated by centrifuging at 4 ^{o}C and 15.000g 30 min. The dry precipitate was dissolved in phosphate- buffered saline. Protein concentration was determined with a Bio-Rad protein assay kit using BSA as standard.

6.7.3. Western blotting

By adding an aliquot of Laemmli SDS sample buffer followed by 5 min boiling at 95°C, 15 µl of the samples from the heart tissue were separated on 7.5% -15% SDS polyacrylamide gels depending on the size or target protein and electrophoretically transferred to nitrocellulose membranes Plolyvinylidene Fluoride.membranes (Gelman Laboratory). Then, the proteins were transferred to Plolyvinylidene Fluoride membranes (Gelman Laboratory). After transfer, the membranes were blocked for 1 hour using 10% non-fat milk or 3% ABS) in TBST Buffer. Blots are incubated with the primary antibody in TBST buffer overnight at 4˚C with light agitation. After incubation with primary antibody, the membranes are washed 5 times with large volumes of TBST and incubated with a horseradish peroxidase labelled secondary antibody in

TBST buffer for 1 hour at room temperature, the blots were detected by enhanced chemiluminescence (ECL) according to the manufacturer's reonmmendations. The signal was detected by a digital imaging system (ALPHA Innotech ChemiImager 5500).

6.7.4. ELISA

ELISA assay. The TGF-β1 protein and PDGF-BB protein were quantitated using the Quantikine mouse TGF-β1 kit and PDGF-BB kit respectively (R&D System, Minneapolis, MN). SPARC protein was quantitated using Osteonectin (SPARC) ELISA kit (US Biological, Swampscott, USA). Cells were processed and assayed according to the manufacturer's protocol (xx). Briefly, serum starved fibroblasts were treated with vitronectin (VN1μg/ml) 48 hours or PBS with or without 10mM integrin αv inhibotor. For SPARC induction, cells were treated by TGFβ1(5ng/ml) or PDGF-BB(5ng/ml) After treatment, conditioned medium was collected by centrifugation at 600x g for 5 min and stored at -80^0 C until the assay was performed. The TGF and PDGF protein concentration in the conditioned medium was determined by plotting absorbance at dual wavelength of 570 for know on a standard curve derived from dilutions of TGF and PDGF standard. SPARC was determined by plotting absorbance at dual wavelength of 490 for know on a standard curve derived from dilutions of SPARC standard. Each treatment was performed in triplicate. Cell numbers were determined and protein values were normalized to cell number.

6.8. Immunofluorescence

6.8.1. Immunofluorescence for frozen mouse heart tissue

Fresh frozen mice ventricular tissue sections (5 μm) from mouse hearts were mounted on slides Then fixed in 4% paraformaldehyde 15 minutes and 1% Triton X-100 prepared in TBS 20 minutes. After blocking the sections with 10% goat serum in TBS containing 1% bovine serum albumin (TBSA), they were incubated with primary antibodies goat polyclonal IgG anti-SPARC antibody (Santa Cruz Biotechnology, Santa Cruz, CA, USA) at a dilution of 1:100 overnight. The sections were further incubated with fluorescence-labeled secondary antibodies anti-goat 488 (Cy-2-

conjungated), as well as Phalloidin (alex 546) at a dilution of 1:40 and Dapi at a dilution of 1:500. Between steps, sections were washed three times for 5 min with TBS. All dilutions were performed with TBSA. Negative controls wee processed using anti-SPARC exposed blocking peptide at a dilution of 1: 10 one hour, or using TBS alone (without antibody, etc.) in some other incubation step

6.8.2. Duplicate immunofluorescence for isolated cardiomyocytes

Isolated neonatal rats cardiomyocytes were fixed in by immersion for 15 min in 4% paraformaldehyde and 20 min in 1% Triton X-100 prepared in PBS, washed three times by PBS. Goat polyclonal IgG anti-SPARC antibody Anti-SPARC was used at a dilution of 1:100 as the first antibody. Isolated Rats cells from heart were identified as cardiomyocytes by staining with a 1:250 dilution of a rabbit polyclonal antibody raised against a recombinant protein corresponding to amino acids of cardiac muscle Troponin I of human origin. (Anti-Troponin I antibody, from Santa Cruz) After overnight incubation, the sections were further incubated with fluorescence-labeled secondary antibodies anti-goat 580 (Cy-2-conjungated) and anti-rabbit 488 (Cy-3-conjungated) at a dilution of 1: 250 for one hour. Then staining the neucleur by Dapi at a dilution of 1:500 Between steps, sections were washed three times for 5 min with PBS. Negative controls wee processed using anti-SPARC exposed blocking peptide at a dilution of 1: 10 one hour, or using PBS alone (without antibody, etc.) in some other incubation step.Microscopy: Sections were observed and photographed using a microscope (Olympus, Tokyo, Japan)

6.9. Migration Assay
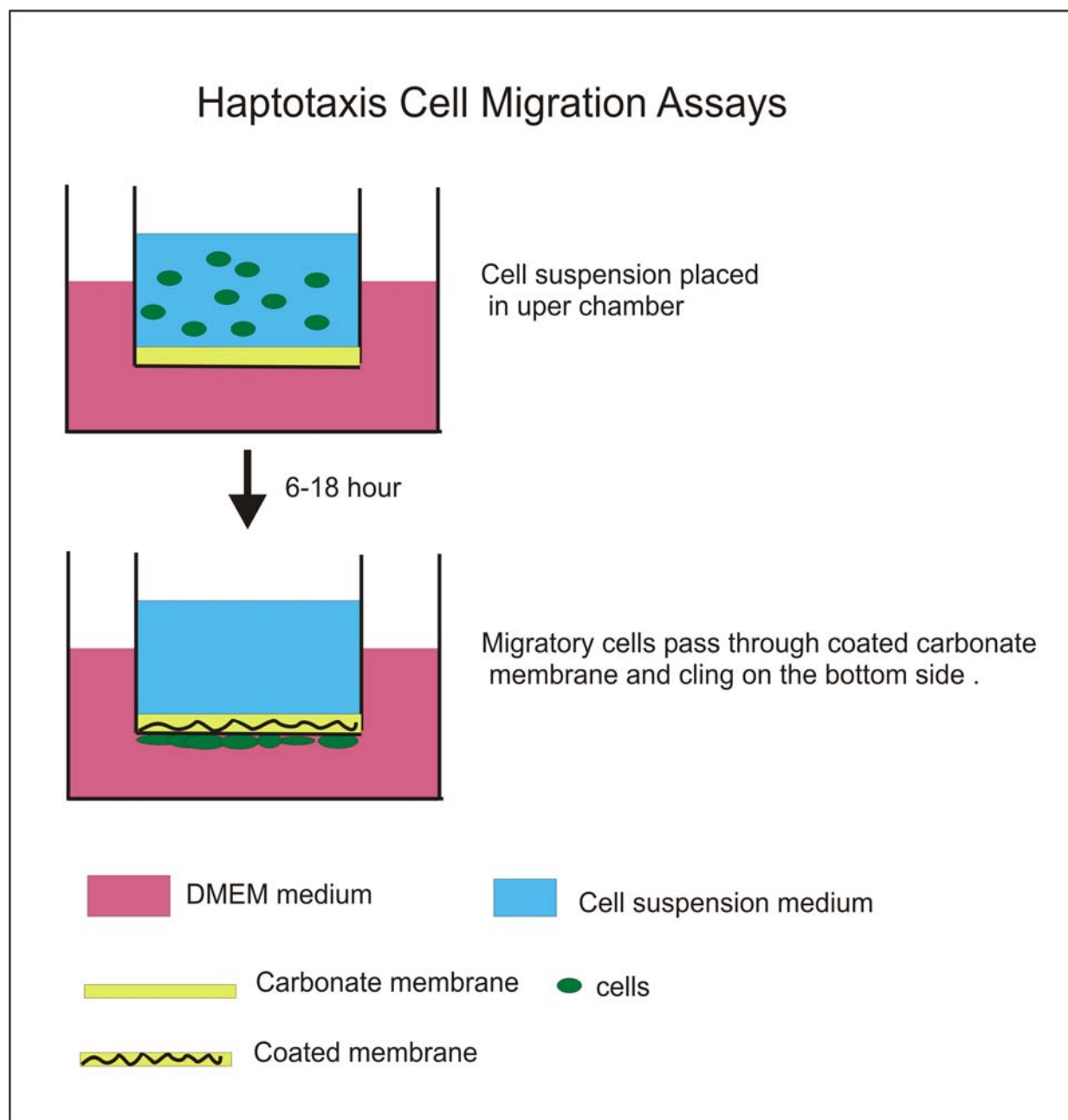
Figure. 6.6. Schematic drawing of haptotaxis cell migration. Cell Migration Assay Kit contains polycarbonate membrane (8µl pore size) in a 24 –well palte. The membrane serves as a barrier to discriminate and ultimately pass through the pores of the polycarbonate membrane. After 6-18 hours, the cells from the top of the membrane are removed and the migratory cells are stained and quantified.

Millicell modified Boyden chambers (8 µm pore size; Millipore, Bedford, MA) were employed in haptotaxis assays as previously described (Hauck, Hsia et al. 2002). Briefly, the lower surface of the Millicell polycarbonate membrane was coated with

100 µl of the indicated proteins or 0.5% BSA in DMEM for 2 hours at room temperature. After washing the chambers with PBS and air-drying, $1x10^5$ serum-starved cells were added in 0.3 ml migration medium (DMEM with 0.5% BSA). Cambers were placed into 24-well plates containing 0.4 ml migration medium. After 7 hours at 37°C, the cells on the upper surface of the membrane were removed by a cotton tip. The migratory cells on the lower membrane surface were fixed by methanol/acid treatment and stained with crystal violet (0.1% crystal violet, 0.1 M borate pH 9.0, 2% ethanol). Haptotaxis was quantified by counting cells in 5 random fields/chamber using a 20x objective in three individual chambers per sample or/ and by measuring absorbance at 600 nM. Each determination represents the average of three individual wells and error bars represent standard deviation (s.d). By cell counting methods background levels of cell migration to 0.5% BSA were <1%of values obtained with FN. Data presented are representative of at least three separate experiments.

6.10. Software and websites

- Microsoft Office ,
- EndNote program
- Microsoft Access
- Adobe photoshop
- Adobe reader
- ScanAlyze 2
- Sigma
- Startview
- CorelDRAW

WebPrimer-http://genome-www2.stanford.edu/cgi-bin/SGD/web-primer

The Web Primer provides tools for the purpose to design primers. Current choices are limited to sequencing and PCR alignment

NCBI Nucleotide- ttp://www.ncbi.nlm.nih.gov/entrez/query.fcgi

The Entrez Nucleotides database is a collection of sequences from several sources, including GenBank.

NCBI BLAST-http://www.ncbi.nlm.nih.gov/BLAST/

(Basic Local Alignment Search Tool) is a set of similarity search programs designed to explore all of the available sequence databases regardless of whether the query is protein or DNA. The program compares nucleotide or protein sequences to sequence databases and calculates the statistical significance of matches. BLAST can be used to infer functional and evolutionary relationships between sequences as well as help identify members of gene families.

6.11. Lab devices

- ChemiImager^{TM} 5500 from ALPHA Innotech. (San Leandro, CA).
- Mastercycler PCR System from eppendof (Hamburg, Germany)
- Ultrospec 3000 spectrophotometer from Pharmacia Biotech AB (Cambridge, England)
- Microscopes
- UV lamp from Bio RAD
- Incubators
- Vacuum dryer
- Autoclaves
- Centrifuges
- Heating blocks
- Water bath

Appendices

Reference

Abbate, A., Biondi-Zoccai, G., Petrolini, A., Biasucci, L. M., & Baldi, A. (2002). Clinical relevance of apoptosis in early and late post-infarction left ventricular remodeling. *Ital Heart J, 3*(12), 699-705.

Abbate, A., Biondi-Zoccai, G. G., & Baldi, A. (2002). Pathophysiologic role of myocardial apoptosis in post-infarction left ventricular remodeling. *J Cell Physiol, 193*(2), 145-153.

Abremski, K., & Hoess, R. (1984). Bacteriophage P1 site-specific recombination. Purification and properties of the Cre recombinase protein. *J Biol Chem, 259*(3), 1509-1514.

Anger, M., Lompre, A. M., Vallot, O., Marotte, F., Rappaport, L., & Samuel, J. L. (1998). Cellular distribution of Ca2+ pumps and Ca2+ release channels in rat cardiac hypertrophy induced by aortic stenosis. *Circulation, 98*(22), 2477-2486.

Barki-Harrington, L., & Rockman, H. A. (2003). Sensing heart stress. *Nat Med, 9*(1), 19-20.

Basu, A., Kligman, L. H., Samulewicz, S. J., & Howe, C. C. (2001). Impaired wound healing in mice deficient in a matricellular protein SPARC (osteonectin, BM-40). *BMC Cell Biol, 2*(1), 15.

Bloom, S., Lockard, V. G., & Bloom, M. (1996). Intermediate filament-mediated stretch-induced changes in chromatin: a hypothesis for growth initiation in cardiac myocytes. *J Mol Cell Cardiol, 28*(10), 2123-2127

.

Bornstein, P., & Sage, E. H. (2002). Matricellular proteins: extracellular modulators of cell function. *Curr Opin Cell Biol, 14*(5), 608-616.

Boulton, T. G., Nye, S. H., Robbins, D. J., Ip, N. Y., Radziejewska, E., Morgenbesser, S. D., DePinho, R. A., Panayotatos, N., Cobb, M. H., & Yancopoulos, G. D. (1991). ERKs: a family of protein-serine/threonine kinases that are activated and tyrosine phosphorylated in response to insulin and NGF. *Cell, 65*(4), 663-675.

Bradshaw, A. D., Reed, M. J., & Sage, E. H. (2002). SPARC-null mice exhibit accelerated cutaneous wound closure. *J Histochem Cytochem, 50*(1), 1-10.

Brand, T., & Schneider, M. D. (1995). The TGF beta superfamily in myocardium: ligands, receptors, transduction, and function. *J Mol Cell Cardiol, 27*(1), 5-18.

Braunwald, E., & Kloner, R. A. (1982). The stunned myocardium: prolonged, postischemic ventricular dysfunction. *Circulation, 66*(6), 1146-1149.

Brekken, R. A., & Sage, E. H. (2000). SPARC, a matricellular protein: at the crossroads of cell-matrix. *Matrix Biol, 19*(7), 569-580.

Brown, P. O., & Botstein, D. (1999). Exploring the new world of the genome with DNA microarrays. *Nat Genet, 21*(1 Suppl), 33-37.

Burkard, N., Becher, J., Heindl, C., Neyses, L., Schuh, K., & Ritter, O. (2005). Targeted proteolysis sustains calcineurin activation. *Circulation, 111*(8), 1045-1053.

Chen, H., Huang, X. N., Stewart, A. F., & Sepulveda, J. L. (2004). Gene expression changes associated with fibronectin-induced cardiac myocyte hypertrophy. *Physiol Genomics, 18*(3), 273-283.

Chen, J., Kubalak, S. W., & Chien, K. R. (1998). Ventricular muscle-restricted targeting of the RXRalpha gene reveals a non-cell-autonomous requirement in cardiac chamber morphogenesis. *Development, 125*(10), 1943-1949.

Cheng, W., Kajstura, J., Nitahara, J. A., Li, B., Reiss, K., Liu, Y., Clark, W. A., Krajewski, S., Reed, J. C., Olivetti, G., & Anversa, P. (1996). Programmed myocyte cell death affects the viable myocardium after infarction in rats. *Exp Cell Res, 226*(2), 316-327.

Chien, K. R. (1999). Stress pathways and heart failure. *Cell, 98*(5), 555-558.

Clerk, A., & Sugden, P. H. (1997). Cell stress-induced phosphorylation of ATF2 and c-Jun transcription factors in rat ventricular myocytes. *Biochem J, 325 (Pt 3)*, 801-810.

Cohn, J. N. (1993). Post-MI remodeling. *Clin Cardiol, 16*(5 Suppl 2), II21-24.

Cooper, G. t. (1987). Cardiocyte adaptation to chronically altered load. *Annu Rev Physiol, 49*, 501-518.

Cooper, G. t., Kent, R. L., Uboh, C. E., Thompson, E. W., & Marino, T. A. (1985). Hemodynamic versus adrenergic control of cat right ventricular hypertrophy. *J Clin Invest, 75*(5), 1403-1414.

D'Armiento, J. (2002). Matrix metalloproteinase disruption of the extracellular matrix and cardiac dysfunction. *Trends Cardiovasc Med, 12*(3), 97-101.

Dai, R. P., Dheen, S. T., & Tay, S. S. (2002). Induction of cytokine expression in rat post-ischemic sinoatrial node (SAN). *Cell Tissue Res, 310*(1), 59-66.

Daugaard, G., Lassen, U., Bie, P., Pedersen, E. B., Jensen, K. T., Abildgaard, U., Hesse, B., & Kjaer, A. (2005). Natriuretic peptides in the monitoring of anthracycline induced reduction in left ventricular ejection fraction. *Eur J Heart Fail, 7*(1), 87-93.

De, S., Chen, J., Narizhneva, N. V., Heston, W., Brainard, J., Sage, E. H., & Byzova, T. V. (2003). Molecular pathway for cancer metastasis to bone. *J Biol Chem, 278*(40), 39044-39050.

Deten, A., Holzl, A., Leicht, M., Barth, W., & Zimmer, H. G. (2001). Changes in extracellular matrix and in transforming growth factor beta isoforms after coronary artery ligation in rats. *J Mol Cell Cardiol, 33*(6), 1191-1207.

Edin, M. L., Howe, A. K., & Juliano, R. L. (2001). Inhibition of PKA blocks fibroblast migration in response to growth factors. *Exp Cell Res, 270*(2), 214-222.

El Jamali, A., Freund, C., Rechner, C., Scheidereit, C., Dietz, R., & Bergmann, M. W. (2004). Reoxygenation after severe hypoxia induces cardiomyocyte hypertrophy in vitro: activation of CREB downstream of GSK3beta. *Faseb J, 18*(10), 1096-1098.

Ertl, G., Gaudron, P., & Hu, K. (1993). Ventricular remodeling after myocardial infarction. Experimental and clinical studies. *Basic Res Cardiol, 88 Suppl 1*, 125-137.

Farhadian, F., Contard, F., Corbier, A., Barrieux, A., Rappaport, L., & Samuel, J. L. (1995). Fibronectin expression during physiological and pathological cardiac growth. *J Mol Cell Cardiol, 27*(4), 981-990.

Fassler, R., & Meyer, M. (1995). Consequences of lack of beta 1 integrin gene expression in mice. *Genes Dev, 9*(15), 1896-1908.

Fishbein, M. C., Maclean, D., & Maroko, P. R. (1978). The histopathologic evolution of myocardial infarction. *Chest, 73*(6), 843-849.

Floege, J., Alpers, C. E., Sage, E. H., Pritzl, P., Gordon, K., Johnson, R. J., & Couser, W. G. (1992). Markers of complement-dependent and complement-independent glomerular visceral epithelial cell injury in vivo. Expression of antiadhesive proteins and cytoskeletal changes. *Lab Invest, 67*(4), 486-497.

Francki, A., Bradshaw, A. D., Bassuk, J. A., Howe, C. C., Couser, W. G., & Sage, E. H. (1999). SPARC regulates the expression of collagen type I and transforming growth factor-beta1 in mesangial cells. *J Biol Chem, 274*(45), 32145-32152.

Francki, A., McClure, T. D., Brekken, R. A., Motamed, K., Murri, C., Wang, T., & Sage, E. H. (2004). SPARC regulates TGF-beta1-dependent signaling in primary glomerular mesangial cells. *J Cell Biochem, 91*(5), 915-925.

Funk, S. E., & Sage, E. H. (1993). Differential effects of SPARC and cationic SPARC peptides on DNA synthesis by endothelial cells and fibroblasts. *J Cell Physiol, 154*(1), 53-63.

Giancotti, F. G., & Ruoslahti, E. (1999). Integrin signaling. *Science, 285*(5430), 1028-1032 .

Gilles, C., Bassuk, J. A., Pulyaeva, H., Sage, E. H., Foidart, J. M., & Thompson, E. W. (1998). SPARC/osteonectin induces matrix metalloproteinase 2 activation in human breast cancer cell lines. *Cancer Res, 58*(23), 5529-5536.

Gu, H., Zou, Y. R., & Rajewsky, K. (1993). Independent control of immunoglobulin switch recombination at individual switch regions evidenced through Cre-loxP-mediated gene targeting. *Cell, 73*(6), 1155-1164.

Harada, M., Qin, Y., Takano, H., Minamino, T., Zou, Y., Toko, H., Ohtsuka, M., Matsuura, K., Sano, M., Nishi, J., Iwanaga, K., Akazawa, H., Kunieda, T., Zhu, W., Hasegawa, H., Kunisada, K., Nagai, T., Nakaya, H., Yamauchi-Takihara, K., & Komuro, I. (2005). G-CSF prevents cardiac remodeling after myocardial infarction by activating the Jak-Stat pathway in cardiomyocytes. *Nat Med, 11*(3), 305-311.

Hauck, C. R., Hsia, D. A., Puente, X. S., Cheresh, D. A., & Schlaepfer, D. D. (2002). FRNK blocks v-Src-stimulated invasion and experimental metastases without effects on cell motility or growth. *Embo J, 21*(23), 6289-6302.

Hefti, M. A., Harder, B. A., Eppenberger, H. M., & Schaub, M. C. (1997). Signaling pathways in cardiac myocyte hypertrophy. *J Mol Cell Cardiol, 29*(11), 2873-2892.

Hirota, H., Chen, J., Betz, U. A., Rajewsky, K., Gu, Y., Ross, J., Jr., Muller, W., & Chien, K. R. (1999). Loss of a gp130 cardiac muscle cell survival pathway is a critical event in the onset of heart failure during biomechanical stress. *Cell, 97*(2), 189-198.

Hoess, R. H., Ziese, M., & Sternberg, N. (1982). P1 site-specific recombination: nucleotide sequence of the recombining sites. *Proc Natl Acad Sci U S A, 79*(11), 3398-3402.

Holland, P. W., Harper, S. J., McVey, J. H., & Hogan, B. L. (1987). In vivo expression of mRNA for the Ca++-binding protein SPARC (osteonectin) revealed by in situ hybridization. *J Cell Biol, 105*(1), 473-482.

Holtta, T., Happonen, J. M., Ronnholm, K., Fyhrquist, F., & Holmberg, C. (2001). Hypertension, cardiac state, and the role of volume overload during peritoneal dialysis. *Pediatr Nephrol, 16*(4), 324-331.

Holtz, J. (1998). Role of ACE inhibition or AT1 blockade in the remodeling following myocardial infarction. *Basic Res Cardiol, 93 Suppl 2*, 92-100.

Hu, K., Gaudron, P., Schmidt, T. J., Hoffmann, K. D., & Ertl, G. (1998). Aggravation of left ventricular remodeling by a novel specific endothelin ET(A) antagonist EMD94246 in rats with experimental myocardial infarction. *J Cardiovasc Pharmacol, 32*(3), 505-508.

Ingber, D. (1991). Integrins as mechanochemical transducers. *Curr Opin Cell Biol, 3*(5), 841-848.

Izumo, S., Nadal-Ginard, B., & Mahdavi, V. (1988). Protooncogene induction and reprogramming of cardiac gene expression produced by pressure overload. *Proc Natl Acad Sci U S A, 85*(2), 339-343.

Keller, R. S., Shai, S. Y., Babbitt, C. J., Pham, C. G., Solaro, R. J., Valencik, M. L., Loftus, J. C., & Ross, R. S. (2001). Disruption of integrin function in the murine myocardium leads to perinatal lethality, fibrosis, and abnormal cardiac performance. *Am J Pathol, 158*(3), 1079-1090.

Kilby, N. J., Snaith, M. R., & Murray, J. A. (1993). Site-specific recombinases: tools for genome engineering. *Trends Genet, 9*(12), 413-421.

Kim, H. E., Dalal, S. S., Young, E., Legato, M. J., Weisfeldt, M. L., & D'Armiento, J. (2000). Disruption of the myocardial extracellular matrix leads to cardiac dysfunction. *J Clin Invest, 106*(7), 857-866.

Kingsley, D. M. (1994). The TGF-beta superfamily: new members, new receptors, and new genetic tests of function in different organisms. *Genes Dev, 8*(2), 133-146.

Kira, Y., Kochel, P. J., Gordon, E. E., & Morgan, H. E. (1984). Aortic perfusion pressure as a determinant of cardiac protein synthesis. *Am J Physiol, 246*(3 Pt 1), C247-258.

Kira, Y., Nakaoka, T., Hashimoto, E., Okabe, F., Asano, S., & Sekine, I. (1994). Effect of long-term cyclic mechanical load on protein synthesis and morphological changes in cultured myocardial cells from neonatal rat. *Cardiovasc Drugs Ther, 8*(2), 251-262.

Knepp, J. H., Geahr, M. A., Forman, M. S., & Valsamakis, A. (2003). Comparison of automated and manual nucleic acid extraction methods for detection of enterovirus RNA. *J Clin Microbiol, 41*(8), 3532-3536.

Komatsubara, I., Murakami, T., Kusachi, S., Nakamura, K., Hirohata, S., Hayashi, J., Takemoto, S., Suezawa, C., Ninomiya, Y., & Shiratori, Y. (2003). Spatially and temporally different expression of osteonectin and osteopontin in the infarct zone of experimentally induced myocardial infarction in rats. *Cardiovasc Pathol, 12*(4), 186-194.

Komuro, I., Kaida, T., Shibazaki, Y., Kurabayashi, M., Katoh, Y., Hoh, E., Takaku, F., & Yazaki, Y. (1990). Stretching cardiac myocytes stimulates protooncogene expression. *J Biol Chem, 265*(7), 3595-3598.

Kretzschmar, M., Liu, F., Hata, A., Doody, J., & Massague, J. (1997). The TGF-beta family mediator Smad1 is phosphorylated directly and activated functionally by the BMP receptor kinase. *Genes Dev, 11*(8), 984-995.

Kupprion, C., Motamed, K., & Sage, E. H. (1998). SPARC (BM-40, osteonectin) inhibits the mitogenic effect of vascular endothelial growth factor on microvascular endothelial cells. *J Biol Chem, 273*(45), 29635-29640.

Kuppuswamy, D., Kerr, C., Narishige, T., Kasi, V. S., Menick, D. R., & Cooper, G. t. (1997). Association of tyrosine-phosphorylated c-Src with the cytoskeleton of hypertrophying myocardium. *J Biol Chem, 272*(7), 4500-4508.

Kyriakides, T. R., & Bornstein, P. (2003). Matricellular proteins as modulators of wound healing and the foreign body response. *Thromb Haemost, 90*(6), 986-992.

Lane, T. F., & Sage, E. H. (1994). The biology of SPARC, a protein that modulates cell-matrix interactions. *Faseb J, 8*(2), 163-173.

Laser, M., Willey, C. D., Jiang, W., Cooper, G. t., Menick, D. R., Zile, M. R., & Kuppuswamy, D. (2000). Integrin activation and focal complex formation in cardiac hypertrophy. *J Biol Chem, 275*(45), 35624-35630.

Levy, D., Garrison, R. J., Savage, D. D., Kannel, W. B., & Castelli, W. P. (1990). Prognostic implications of echocardiographically determined left ventricular mass in the Framingham Heart Study. *N Engl J Med, 322*(22), 1561-1566.

Lodge-Patch, I. (1951). The ageing of cardiac infarcts, and its influence on cardiac rupture. *Br Heart J, 13*(1), 37-42.

MacKenna, D. A., Dolfi, F., Vuori, K., & Ruoslahti, E. (1998). Extracellular signal-regulated kinase and c-Jun NH2-terminal kinase activation by mechanical stretch is integrin-dependent and matrix-specific in rat cardiac fibroblasts. *J Clin Invest, 101*(2), 301-310.

Maillard, C., Malaval, L., & Delmas, P. D. (1992). Immunological screening of SPARC/Osteonectin in nonmineralized tissues. *Bone, 13*(3), 257-264.

Marth, J. D. (1996). Recent advances in gene mutagenesis by site-directed recombination. *J Clin Invest, 97*(9), 1999-2002.

Masson, S., Arosio, B., Fiordaliso, F., Gagliano, N., Calvillo, L., Santambrogio, D., D'Aquila, S., Vergani, C., Latini, R., & Annoni, G. (2000). Left ventricular

response to beta-adrenergic stimulation in aging rats. *J Gerontol A Biol Sci Med Sci, 55*(1), B35-41; discussion B42-33.

Masson, S., Arosio, B., Luvara, G., Gagliano, N., Fiordaliso, F., Santambrogio, D., Vergani, C., Latini, R., & Annoni, G. (1998). Remodelling of cardiac extracellular matrix during beta-adrenergic stimulation: upregulation of SPARC in the myocardium of adult rats. *J Mol Cell Cardiol, 30*(8), 1505-1514.

Matrisian, L. M. (1990). Metalloproteinases and their inhibitors in matrix remodeling. *Trends Genet, 6*(4), 121-125.

Meerson, F. Z., & Javich, M. P. (1982). Isoenzyme pattern and activity of myocardial creatine phosphokinase under heart adaptation to prolonged overload. *Basic Res Cardiol, 77*(4), 349-358.

Meggs, L. G., Tillotson, J., Huang, H., Sonnenblick, E. H., Capasso, J. M., & Anversa, P. (1990). Noncoordinate regulation of alpha-1 adrenoreceptor coupling and reexpression of alpha skeletal actin in myocardial infarction-induced left ventricular failure in rats. *J Clin Invest, 86*(5), 1451-1458.

Mendez, R. E., Pfeffer, J. M., Ortola, F. V., Bloch, K. D., Anderson, S., Seidman, J. G., & Brenner, B. M. (1987). Atrial natriuretic peptide transcription, storage, and release in rats with myocardial infarction. *Am J Physiol, 253*(6 Pt 2), H1449-1455.

Mercadier, J. J., Samuel, J. L., Michel, J. B., Zongazo, M. A., de la Bastie, D., Lompre, A. M., Wisnewsky, C., Rappaport, L., Levy, B., & Schwartz, K. (1989). Atrial natriuretic factor gene expression in rat ventricle during experimental hypertension. *Am J Physiol, 257*(3 Pt 2), H979-987.

Miyamoto, S., Teramoto, H., Coso, O. A., Gutkind, J. S., Burbelo, P. D., Akiyama, S. K., & Yamada, K. M. (1995). Integrin function: molecular hierarchies of cytoskeletal and signaling molecules. *J Cell Biol, 131*(3), 791-805.

Murakami, M., Kusachi, S., Nakahama, M., Naito, I., Murakami, T., Doi, M., Kondo, J., Higashi, T., Ninomiya, Y., & Tsuji, T. (1998). Expression of the alpha 1 and alpha 2 chains of type IV collagen in the infarct zone of rat myocardial infarction. *J Mol Cell Cardiol, 30*(6), 1191-1202.

Murphy-Ullrich, J. E. (2001). The de-adhesive activity of matricellular proteins: is intermediate cell adhesion an adaptive state? *J Clin Invest, 107*(7), 785-790.

Nebe, B., Rychly, J., Knopp, A., & Bohn, W. (1995). Mechanical induction of beta 1-integrin-mediated calcium signaling in a hepatocyte cell line. *Exp Cell Res, 218*(2), 479-484.

O'Brien, T. X., Lee, K. J., & Chien, K. R. (1993). Positional specification of ventricular myosin light chain 2 expression in the primitive murine heart tube. *Proc Natl Acad Sci U S A, 90*(11), 5157-5161.

Olivetti, G., Abbi, R., Quaini, F., Kajstura, J., Cheng, W., Nitahara, J. A., Quaini, E., Di Loreto, C., Beltrami, C. A., Krajewski, S., Reed, J. C., & Anversa, P. (1997). Apoptosis in the failing human heart. *N Engl J Med, 336*(16), 1131-1141.

Pan, J., Fukuda, K., Kodama, H., Makino, S., Takahashi, T., Sano, M., Hori, S., & Ogawa, S. (1997). Role of angiotensin II in activation of the JAK/STAT pathway induced by acute pressure overload in the rat heart. *Circ Res, 81*(4), 611-617

Parsons, J. T., & Parsons, S. J. (1997). Src family protein tyrosine kinases: cooperating with growth factor and adhesion signaling pathways. *Curr Opin Cell Biol, 9*(2), 187-192.

Paulsson, M., Deutzmann, R., Dziadek, M., Nowack, H., Timpl, R., Weber, S., & Engel, J. (1986). Purification and structural characterization of intact and fragmented nidogen obtained from a tumor basement membrane. *Eur J Biochem, 156*(3), 467-478.

Pauschinger, M., Chandrasekharan, K., & Schultheiss, H. P. (2004). Myocardial remodeling in viral heart disease: possible interactions between inflammatory mediators and MMP-TIMP system. *Heart Fail Rev, 9*(1), 21-31.

Pelouch, V., Dixon, I. M., Golfman, L., Beamish, R. E., & Dhalla, N. S. (1993). Role of extracellular matrix proteins in heart function. *Mol Cell Biochem, 129*(2), 101-120.

Pelzer, T., Loza, P. A., Hu, K., Bayer, B., Dienesch, C., Calvillo, L., Couse, J. F., Korach, K. S., Neyses, L., & Ertl, G. (2005). Increased mortality and aggravation of heart failure in estrogen receptor-beta knockout mice after myocardial infarction. *Circulation, 111*(12), 1492-1498.

Pfeffer, M. A., & Braunwald, E. (1990). Ventricular remodeling after myocardial infarction. Experimental observations and clinical implications. *Circulation, 81*(4), 1161-1172.

Pham, C. G., Harpf, A. E., Keller, R. S., Vu, H. T., Shai, S. Y., Loftus, J. C., & Ross, R. S. (2000). Striated muscle-specific beta(1D)-integrin and FAK are involved in cardiac myocyte hypertrophic response pathway. *Am J Physiol Heart Circ Physiol, 279*(6), H2916-2926.

Porter, P. L., Sage, E. H., Lane, T. F., Funk, S. E., & Gown, A. M. (1995). Distribution of SPARC in normal and neoplastic human tissue. *J Histochem Cytochem, 43*(8), 791-800.

Raines, E. W., Lane, T. F., Iruela-Arispe, M. L., Ross, R., & Sage, E. H. (1992). The extracellular glycoprotein SPARC interacts with platelet-derived growth factor (PDGF)-AB and -BB and inhibits the binding of PDGF to its receptors. *Proc Natl Acad Sci U S A, 89*(4), 1281-1285.

Reed, M. J., Bradshaw, A. D., Shaw, M., Sadoun, E., Han, N., Ferara, N., Funk, S., Puolakkainen, P., & Sage, E. H. (2005). Enhanced angiogenesis characteristic of SPARC-null mice disappears with age. *J Cell Physiol*.

Reed, M. J., Puolakkainen, P., Lane, T. F., Dickerson, D., Bornstein, P., & Sage, E. H. (1993). Differential expression of SPARC and thrombospondin 1 in wound repair: immunolocalization and in situ hybridization. *J Histochem Cytochem, 41*(10), 1467-1477.

Reed, M. J., Vernon, R. B., Abrass, I. B., & Sage, E. H. (1994). TGF-beta 1 induces the expression of type I collagen and SPARC, and enhances contraction of collagen gels, by fibroblasts from young and aged donors. *J Cell Physiol, 158*(1), 169-179.

Rempel, S. A., Golembieski, W. A., Fisher, J. L., Maile, M., & Nakeff, A. (2001). SPARC modulates cell growth, attachment and migration of U87 glioma cells on brain extracellular matrix proteins. *J Neurooncol, 53*(2), 149-160.

Revis, N. W., Thomson, R. Y., & Cameron, A. J. (1977). Lactate dehydrogenase isoenzymes in the human hypertrophic heart. *Cardiovasc Res, 11*(2), 172-176.

Ross, R. S. (2002). The extracellular connections: the role of integrins in myocardial remodeling. *J Card Fail, 8*(6 Suppl), S326-331.

Ross, R. S., Pham, C., Shai, S. Y., Goldhaber, J. I., Fenczik, C., Glembotski, C. C., Ginsberg, M. H., & Loftus, J. C. (1998). Beta1 integrins participate in the hypertrophic response of rat ventricular myocytes. *Circ Res, 82*(11), 1160-1172.

Ruwhof, C., & van der Laarse, A. (2000). Mechanical stress-induced cardiac hypertrophy: mechanisms and signal transduction pathways. *Cardiovasc Res, 47*(1), 23-37.

Sacca, L., Napoli, R., & Cittadini, A. (2003). Growth hormone, acromegaly, and heart failure: an intricate triangulation. *Clin Endocrinol (Oxf), 59*(6), 660-671.

Sadoshima, J., & Izumo, S. (1993). Mechanical stretch rapidly activates multiple signal transduction pathways in cardiac myocytes: potential involvement of an autocrine/paracrine mechanism. *Embo J, 12*(4), 1681-1692.

Sadoshima, J., Jahn, L., Takahashi, T., Kulik, T. J., & Izumo, S. (1992). Molecular characterization of the stretch-induced adaptation of cultured cardiac cells. An in vitro model of load-induced cardiac hypertrophy. *J Biol Chem, 267*(15), 10551-10560.

Sage, E. H., & Bornstein, P. (1991). Extracellular proteins that modulate cell-matrix interactions. SPARC, tenascin, and thrombospondin. *J Biol Chem, 266*(23), 14831-14834.

Sage, E. H., & Vernon, R. B. (1994). Regulation of angiogenesis by extracellular matrix: the growth and the glue. *J Hypertens Suppl, 12*(10), S145-152.

Sage, H., Decker, J., Funk, S., & Chow, M. (1989). SPARC: a Ca2+-binding extracellular protein associated with endothelial cell injury and proliferation. *J Mol Cell Cardiol, 21 Suppl 1*, 13-22.

Sage, H., Johnson, C., & Bornstein, P. (1984). Characterization of a novel serum albumin-binding glycoprotein secreted by endothelial cells in culture. *J Biol Chem, 259*(6), 3993-4007.

Sage, H., Vernon, R. B., Decker, J., Funk, S., & Iruela-Arispe, M. L. (1989). Distribution of the calcium-binding protein SPARC in tissues of embryonic and adult mice. *J Histochem Cytochem, 37*(6), 819-829.

Sage, H., Vernon, R. B., Funk, S. E., Everitt, E. A., & Angello, J. (1989). SPARC, a secreted protein associated with cellular proliferation, inhibits cell spreading in vitro and exhibits Ca+2-dependent binding to the extracellular matrix. *J Cell Biol, 109*(1), 341-356.

Sauer, B. (1998). Inducible gene targeting in mice using the Cre/lox system. *Methods, 14*(4), 381-392.

Schellings, M. W., Pinto, Y. M., & Heymans, S. (2004). Matricellular proteins in the heart: possible role during stress and remodeling. *Cardiovasc Res, 64*(1), 24-31.

Schiemann, B. J., Neil, J. R., & Schiemann, W. P. (2003). SPARC inhibits epithelial cell proliferation in part through stimulation of the transforming growth factor-beta-signaling system. *Mol Biol Cell, 14*(10), 3977-3988.

Schwartz, K., de la Bastie, D., Bouveret, P., Oliviero, P., Alonso, S., & Buckingham, M. (1986). Alpha-skeletal muscle actin mRNA's accumulate in hypertrophied adult rat hearts. *Circ Res, 59*(5), 551-555.

Schwarzbauer, J. E., Musset-Bilal, F., & Ryan, C. S. (1994). Extracellular calcium-binding protein SPARC/osteonectin in Caenorhabditis elegans. *Methods Enzymol, 245*, 257-270.

Seger, R., & Krebs, E. G. (1995). The MAPK signaling cascade. *Faseb J, 9*(9), 726-735.

Shai, S. Y., Harpf, A. E., Babbitt, C. J., Jordan, M. C., Fishbein, M. C., Chen, J., Omura, M., Leil, T. A., Becker, K. D., Jiang, M., Smith, D. J., Cherry, S. R., Loftus, J. C., & Ross, R. S. (2002). Cardiac myocyte-specific excision of the beta1 integrin gene results in myocardial fibrosis and cardiac failure. *Circ Res, 90*(4), 458-464.

Shankavaram, U. T., DeWitt, D. L., Funk, S. E., Sage, E. H., & Wahl, L. M. (1997). Regulation of human monocyte matrix metalloproteinases by SPARC. *J Cell Physiol, 173*(3), 327-334.

Shiba, H., Fujita, T., Doi, N., Nakamura, S., Nakanishi, K., Takemoto, T., Hino, T., Noshiro, M., Kawamoto, T., Kurihara, H., & Kato, Y. (1998). Differential effects of various growth factors and cytokines on the syntheses of DNA, type I collagen, laminin, fibronectin, osteonectin/secreted protein, acidic and rich in cysteine (SPARC), and alkaline phosphatase by human pulp cells in culture. *J Cell Physiol, 174*(2), 194-205.

Simkhovich, B. Z., Kloner, R. A., Poizat, C., Marjoram, P., & Kedes, L. H. (2003). Gene expression profiling--a new approach in the study of myocardial ischemia. *Cardiovasc Pathol, 12*(4), 180-185.

Simpson, D. G., Terracio, L., Terracio, M., Price, R. L., Turner, D. C., & Borg, T. K. (1994). Modulation of cardiac myocyte phenotype in vitro by the composition and orientation of the extracellular matrix. *J Cell Physiol, 161*(1), 89-105.

Spinale, F. G. (2002). Matrix metalloproteinases: regulation and dysregulation in the failing heart. *Circ Res, 90*(5), 520-530.

Stanton, L. W., Garrard, L. J., Damm, D., Garrick, B. L., Lam, A., Kapoun, A. M., Zheng, Q., Protter, A. A., Schreiner, G. F., & White, R. T. (2000). Altered patterns of gene expression in response to myocardial infarction. *Circ Res, 86*(9), 939-945.

Stephens, L. E., Sutherland, A. E., Klimanskaya, I. V., Andrieux, A., Meneses, J., Pedersen, R. A., & Damsky, C. H. (1995). Deletion of beta 1 integrins in mice results in inner cell mass failure and peri-implantation lethality. *Genes Dev, 9*(15), 1883-1895.

Sturm, R. A., Satyamoorthy, K., Meier, F., Gardiner, B. B., Smit, D. J., Vaidya, B., & Herlyn, M. (2002). Osteonectin/SPARC induction by ectopic beta(3) integrin in human radial growth phase primary melanoma cells. *Cancer Res, 62*(1), 226-232.

Sun, Y., & Weber, K. T. (2000). Infarct scar: a dynamic tissue. *Cardiovasc Res, 46*(2), 250-256.

Tamamori-Adachi, M., Hayashida, K., Nobori, K., Omizu, C., Yamada, K., Sakamoto, N., Kamura, T., Fukuda, K., Ogawa, S., Nakayama, K. I., & Kitajima, S. (2004). Down-regulation of p27Kip1 promotes cell proliferation of rat neonatal cardiomyocytes induced by nuclear expression of cyclin D1 and CDK4. Evidence for impaired Skp2-dependent degradation of p27 in terminal differentiation. *J Biol Chem, 279*(48), 50429-50436.

Tanaka, N., Dalton, N., Mao, L., Rockman, H. A., Peterson, K. L., Gottshall, K. R., Hunter, J. J., Chien, K. R., & Ross, J., Jr. (1996). Transthoracic echocardiography in models of cardiac disease in the mouse. *Circulation, 94*(5), 1109-1117.

Termine, J. D., Kleinman, H. K., Whitson, S. W., Conn, K. M., McGarvey, M. L., & Martin, G. R. (1981). Osteonectin, a bone-specific protein linking mineral to collagen. *Cell, 26*(1 Pt 1), 99-105.

Thompson, N. L., Bazoberry, F., Speir, E. H., Casscells, W., Ferrans, V. J., Flanders, K. C., Kondaiah, P., Geiser, A. G., & Sporn, M. B. (1988). Transforming growth factor beta-1 in acute myocardial infarction in rats. *Growth Factors, 1*(1), 91-99.

Thorburn, J., Xu, S., & Thorburn, A. (1997). MAP kinase- and Rho-dependent signals interact to regulate gene expression but not actin morphology in cardiac muscle cells. *Embo J, 16*(8), 1888-1900.

Tian, Z. J., Cui, W., Li, Y. J., Hao, Y. M., Du, J., Liu, F., Zhang, H., Zu, X. G., Liu, S. Y., Chen, L., & An, W. (2004). Different contributions of STAT3, ERK1/2, and PI3-K signaling to cardiomyocyte hypertrophy by cardiotrophin-1. *Acta Pharmacol Sin, 25*(9), 1157-1164.

Tran, K. L., Lu, X., Lei, M., Feng, Q., & Wu, Q. (2004). Upregulation of corin gene expression in hypertrophic cardiomyocytes and failing myocardium. *Am J Physiol Heart Circ Physiol, 287*(4), H1625-1631.

Vandenburgh, H. H., Solerssi, R., Shansky, J., Adams, J. W., Henderson, S. A., & Lemaire, J. (1995). Response of neonatal rat cardiomyocytes to repetitive mechanical stimulation in vitro. *Ann N Y Acad Sci, 752*, 19-29.

Wang, H., Fertala, A., Ratner, B. D., Sage, E. H., & Jiang, S. (2005). Identifying the SPARC Binding Sites on Collagen I and Procollagen I by Atomic Force Microscopy. *Anal Chem, 77*(21), 6765-6771.

Wang, Y., Huang, S., Sah, V. P., Ross, J., Jr., Brown, J. H., Han, J., & Chien, K. R. (1998). Cardiac muscle cell hypertrophy and apoptosis induced by distinct members of the p38 mitogen-activated protein kinase family. *J Biol Chem, 273*(4), 2161-2168.

Wang, Z., Harkins, P. C., Ulevitch, R. J., Han, J., Cobb, M. H., & Goldsmith, E. J. (1997). The structure of mitogen-activated protein kinase p38 at 2.1-A resolution. *Proc Natl Acad Sci U S A, 94*(6), 2327-2332.

Weber, K. T. (1989). Cardiac interstitium in health and disease: the fibrillar collagen network. *J Am Coll Cardiol, 13*(7), 1637-1652.

Wrana, J. L., Overall, C. M., & Sodek, J. (1991). Regulation of the expression of a secreted acidic protein rich in cysteine (SPARC) in human fibroblasts by transforming growth factor beta. Comparison of transcriptional and post-transcriptional control with fibronectin and type I collagen. *Eur J Biochem, 197*(2), 519-528.

Yamazaki, T., Komuro, I., & Yazaki, Y. (1995). Molecular mechanism of cardiac cellular hypertrophy by mechanical stress. *J Mol Cell Cardiol, 27*(1), 133-140.

Yan, Q., & Sage, E. H. (1999). SPARC, a matricellular glycoprotein with important biological functions. *J Histochem Cytochem, 47*(12), 1495-1506.

Yan, Q., Sage, E. H., & Hendrickson, A. E. (1998). SPARC is expressed by ganglion cells and astrocytes in bovine retina. *J Histochem Cytochem, 46*(1), 3-10.

Zhou, H., Hammonds, R. G., Jr., Findlay, D. M., Martin, T. J., & Ng, K. W. (1993). Differential effects of transforming growth factor-beta 1 and bone morphogenetic protein 4 on gene expression and differentiated function of preosteoblasts. *J Cell Physiol, 155*(1), 112-119.

Abbreviations

A_{260}	absorbance at 260 nm
aa	amino acids
Ag	antigen
ANP	atrial natriuretic peptide
ATG	Base triplet coding for methionine; translational start site
BNP	brain natriuretic peptide
BSA	bovine serum albumin
BW	body weignt
cDNA	complementary DNA
CF	cardiac failure
Cre	Cre (causes recombination) recombinase
DMEM	Dulbecco's minimum essential medium
DMSO	dimethylsulfoxid
DNA	desoxyribonucleic acid
dp/dt max	velocity of systolic LV pressure development
dp/dt min	velocity of diastolic LV relaxation
ECM	extracellular matrix
EDTA	ethylenediaminetetraacetic acid
EGF	epidermal growth factor
Erk	Extracellular signal-regulated kinase
FAK	focal adhesion kinase
FCS	fetal calf serum
FGF	fibroblast growth factor
FN	fibronectin
FS	fractional shortening
HW	heart weight
IGF	Insulin-like growth fachor
IVS	inventricular septum

Jnk	c-jun N-terminal kinase
Kb	kilobases
kDa	kilodalton
loxP	recognition site for Cre recombinase
LV	left ventricle
LVEDP	LV end diastolic pressure
MAPK	mitogen-activated protein kinase
MHC	major histocompatibility complex
MI	myocardial infarction
mRNA	messenger RNA
OD	optical density
PBS	phosphate-buffered saline
PCR	polymerase chain reaction
PDGF	platelet derived growth factor
PFA	paraformaldehyd
RGD	arginine glycine aspartate
RNA	ribonucleic acid
Rnase	ribonuclease
rpm	rotations per minute
RT-PCR	reverse-transcriptase polymerase chain reaction
SDS	sodium dodecyl sulphate
SPARC	secreted protein, acidic and rich in cystein
c-Src	c-Src-kinase
TGF	transforming growth factor
VN	vitronectin
WT	wildtype

Publications and poster presentations from this work

1. Original articles

- **Wu R**., Laser M., Han H., Varadarajulu J., Schuh K., Hallhuber M., Hu K., Ertl G., Hauck C., Ritter O. (2006) Fibroblast migration after myocardial infarction is regulated by SPARC expression. *Journal of Molecular Medicine* March 84 (3): 241-252

- Varadarajulu J., Laser M., Hupp M., **Wu R.,** Hauck C.(2005)Targeting of alpha(v) integrins interferes with FAK activation and smooth muscle cell migration and invasion. *Biochem Biophys Res Commun.* Jun 3;331 (2):404-12.

- **Wu R.,** Laser M., Han H., Hu K., Schuh K., Ertl G., Hauck C., Ritter O. Characterization of cardiac specific excision of the β1 integrin gene in mice- influence on the transcriptional response after transversal aortic constriction (manuscript in preparation)

- **Wu R.,** Laser M., Han H., Hu K., Schuh K., Ertl G., Hauck C., Ritter O. Targeting of alpha(v) integrins interferes with gene expression and signal transduction after aortic banding in mice (manuscript in preparation)

2.Abstracts

- **Wu R**., Laser M., Han H., Varadarajulu J., Schuh K., Hallhuber M., Hu K., Ertl G., Hauck C., Ritter O. (2005) The matricelluar protein SPARC is induced after myocardial infarction in mice and orchestrates. *Kardiologie* 94 suppl (1) P 1283

- Laser M., Han H., **Wu R.,** Ertl G.(2004) Integrin signaling is activated and required after myocardial infarction and aortic banding in mice for early compensation and survival. 93suppl (3)172

3. Posters and oral presentations

- Transient expression of SPARC upon myocardial infarction orchestrates fibroblast migration and tissue remodelling in the heart. Congress *of the European Society of Cardiology* September, 03-09, 2005 (Stockholm, Sweden)

- The matricellular protein SPARC is induced after myocardial infarction in mice. *"71. Jahrestagung der Deutschen Gesellschaft für Kardiologie - Herz- und Kreislaufforschung"* Mach 31.- April 0 2. 2005 (Mannheim, Germany)

- Transient expression of SPARC upon myocardial infarction orchestrates fibroblast migration and tissue remodelling in the heart. Meeting of Mediziische Klinik Universität Würzburg *"Bad Brückenauer Wintertagung"*. 16-17. Februar 2005 (Bad Brückenau)

- Characterization of cardiac specific excision of the β1 integrin gene in mice. *8th annual symposium of Chinese Medical Association in Germany*. October 30-31,2004, (Hamburg, Germany)

- Integrin-dependent upregulation of sparc during early remodelling after myocardial infarction in mice. *"Herzinsuffizienz 2004"* September 23-25, 2004 (Würzburg, Germany)

- Integrin signaling in the hypertrophy in myocardium is required for survival and hypertrophic growth. *Congress of the European Society of Cardiology*, August 28 – September 01, 2004 (Munich Germany)

- Integrin signalling is activated and required after myocardial infarction and aortic banding in mice for early compensation and survival. *70. Jahrestagung der Deutschen Gesellschaft für Kardiologie - Herz- und Kreislaufforschung"* April 15-17, 2005 (Mannheim, Germany)

Honours

- **"Rudolf Thauer poster prize"** at the 71. Annual Conference of the German Society for Cardiology - heart research and circulatory research, Mannheim, Germany, 2005.

- **"Chinese government award for outstanding student abroad " 2005**

- Second place of the "**Contest of Excellent Medical Lecturer**" by Kunming Medical College. China, 2001.

- "**Advanced science and technique prize**" for research on anti-fibrotic effect of traditional Chinese medicine on animal model. Awarded by the city of Kunming, China.2000.

- "**Advanced science and technique prize**" for research on anti-fibrotic effect of traditional Chinese medicine "kan qian fang" Awarded by the Yunnan province, China, 1998.

- "Exploration of the diagnosing law for hepatitis C in Yunnan province" Awarded the second place of "**Science Research**" by 1stAffiliated Hospital of Kunming Medical College, China, 1997.

- Awarded the name of "**Excellent Doctor**" by Public Health Department of Yunnan province, China, 1992.

- Honor "**The best graduate student of Kunming Medical College**" awarded by Kunming Medical College, China, 1991.

CURRICULUM VITAE

Name: Rongxue Wu
Date and place of birth: 10. 10. 1969, Kunming, P. R. China

Academic Education

Since April 2003   PhD student of biology at the Center for Infections Diseases
                           University of Würzburg, Germany.
                           Supervisor: Prof. Christof Hauck.

Since January 2002   MD student in Institute of Medizinische Universitätskllinik,
                           Würzburg, Germany.
                           Supervisor: Prof Georg Ertl and Dr Oliver Ritter

08.1994-07.1997   Master Degree of Medicine, Department of infection diseases
                           Kunming Medical College (KMC), Kunming,P.R China.
                           Supervisor: Prof. Lianxian Gao .Prof. Xianni Rao

08.1986-07.1991   Bachelor Degree of Medicine,
                           Kunming Medical College, Kunming, P.R. China

Professional experience

07.1999 - 01.2002   Attending physician and lecturer, 1st Affiliated Hospital of
                           Kunming medical university.

08.1997-08.1999   Resident, 1st Affiliated Hospital of Kunming medical college

08.1991-08.1994   Intern in 1st Affiliated Hospital, Kunming medical college,
                           attending a rotation training course in every department of
                           internal medicine and the relevant auxiliary departments.

Eidesstattliche Erklärungen

Hiermit erkläre ich ehrenwörtlich, dass ich die vorliegende Dissertation in allen Teilen selbständig angefertigt und keine anderen als die genannten Quellen und Hilfsmittel verwendet habe.

Weiterhin versichere ich, dass ich bisher keinen Promotionsversuch unternommen oder die vorliegende Dissertation weder in gleicher noch in ähnlicher Form in einem anderen Prüfungsverfahren vorgelegt habe.

Hiermit bewerbe ich mich erstmals um den Doktorgrad der Naturwissenschaften an der Bayerischen Julius-Maximilians-Universität Würzburg.

Würzburg, den 12. 1. 2006